USGS
science for a changing world

Field Trip Guide to Mount St. Helens, Washington—Recent and Ancient Volcaniclastic Processes and Deposits

Scientific Investigations Report 2017–5022–E

U.S. Department of the Interior
U.S. Geological Survey

Cover: Photograph of open breach of the Mount St. Helens crater taken from Johnston Ridge looking south-southeast. Eroded deposits in foreground are 1980 pyroclastic density current deposits. The ramp leading up to the crater floor is the sliding surface of the 1980 debris avalanche. The composite lava dome (1980–86 and 2004–08) is barely visible. Photograph by Amanda Lucier, September 2019, used with permission.

Field Trip Guide to Mount St. Helens, Washington—Recent and Ancient Volcaniclastic Processes and Deposits

By Richard B. Waitt, Jon J. Major, Richard P. Hoblitt, Alexa R. Van Eaton, and Michael A. Clynne

Scientific Investigations Report 2017–5022–E

U.S. Department of the Interior
U.S. Geological Survey

U.S. Department of the Interior
DAVID BERNHARDT, Secretary

U.S. Geological Survey
James F. Reilly, II, Director

U.S. Geological Survey, Reston, Virginia: 2019

Suggested citation:
Waitt, R.B., Major, J.J., Hoblitt, R.P., Van Eaton, A.R., and Clynne, M.A., 2019, Field trip guide to Mount St. Helens, Washington—Recent and ancient volcaniclastic processes and deposits: U.S. Geological Survey Scientific Investigations Report 2017–5022–E, 68 p., https://doi.org/10.3133/sir20175022E.

ISSN 2328-0328 (online)

Preface

The North American Cordillera is home to a greater diversity of volcanic provinces than any comparably sized region in the world. The interplay between changing plate-margin interactions, tectonic complexity, intra-crustal magma differentiation, and mantle melting have resulted in a wealth of volcanic landscapes. Field trips in this series visit many of these landscapes, including (1) active subduction-related arc volcanoes in the Cascade Range; (2) flood basalts of the Columbia Plateau; (3) bimodal volcanism of the Snake River Plain-Yellowstone volcanic system; (4) some of the world's largest known ignimbrites from southern Utah, central Colorado, and northern Nevada; (5) extension-related volcanism in the Rio Grande Rift and Basin and Range Province; and (6) the spectacular eastern Sierra Nevada featuring Long Valley Caldera and the iconic Bishop Tuff. Some of the field trips focus on volcanic eruptive and emplacement processes, calling attention to the fact that the western United States provides opportunities to examine a wide range of volcanological phenomena at many scales.

The 2017 Scientific Assembly of the International Association of Volcanology and Chemistry of the Earth's Interior (IAVCEI) in Portland, Oregon, marks the first time that the U.S. volcanological community has hosted this quadrennial meeting since 1989, when it was held in Santa Fe, New Mexico. The 1989 field-trip guides are still widely used by students and professionals alike. This new set of field guides is similarly a legacy collection that summarizes decades of advances in our understanding of magmatic and tectonic processes of volcanic western North America.

The field of volcanology has flourished since the 1989 IAVCEI meeting, and it has profited from detailed field investigations coupled with emerging new analytical methods. Mapping has been enhanced by plentiful major- and trace-element whole-rock and mineral data, technical advances in radiometric dating and collection of isotopic data, GPS (Global Positioning System) advances, and the availability of lidar (light detection and ranging) imagery. Spectacularly effective microbeam instruments, geodetic and geophysical data collection and processing, paleomagnetic determinations, and modeling capabilities have combined with mapping to provide new information and insights over the past 30 years. The collective works of the international community have made it possible to prepare wholly new guides to areas across the western United States. These comprehensive field guides are available, in large part, because of enormous contributions from many experienced geologists who have devoted entire careers to their field areas. Early career scientists are carrying forward and refining their foundational work with impressive results.

Our hope is that future generations of scientists as well as the general public will use these field guides as introductions to these fascinating areas and will be enticed toward further exploration and field-based research.

Michael Dungan, University of Oregon
Judy Fierstein, U.S. Geological Survey
Cynthia Gardner, U.S. Geological Survey
Dennis Geist, National Science Foundation
Anita Grunder, Oregon State University
John Wolff, Washington State University
Field-trip committee, IAVCEI 2017

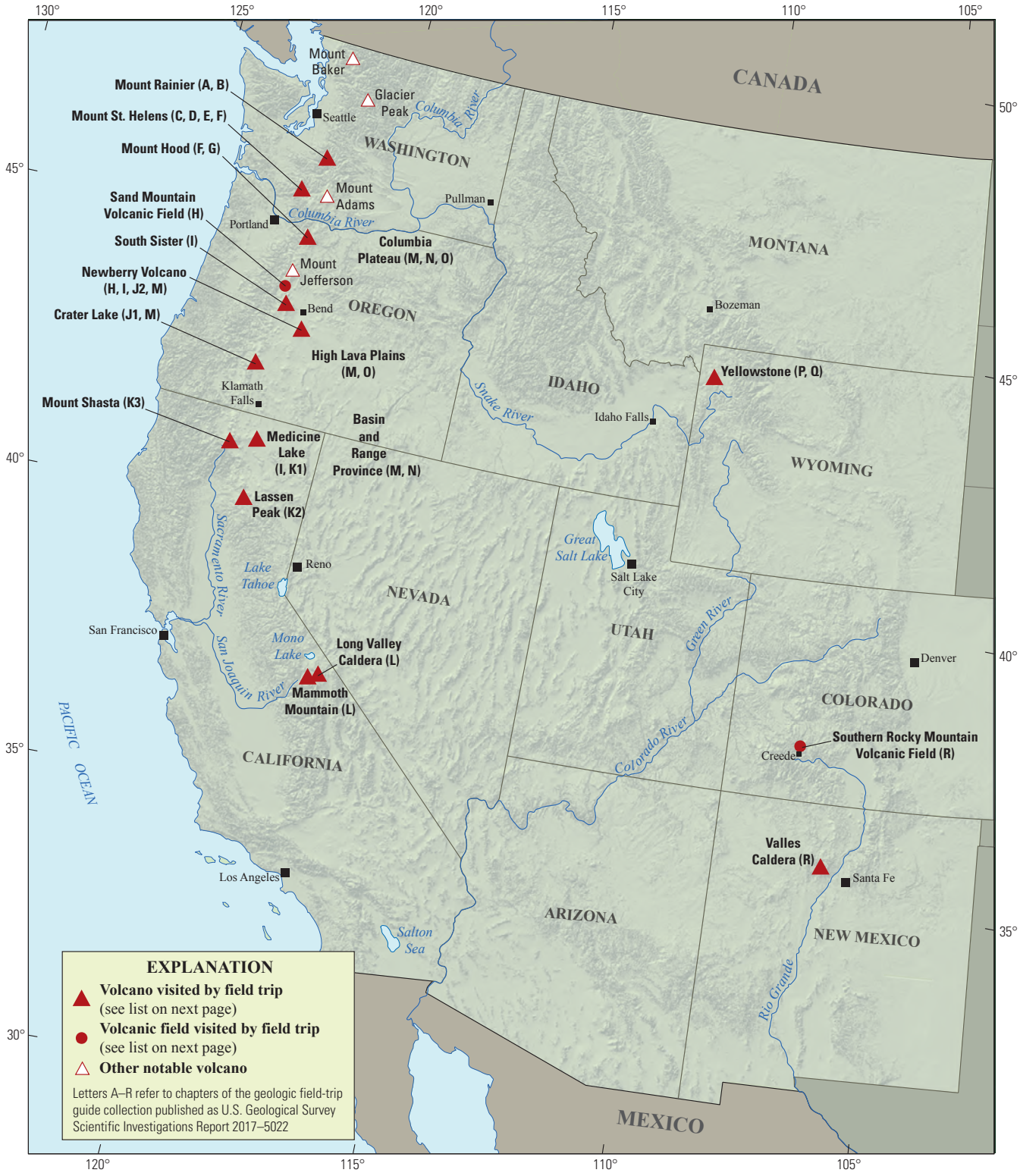

Map of the western United States showing volcanoes and volcanic fields visited by geologic field trips scheduled in conjunction with the 2017 meeting of the International Association of Volcanology and Chemistry of the Earth's Interior (IAVCEI) in Portland, Oregon, and available as chapters in U.S. Geological Survey Scientific Investigations Report 2017–5022. Shaded-relief base from U.S. Geological Survey National Elevation Dataset 30-meter digital elevation model data.

Contributing Authors

Boise State University
Brittany D. Brand
Nicholas Pollock

Colgate University
Karen Harpp
Alison Koleszar

Durham University
Richard J. Brown

Eastern Oregon University
Mark L. Ferns

ETH Zurich
Olivier Bachmann

Georgia Institute of Technology
Josef Dufek

GNS Science, New Zealand
Natalia I. Deligne

Hamilton College
Richard M. Conrey

Massachusetts Institute of Technology
Timothy Grove

National Science Foundation
Dennis Geist (also with Colgate University and University of Idaho)

New Mexico Bureau of Geology and Mineral Resources
Paul W. Bauer
William C. McIntosh
Matthew J. Zimmerer

New Mexico State University
Emily R. Johnson

Northeastern University
Martin E. Ross

Oregon Department of Geology and Mineral Industries
William J. Burns
Lina Ma
Ian P. Madin
Jason D. McClaughry

Oregon State University
Adam J.R. Kent
Benjamin J. Drenth
William C. Evans
Judy Fierstein
Cynthia A. Gardner
V.J.S. Grauch
Christopher J. Harpel
Wes Hildreth
Richard P. Hoblitt
Peter W. Lipman
Jacob B. Lowenstern
Jon J. Major
Seth C. Moran
Lisa A. Morgan
Leah E. Morgan
L.J. Patrick Muffler
Jim O'Connor
John S. Pallister
Thomas C. Pierson
Joel E. Robinson
Juliet Ryan-Davis
Kevin M. Scott
William E. Scott
Wayne (Pat) Shanks
David R. Sherrod
Thomas W. Sisson
Mark Evan Stelten
Weston Thelen
Ren A. Thompson
Kenzie J. Turner
James W. Vallance
Alexa R. Van Eaton
Jorge A. Vazquez
Richard B. Waitt
Heather M. Wright

Portland State University
Jonathan H. Fink (also with University of British Columbia)
Martin J. Streck
Ashley R. Streig

San Diego State University
Victor E. Camp

Smithsonian Institution
Lee Siebert

Universidad Nacional Autónoma de San Luis Potosi
Damiano Sarocchi

University of California, Davis
Kari M. Cooper

University of Liverpool
Peter B. Kokelaar

University of Northern Colorado
Steven W. Anderson

University of Oregon
Ilya N. Binderman
Michael A. Dungan
Daniele Mckay (also with Oregon State University and Oregon State University, Cascades)

University of Portland
Kristin Sweeney

University of Tasmania
Martin Jutzeler
Jocelyn McPhie

University of Utah
Jamie Farrell

U.S. Army Corps of Engineers
Keith I. Kelson

U.S. Forest Service
Gordon E. Grant (also with Oregon State University)

U.S. Geological Survey
Charles R. Bacon
Andrew T. Calvert
Christine F. Chan
Robert L. Christiansen
Michael A. Clynne
Michael A. Cosca
Julie M. Donnelly-Nolan

U.S. Nuclear Regulatory Commission
Stephen Self (also with University of California, Berkeley)

Washington State University
Joseph R. Boro
Owen K. Neill
Stephen P. Reidel
John A. Wolff

Acknowledgments
Juliet Ryan-Davis and Kate Sullivan created the overview map, and Vivian Nguyen created the cover design for this collection of field-trip guide books. The field trip committee is grateful for their contributions.

Contents

Figures

Tables

Sidebars

Abbreviations

B.P.	before present ("present" is year 1950; see sidebar 2 on dating)
DRE	dense-rock equivalent
ka	thousands of years ago
km^3	cubic kilometers
m^3	cubic meters
Ma	millions of years ago
m.y.	millions of years
PDT	Pacific Daylight Time (in 1980 shifted from Standard Time 27 April)

Itinerary

Day 0: Drive from Portland, Oreg., to Packwood, Wash. Arrive by late afternoon.

Day 1: Northeast sector: Tertiary volcanic rocks, prehistoric tephra falls, 18 May 1980 pyroclastic surge along NE radial, 1980 eyewitness vignettes, Spirit Lake story.

Day 2: Northeast sector: Big trees, Harmony Falls basin, Norway Pass trail. Spirit Lake story; prehistoric tephra falls.

Day 3: East, southeast, and south flanks: surge, lahars, prehistoric debris avalanche, pumice flows, tephra falls, lava flow. Drive from Packwood to Woodland.

Day 4: Kalama eruptive stage on southwest and south flanks: flows, lahars, falls, domes, lava flows. Drive to Castle Rock.

Day 5: 18 May 1980 debris-avalanche and pyroclastic surge near Elk Rock and Coldwater Lake, North Fork Toutle valley; modern and ancient volcaniclastic sedimentation in Toutle River valley. Drive to Portland, Oreg. Arrive evening.

Sources and Acknowledgments

Much of this report is newly composed, but it partly derives from earlier field guides (Waitt and others, 1989; Waitt and Pierson, 1994; Major and others, 2009). From many years of mapping and chronology, Michael A. Clynne contributed an updated summary of Mount St. Helens history. Stop 3.6 derives from Clynne (2003) and stop 2.7 from Pallister and others (2003). Accessible earlier field guides include Doukas (1990) and Pat Pringle's nice duo on Mount St. Helens (2002) and on Mount Rainier (2008). Pringle's Mount St. Helens guide includes road logs to all approaches and many notes on the Tertiary bedrock.

Field Trip Guide to Mount St. Helens, Washington—Recent and Ancient Volcaniclastic Processes and Deposits

By Richard B. Waitt, Jon J. Major, Richard P. Hoblitt, Alexa R. Van Eaton, and Michael A. Clynne

Introduction—Overview and Background for Days 1–3

Setting and Structure

Mount St. Helens is part of a volcanic arc where the oceanic Juan de Fuca Plate subducts beneath the continental North American Plate. The west edge of the continental plate has been distorting for most of Cenozoic time. Crustal blocks in California translating northwest along transform faults like the San Andreas compress and rotate clockwise the forearc region to the north. That block in turn compresses the forearc and Cascade region farther north in Washington (Wells and others, 1998) (fig. 1).

Hundreds of analyzed folds and faults and dike intrusions show that the Pacific Northwest has experienced NNW–SSE crustal shortening and WSW–ENE extension (Hooper and Conrey, 1989). Throughgoing WNW–ESE dextral-shear zones like the Olympic-Wallowa lineament and the Brothers fault zone (fig. 2) take up some deformation—regional structures probably active for 40 million years. The Olympic-Wallowa shows evidence of dextral movement into Late Pleistocene and Holocene times (Sherrod and others, 2016). Smaller structures also reveal NNW–SSE compression (Hammond, 2013). To the south in Columbia gorge, a dozen northwest-striking dextral strike-slip faults cut the mid-Miocene Columbia River Basalt and even Pleistocene sediment (Anderson and others, 2013).

Tertiary (Paleogene-Neogene) Rocks

An intermittently active magmatic arc has erupted in the area of the Cascade Range since late Eocene time. Detailed geologic maps around Mount St. Helens portray stratified east-dipping basalt, basaltic andesite, and andesite lava flows interbedded with dacite tuffs, welded tuffs, tuff breccias, and volcaniclastic sedimentary rocks (fig. 3) (Evarts and Ashley, 1990, 1992, 1993a,b,c,d; Evarts and others, 1987). The rocks range from about 36 million years ago (Ma) in the west to 23 Ma upsection in the east (Evarts and others, 1994; Evarts and Swanson, 1994). Most of the rocks—lava flows, coarse breccias and conglomerates, pumiceous pyroclastic flows—seem fairly near their vents. The many separate eruption centers include Strawberry Mountain, Vanson Peak, Bismark Mountain, Spud Mountain, Cinnamon Peak, and others.

The rock sequence is regionally burial-metamorposed to zeolite facies. Smectite clays, a common alteration element, impart a greenish cast to many rocks. Younger plutons—the ~120 square kilometer (km^2) Spirit Lake pluton (granodiorite, other variants isotopically dated to 23–20 Ma)—and mafic to silicic small stocks, dikes, and small sills intrude the layered rocks and in places have contact-metamorphosed them to hornfels. In the southern Washington Cascades, Hammond (1998) identifies 41 major andesitic stratovolcanoes or shield volcanoes dated to between 37 and 20 Ma.

Cheney and Hayman (2009) and Cheney (2016) have suggested that before 17 Ma the area of the southern Cascade Range had been beveled to a plain and that 16–15 Ma Columbia River Basalt flows from the east covered this area. The basalt has been since stripped off, they infer, by erosion caused by late Miocene to Pliocene rise of the Cascade Range.

But the rocks surrounding Mount St. Helens reveal Oligocene volcanic centers and terrestrial volcaniclastic debris shed from them—evidence of high terrain here. Oligocene to early Miocene silicic intrusions—Snoqualmie batholith, Tatoosh and Spirit Lake plutons—probably had fed surface volcanoes. Northeast of Mount Rainier, Hammond (2013) mapped the west edge of Columbia River basalt surrounding older volcanic highs. Smith (1988) shows silicic volcaniclastic debris shed from the southern Cascades that interfingers eastward with several 16–10.5 Ma Columbia River basalt members. All these show that a moderate north-south high existed here since the late Eocene.

Prehistoric Mount St. Helens

Mount St. Helens, a geologically young volcano built atop the mid-Tertiary rocks (fig. 4), has been the most active Cascade Range volcano during the past 4,000 years. Our 2017 IAVCEI field excursion investigates some of its deposits, ancient to recent. During five days we visit most flanks of the volcano (fig. 5) focusing on effects of the 18 May 1980 eruption that made this volcano famous.

Continuing fieldwork by Michael A. Clynne and more $^{40}Ar/^{39}Ar$ dating by Andy T. Calvert add to Mount St. Helens' prehistoric story as laid out by Clynne and others (2008).

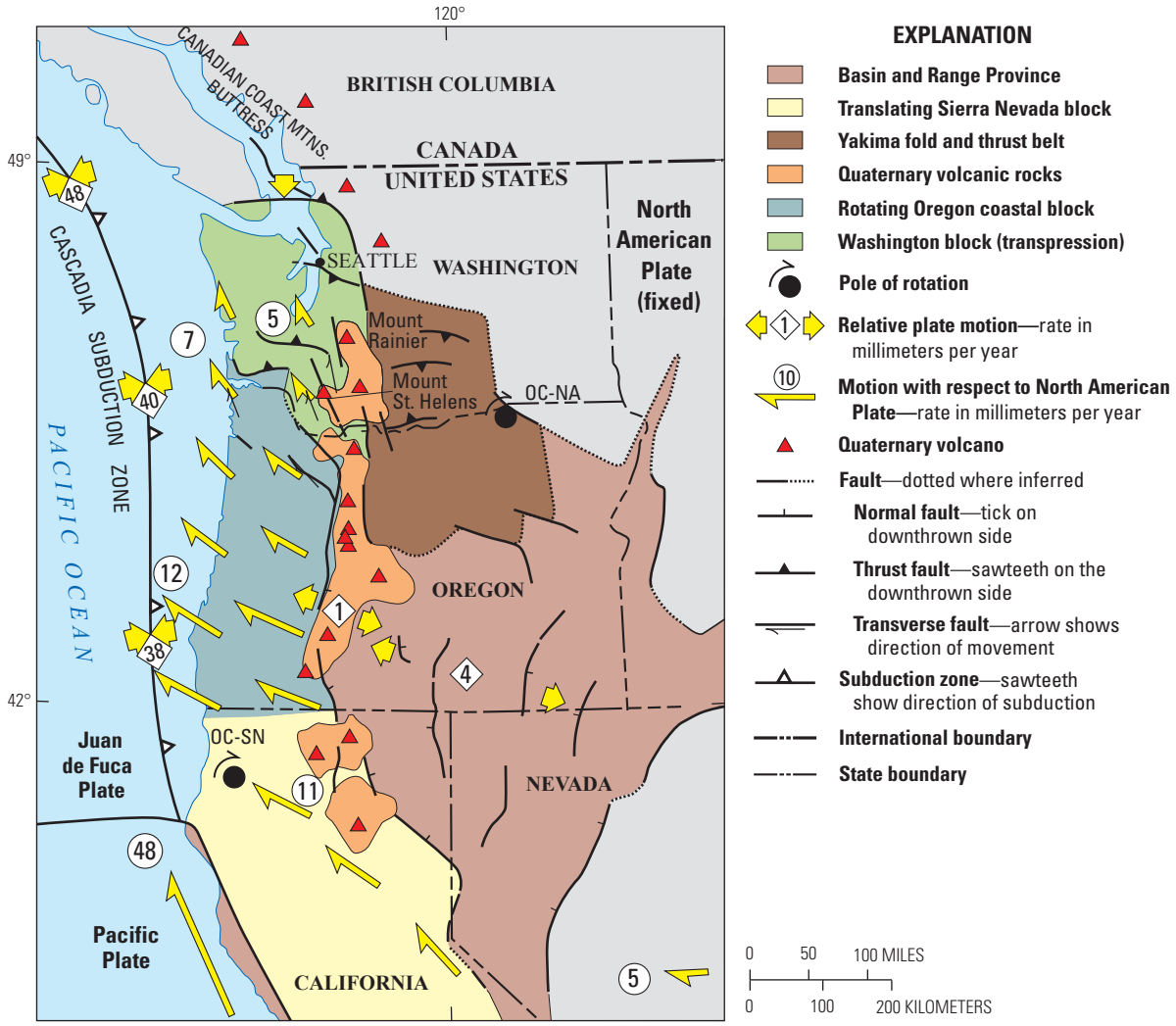

Figure 1. Map of the tectonic setting of Cascadia. The oceanic Juan de Fuca Plate dives beneath the continental North American Plate along the Cascadia subduction zone (white toothed). The migrating Cascadia forearc terrane is parceled into Sierra Nevada (SN), Oregon coastal (OC), and Washington blocks. Velocity of the tectonic blocks (yellow arrows) is calculated from a pole of rotation at point OC–NA (North America). The Oregon block is also rotating around pole OC–SN. Velocity of the Oregon coastal block is for post-Eocene time. The north end of the Oregon block squeezes the forearc area of Washington (green) against a buttress of crystalline rocks of the Canadian Coast Mountains. This north-south compression causes uplift and thrust faulting. Orange areas are Quaternary volcanic rocks; red triangles spot modern large stratovolcanoes including Mount St. Helens. From Pringle (2008), modified from a Ray E. Wells diagram.

Coming publications will update the Mount St. Helens numbers including argon plateau and isochron diagrams.

Dacite and silicic-andesite flowage deposits of the past 20,000 years dominate Mount St. Helens's flanks. These deposits partly fill several valleys that streams and glaciers had carved into Tertiary rocks (fig. 6). In the 1960s–1980s D.R. Mullineaux and D.R. Crandell deciphered these flows using tephras as marker beds to parcel out eruptive history (Crandell and Mullineaux, 1978; Mullineaux and Crandell, 1981). Mullineaux (1986, 1996) grouped 13 coarse pumiceous tephra layers (fig. 7) and several finer or thinner ones into "sets" of similar age and composition. (A sidebar elaborates some mineralogical characteristics.) Distribution plots reveal wind directions during the eruptions—mostly toward the northeast, east, or southeast. Some ash layers trace out tens to hundreds of kilometers downwind.

Crandell and Mullineaux defined four eruptive stages, the most recent subdivided into seven periods within which tephra is correlated with lava flows, domes, and fragmental deposits (fig. 7) (Crandell, 1987). R.P. Hoblitt worked out details of deposits emplaced in the past 500 years (Hoblitt and others, 1980). About 42 conventional radiocarbon dates roughly timed most intervals. This team thought Mount St. Helens about 50,000 years old.[1]

[1]Radiocarbon ages here in calibrated time. Crandell's and Mullineaux's reports in the 1960s–1990s had radiocarbon time uncalibrated. Clynne and others (2008) include tables and plots with calibration details for Mount St. Helens deposits.

Figure 2. Map of major tectonic structures of the Pacific Northwest emphasizing NW-SE dextral shear zones. OWL, Olympic-Wallowa lineament; BFZ, Brothers fault zone. From Hooper and Conrey (1989).

Glaciation had removed or buried most deposits older than ~60 ka (thousands of years old). U.S. Geological Survey geologic mapping since the 1990s—aided by $^{40}Ar/^{39}Ar$ dating, paleomagnetic data, and refined radiocarbon dating—shows that the volcano's eruptive history begins much earlier (Clynne and others, 2008). Various rocks from Mount St. Helens as old as 272,000 years (fig. 8) lie within lahars and beneath deposits younger than 60 ka. Figure 7 summarizes Crandell and Mullineaux's eruption history as refined by newer mapping and chronology (M.A. Clynne and A.T. Calvert, written commun., 2016). The newer dates lengthen some eruptive stages and narrow the gaps between. Crandell and Mullineaux emphasized major Plinian eruptions. But less-explosive activity followed each major eruption. Before its present cone, Mount St. Helens had apparently been a long succession of dacite domes (Clynne and others, 2005) intermittently active since the middle Pleistocene (fig. 9).

Ape Canyon Stage (300–35 ka)

During the Ape Canyon Stage, Mount St. Helens erupted quartz-bearing biotite and (or) hornblende dacite domes and the set C tephras. These rocks crop out in spots beneath glacial deposits and younger rocks on Mount St. Helens's southeast and southwest flanks. Figure 8 summarizes the long volcanic history during this stage. Oldest and most prominent is Goat Mountain at 272±1 ka (fig. 8). The other four dates in that cluster ranging back to about 245 ka are from clasts of Mount St. Helens compositions in glacial deposits in Lewis River valley. (The sidebar elaborates some details of dating.) Other older dates are from clasts in lahars or younger Plinian deposits. Zircon as old as about 500 ka in some Ape Canyon rocks suggests that volcanism or intrusion at Mount St. Helens began long before Goat Mountain time (Claiborne and others, 2010). One could split out a Goat Mountain stage for materials older than 160 or 120 ka. An 84.2±21.9-ka dacite on the crater floor—exposures new since the great 1980 landslides—proves that Ape Canyon Stage rocks underlie the present edifice.

Cougar Stage (28–18 ka)

During the Cougar Stage the volcano erupted hypersthene-hornblende dacite domes, pumiceous pyroclastic flows, tephra sets M and K, and two andesite lava flows. A large debris avalanche at ~24.5 ka on the southwest volcano flank dammed Lewis River. Almost immediately several cubic kilometers of pumiceous pyroclastic flows covered the avalanche. When the dammed lake breached, huge lahars swept down Lewis River. A south-flank silicic-andesite lava flow at about 17.8 ka is at volume 0.75 km^3 the largest in Mount St. Helens's history.

Swift Creek Stage (16–10 ka)

During the Swift Creek Stage, widespread tephra sets S and J erupted, and debris from hypersthene-hornblende dacite domes built three broad fans of fragmental debris on the volcano's flanks. Crescent Dome on the west-northwest flank shed Crescent Ridge fan. Domes exposed in the east crater wall may have supplied the Cedar Flats fan on the southeast flank and a fan on the south flank. Most debris started as block-and-ash flows but lower on the fans transformed into lahars. Small lithologic differences suggest the three fans record separate eruptions between about 16 and 10 ka.

Spirit Lake Stage (4–0 ka)

The Spirit Lake Stage is the youngest (it continues today), is the best exposed and dated, and is by far the most understood eruptive interval. It is divided into seven eruptive periods separated by short interludes (figs. 7, 10).

The Smith Creek Period began about 3,900 cal yr B.P. with several set Y tephras. Yn erupted ~3,500 cal yr B.P., at as much as 4 km^3 DRE (Carey and others, 1995) the largest

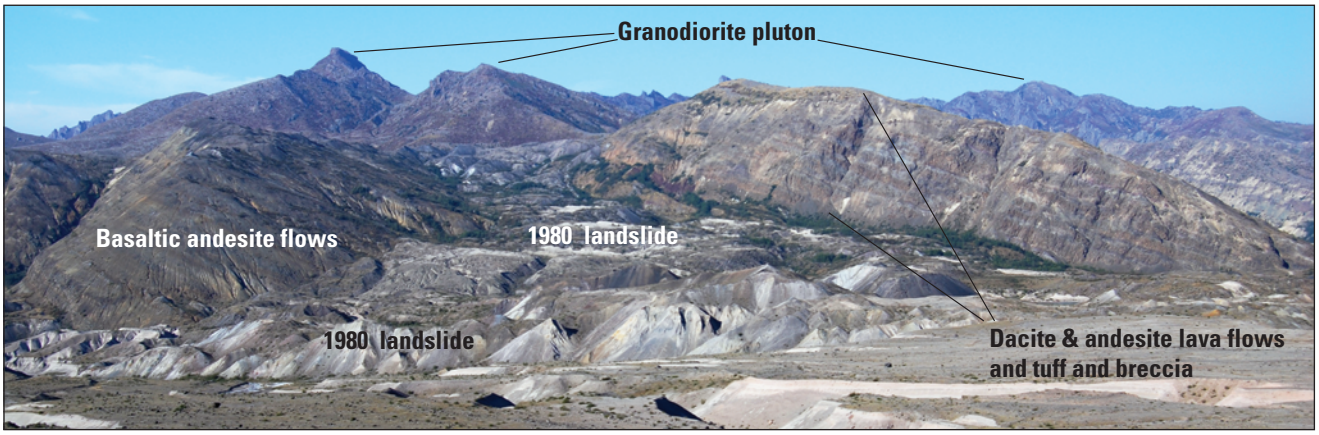

Figure 3. North-northeast-directed view of Spirit Lake area showing homocline of layered Oligocene-Miocene volcanic and volcaniclastic rocks dipping east about 20°. Erosionally resistant lava flows and intervening weaker beds form a series of hogbacks, their topography sharpened by glaciation. USGS oblique-aerial photograph.

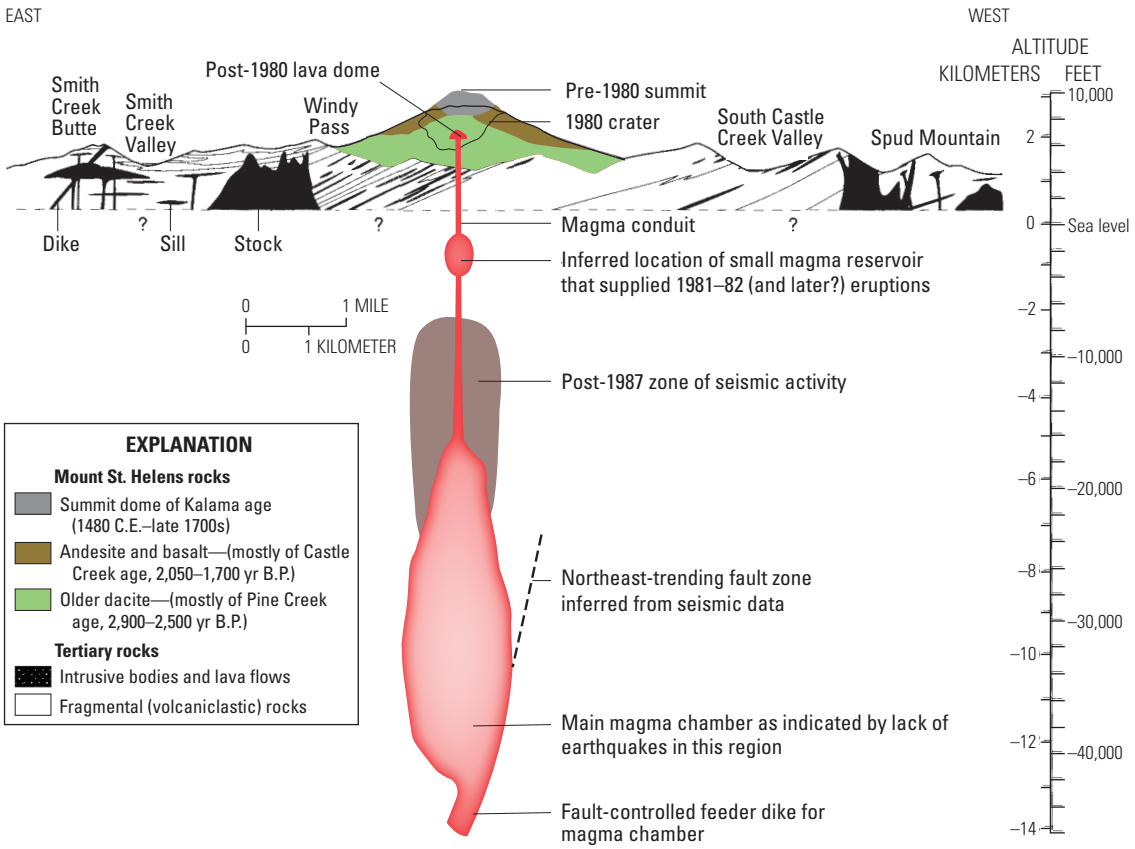

Figure 4. Simplified geologic cross section of Mount St. Helens and the underlying east-tilted Tertiary rocks, viewed from the north. The magmatic plumbing system depicted is inferred from seismic data. From Pringle (2002, fig. 7) as modified by him from Evarts and others (1987) and Pallister and others (1992).

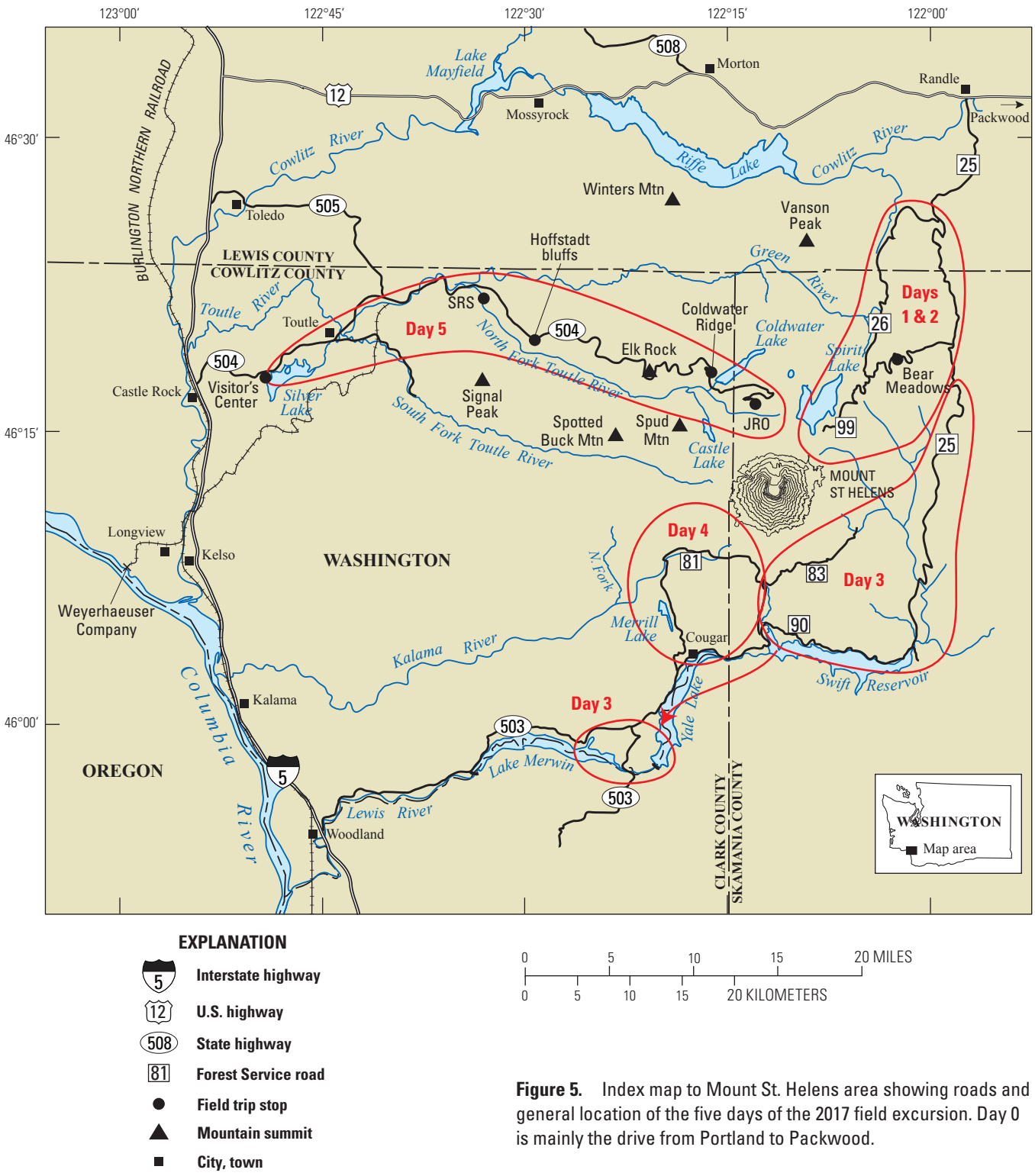

Figure 5. Index map to Mount St. Helens area showing roads and general location of the five days of the 2017 field excursion. Day 0 is mainly the drive from Portland to Packwood.

single eruption in the volcano's history. Large Ye followed at ~3,350 cal yr B.P. Pyroclastic flows, lava domes, and lahars followed each major Y tephra. A fan of fragmental debris on the north dammed ancestral Spirit Lake.

During the Pine Creek Period (~3,000–2,500 cal yr B.P.) the volcano erupted several dacite domes and tephra set P, then several andesitic lava flows, pyroclastic flows, lahars, and two of the set-B tephras (fig. 10). The 1980 crater walls expose Pine Creek-age dacite domes, and large fans of lithic pyroclastic debris and lahars lie on several flanks. Pine Creek-age domes collapsed into two small debris avalanches, one or both damming Spirit Lake. Breakouts from the lake sent huge lahars down lower Toutle valley (Scott, 1988a, b) at ~2,560 cal yr B.P. (fig. 10). The burst of activity about 2,550 cal yr B.P. erupted tephra Bh, andesite lava flows, tephra Bo, and basaltic andesite to andesite lava flows and lahars.

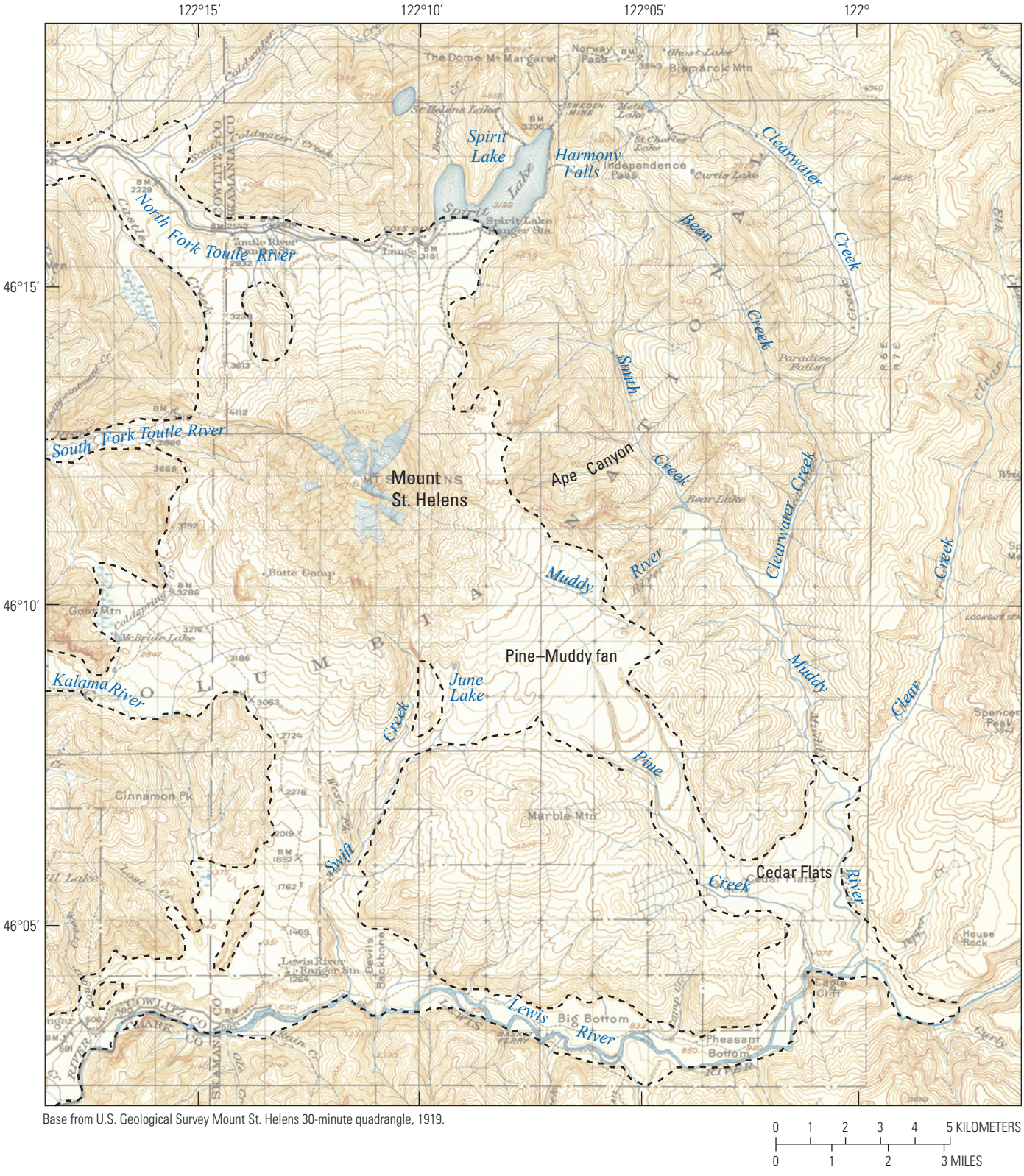

Figure 6. Historical topographic map of Mount St. Helens showing limits of the volcano's pre-1980 debris (dashed line, modified from Clynne and others, 2008). Swift and Yale Lake reservoirs since the 1950s have filled much of Lewis valley in the south.

Eruptive stage	Eruptive period	Tephra set	Major eruptive products	Glacial stage
Spirit Lake 3,900–0 years B.P.	Modern period, 1980–2008 C.E.	1980	Landslides, surge, pyroclastic flows, lahars, dacite domes	
	Goat Rocks period, 1800–1857 C.E.	layer T	Andesite flows, dacite dome,. block-and-ash flows	
	Kalama period, 1479–1725 C.E.	layer Z set X set W	Dacite domes, surge, pyroclastic flows, block-and-ash flows, andesite flows, dacite domes	
	Sugar Bowl period, 1,050–1,000 cal yr B.P.	layer D	Dacite dome, lateral blast	
	Castle Creek period, 2,050–1,700 cal yr B.P.	set B	Dacite domes and flows, block-and-ash flows, basalt to andesite flows, lahars	
	Pine Creek period, 3,000–2,550 cal yr B.P.	set B set P	Dacite domes and block-and-ash flows, andesite flows, debris avalanches, lahars	
	Smith Creek period, 3,900–3,300 cal yr B.P.	set Y	Dacite domes and block-and-ash flows, pyroclastic flows, lahars	
Dormant interval 10–3.9 ka				
Swift Creek 16–10 ka		set J set S	Dacite domes and block-and-ash flows, pyroclastic flows, lahars	
Dormant interval 18–16 ka				
Cougar 28–18 ka		set K set M	Dacite domes and block-and-ash flows, debris avalanche and pyroclastic flows, andesite flows, lahars	Evans Creek, 22–18 ka
Dormant interval 35–28 ka				
Possible dormant interval 240–160 ka				
Ape Canyon 300–35 ka		set C	Dacite domes and block-and-ash flows, lahars	Hayden Creek, ~140 ka pre-Hayden Creek, ~280 ka

Figure 7. Chart of Mount St. Helens eruptive materials in stratigraphic order. Adapted from Clynne and others (2008) updated by Clynne in 2016. It had been in turn adapted from Crandell (1987) and Mullineaux (1996). Ages are in years of the Common Era (C.E.), years before present (cal yr B.P., where "present" is 1950), and thousands of years ago (ka).

Sidebar 1. Minerals in tephra

Many of Mount St. Helens's tephras may be distinguished from each other by mineralogy. Quartz-biotite dacite characterizes only the oldest eruptive stage—the Ape Canyon—and its tephra set C (Mullineaux, 1986; Clynne and others, 2008).

The amphibole cummingtonite—once thought a metamorphic mineral—was in the 1960s identified in dacite tephras at Mount St. Helens. Cummingtonite is a constituent of older silicic tephra sets C to Y (older than 3,000 years) but absent from younger ones P through T and 1980.

Laboratory experiments show cummingtonite to be stable in fairly cool (<800 °C) and wet (>5.5–6.5 weight percent H_2O) magmas (Geschwind and Rutherford, 1992). Gardner and others (1995a) infer that basalt intruded a magma chamber 3,000–2,500 years ago and heated dacitic magma that lay higher in the chamber. Dacite magmas that have erupted tephra in the past 2,500 years were hotter and drier than those before 3,000 years ago—and so they lack cummingtonite.

Sidebar 2. Dating lava flows and deposits

Lava flows may be dated directly by K-Ar and $^{40}Ar/^{39}Ar$ methods. Clasts in fragmental deposits—say a lava clast within a flowage deposit—may too be dated. A dated clast gives only a maximum-limiting age of the flow containing the clast. One hopes it's closely limiting.

Where ash fell into peat bogs or ponds, radiocarbon dating of organic material just below or above gives a maximum or minimum age of the ash. Once an identifiable tephra is dated, it can then proxy-date a flowage deposit that it underlies or overlies at another site.

Four of the youngest Mount St. Helens tephras have been dated to the year by tree rings. Trees stressed by heavy ashfall may grow only narrow rings for some years. Thus by suddenly narrowed growth rings of firs, tephra Wn dates to late 1479 or early 1480 C.E., We to 1482, X to 1680, and T to early 1800 (Yamaguchi, 1983, 1985, 1986) (see Day 4).

By historical precedent radiocarbon dating is expressed by a unique protocol. In its expression "years before present" (yr B.P.), "present" means 1950 C.E. Except for youngest radiocarbon ages, a "thousand years B.P." of radiocarbon protocol approximately equals the "ka" of other dating methods.

Radiocarbon protocol is further complicated by a correction now routinely applied to published radiocarbon dates that calibrates them to calendar time. To distinguish calibrated from traditional "raw" radiocarbon dates as in previous paragraph, the calibrated versions are expressed as "cal yr B.P." All radiocarbon dates in this work are calibrated by the OxCal routine (Bronk Ramsey, 1998, 2001).

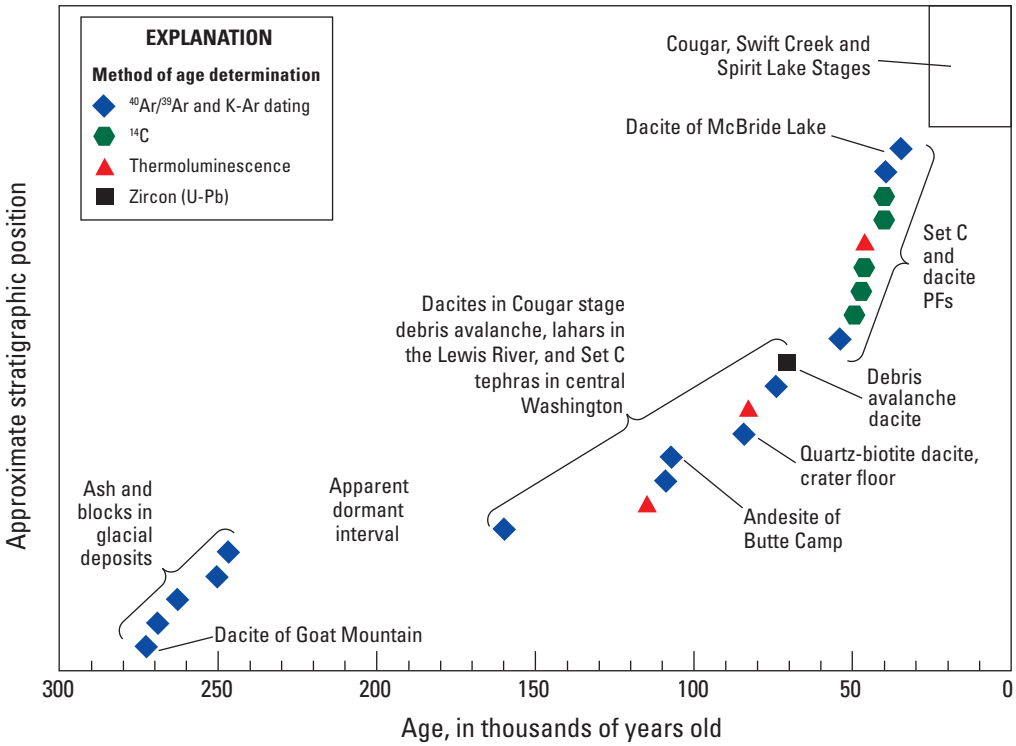

Figure 8. Plot of ages and approximate stratigraphic position for Ape Canyon stage (by Michael A. Clynne, 2016). The three younger stages, represented by box in upper right, occupy only a tenth of the known time of volcano's eruptive history. Thermoluminescence ages from Berger and Busacca (1995). For more age details including error bars, see Clynne and others (2008) and references therein, and Wanke and others (2019).

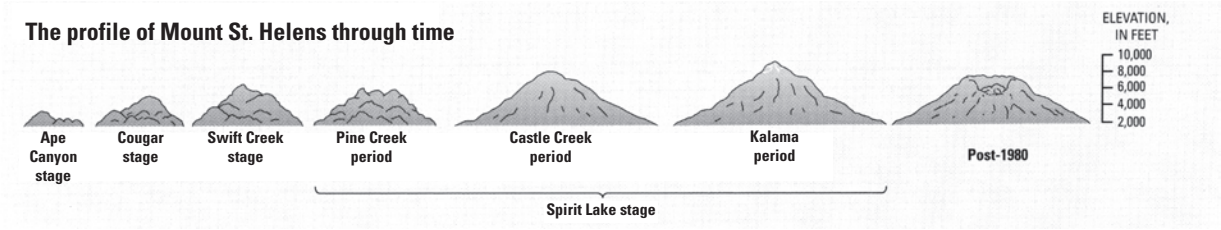

Figure 9. Inferred succession through time of Mount St. Helens dome complexes to modern cone. From Clynne and others (2005).

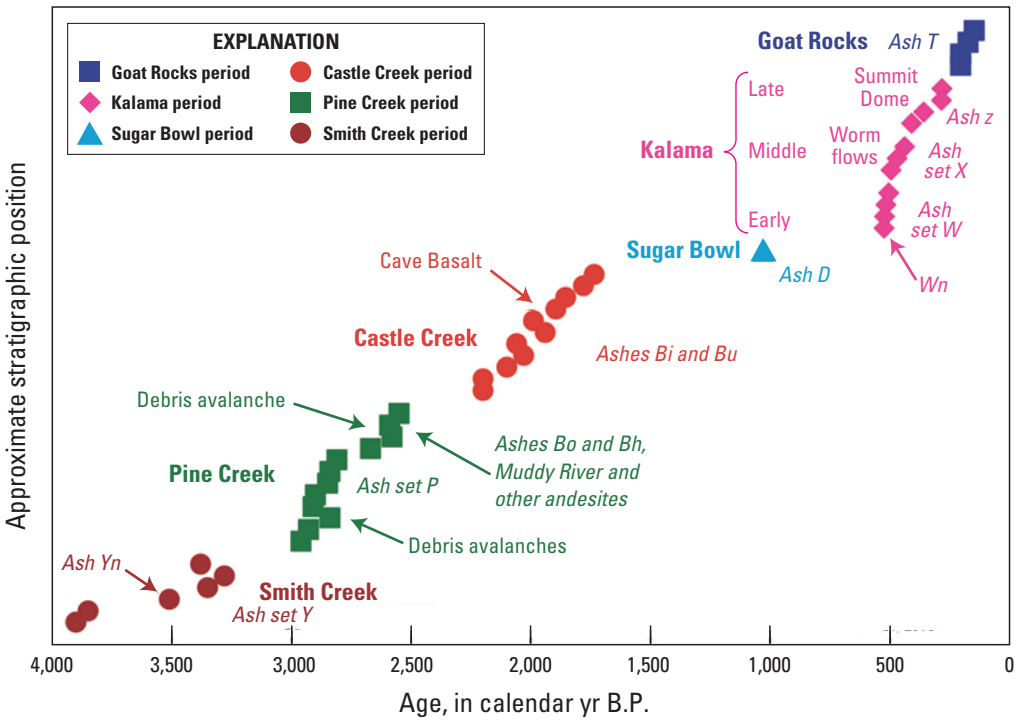

Figure 10. Summary plot of radiocarbon ages and stratigraphic position for eruptive products of Spirit Lake stage. See figure 7 for description of tephra sets. By Michael A. Clynne, data as of April 2016.

Mullineaux (1987) had defined the Castle-Creek/Pine-Creek boundary at a visually sharp color change—from tan in the top of tephra set P to overlying very dark brown of the base of tephra Set B. He inferred a hiatus in time at the base of layer Bh but had no data to prove it. Recent details of $^{40}Ar/^{39}Ar$ dating, paleomagetism, and geochemistry show the hiatus to instead be above tephra layer Bo. We follow Clynne's until-now unpublished interpretation and move the Castle Creek/Pine Creek boundary up to top of tephra Bo.

During the diverse Castle Creek Period, compositions ranging from dacite to basalt erupted in three phases from ~2,025 to ~1,700 cal yr B.P. (fig. 10). The mainly dacitic early phase includes Northwest and Dogs Head domes, pumiceous and lithic pyroclastic flows, several andesite-dacite lava flows (Red Rock Pass and North Rim), and tephra Bi—all in a brief interval ~2,025–1,990 cal yr B.P. Through most of its history Mount St. Helens had erupted dacitic lavas as tephra, domes, and pyroclastic flows. But now basalt also appears. The middle phase begins with basaltic tephra Bu. Then come three south-flank basalt and basaltic-andesite lava flows including Cave Basalt at ~1,895 cal yr B.P. During the late phase the volcano erupts about eight basalt to andesite flows on the north and east flanks between ~1,895 and ~1,700 cal yr B.P. Four radiocarbon dates from 1,795±30 to 1,730±35 cal yr B.P. and paleomagnetic directional data all show that this period was brief. Late Castle Creek Period lava flows cap parts of the modern crater rim.

During the Sugar Bowl Period at least three dacite lava domes erupted: Sugar Bowl dome, East dome, and West dome. A small blast from Sugar Bowl dome threw ballistic blocks a few kilometers northeast, but air currents carried this tephra layer D along a narrow path at least 30 km out (Mullineaux, 1987, fig. 55). The Sugar Bowl Period was probably brief, ~1,050 to ~1,000 cal yr B.P.

The Kalama Period (figs. 7, 10) comprises three phases correlated with tephra sets W and X and layer z. The early Kalama phase began in late 1479 C.E. (Yamaguchi, 1983; Fiacco and others, 1993; Yamaguchi and Hoblitt, 1995) with the major eruption of dacitic tephra Wn. Another major dacite tephra (We) erupted in 1482 C.E., and several smaller tephras and pyroclastic flows accompanied several decades of dacite dome growth. The middle Kalama began ~1505 C.E. and included several small explosive events (andesitic pyroclastic flows and X tephras), lava flows, and lahars. Around 1545–1550 C.E. came many andesite lava flows—the Worm flows and others. During the late Kalama phase the large andesite-dacite summit dome built the upper cone of the volcano (fig. 8) much higher than any earlier summit (until it was deleted in 1980). Emplacement of the summit dome probably began ~1650 C.E. and ended by ~1725 C.E. During this time many pyroclastic and lahar deposits spread down the volcano flanks.

Pleistocene Glaciation

Let us turn back to Ape Canyon and Cougar times and earlier. Several Pleistocene glacial episodes carved cirques and other alpine topography in the Mount Margaret highlands north of Spirit Lake (fig. 6). From there large glaciers widened valleys like upper Schultz Creek, the upper Green, the upper North Fork Toutle, the upper Clearwater, and the head of Bean Creek. Scattered moraines and expanses of till and outwash also reveal Pleistocene glaciation.

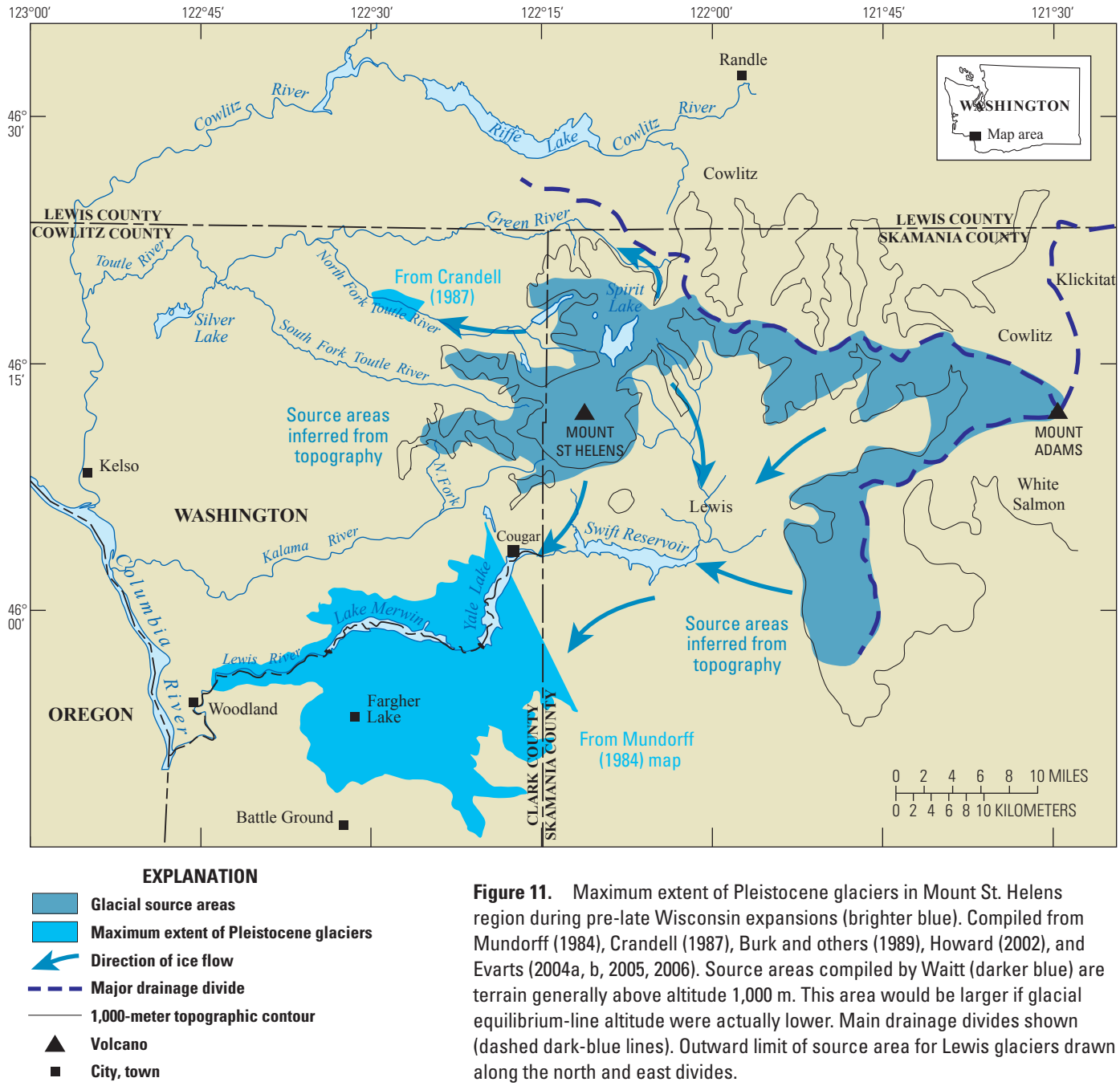

EXPLANATION

- Glacial source areas
- Maximum extent of Pleistocene glaciers
- Direction of ice flow
- Major drainage divide
- 1,000-meter topographic contour
- Volcano
- City, town

Figure 11. Maximum extent of Pleistocene glaciers in Mount St. Helens region during pre-late Wisconsin expansions (brighter blue). Compiled from Mundorff (1984), Crandell (1987), Burk and others (1989), Howard (2002), and Evarts (2004a, b, 2005, 2006). Source areas compiled by Waitt (darker blue) are terrain generally above altitude 1,000 m. This area would be larger if glacial equilibrium-line altitude were actually lower. Main drainage divides shown (dashed dark-blue lines). Outward limit of source area for Lewis glaciers drawn along the north and east divides.

In North Fork Toutle valley, Crandell (1987) correlates nested moraines of weathered till near Hoffstadt Bluffs (fig. 5) with Hayden Creek drift near Mount Rainier (Crandell and Miller, 1974), now thought to have accumulated partly ~140–150 ka during marine isotope stage 6 (Dethier, 1988). Much sharper moraines of scarcely weathered drift—last-glacial Evans Creek age (25–18 ka during marine isotope stage 2)—lie along north Coldwater valley and Harmony Falls basin in the north, Swift Creek in the south, and at other spots.

A small highland 10–24 km west and southwest of Mount St. Helens is carved into many cirques that lead into open tributary valleys whose glaciers fed into large troughs like the upper South Fork Toutle, Kalama, and North Fork Kalama. Evarts and Ashley (1992) mapped drift here they correlate by weathering traits with Evans Creek, Hayden Creek, and pre-Hayden Creek drifts.

In Lewis valley a vast extent of Pleistocene ice reaching far south and west of Mount St. Helens (Mundorf, 1964, 1984) is enigmatic. The south Cascades generally lack cirques or other obvious accumulation areas to support large valley glaciers. Yet weathered till in Lewis valley—the "Amboy drift"—forms moraines that enclose Fargher Lake 45 km southwest of

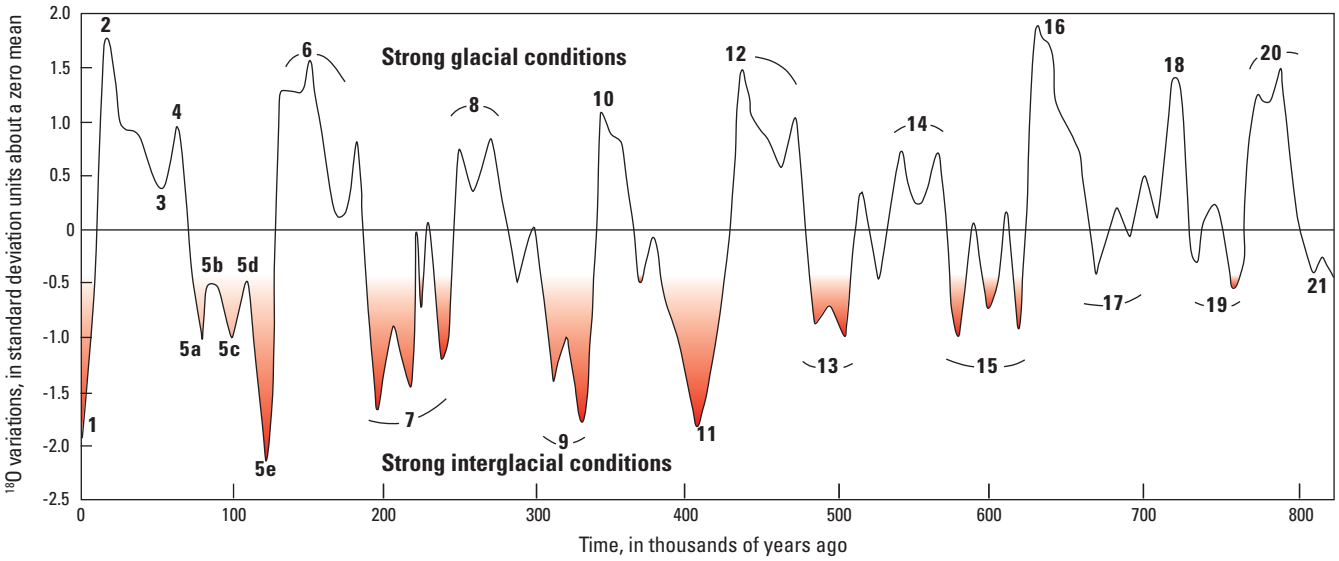

Figure 12. Plot showing marine oxygen-isotope stages for the past 800,000 years (from Pringle, 2008). Graphed variations of the ratio $^{18}O/^{16}O$ in benthic marine foraminifera over time. Even-numbered stage peaks (top) are glacial maxima, odd-numbered troughs (bottom) interglacial minima.

Mount St. Helens (fig. 11). Crandell (1987) correlates this with the Hayden Creek drift. More weathered older drift reaches 5 km farther south and west (Crandell, 1987; Howard, 2002; Evarts, 2004a, 2004b, 2005, 2006). The Hayden Creek drift is overlain by tephra set C (50–36 ka) (Crandell, 1987) and by a basalt flow from Battle Ground Lake area $^{40}Ar/^{39}Ar$ dated to 108±16 ka (Fleck and others, 2014). This pre-last-glacial drift is likely from marine isotope stage 6 (~160–140 ka) or stage 8 (~270–250 ka) (fig. 12) (Lisiecki and Raymo, 2005).

The Lewis valley glaciers seem to have issued from high areas between Mount St. Helens and Mount Adams, especially a broad upland >800 km^2 lying 25–50 km southeast of Mount St. Helens that includes Indian Heaven area (fig. 11). Glassy ice-contact margins of some Pleistocene lava flows there show they indeed erupted among glacier ice (Hammond, 1987). The "dark divide" 15–35 km east of Mount St. Helens must have fed a Lewis valley glacier (but also fed north into Cispus valley glacier). High Mount Adams and ancestral Mount St. Helens too contributed ice to the Lewis glaciers.

Crandell (1987) inferred Mount St. Helens to be younger than 50 ka partly because he found no Mount St. Helens rocks among the gravel stones of Hayden Creek and older drift. But later work found quartz-biotite dacite stones from Mount St. Helens in glacial gravel interbedded with the oldest drift in Lewis valley alluvial and debris-flow deposits. These dacite stones date to around 260 ka (fig. 7) (Clynne and others, 2008; R.C. Evarts, oral commun., 2016). So the oldest drift probably dates to marine isotope stage 8.

These ages and distribution roughly accord with Dethier's (1988) analysis of drift sheets reaching far down Cowlitz valley from uplands near Mount Rainier. This area too was far more widely glaciated during Hayden Creek and an older glaciation than during the last-glacial Evans Creek (Pringle, 2008).

Historical Mount St. Helens

We now return to Mount St. Helens. After a 75-year pause since the Kalama Period ended, the Goat Rocks Period began in early 1800 C.E. with eruption of the dacitic T tephra (fig. 7). Northeast of the volcano it damaged Douglas firs enough as to abruptly cut their annual growth to a small fraction of what it had been (fig 13). This may owe to the roots having been covered in 50–80 cm of fall pumice (Mullineaux, 1996, fig. 71). Ring growth recovered to pre-eruption rates only gradually across a few decades. The andesitic Floating Island lava flow erupted on the north flank later in year 1800 (Yamaguchi, 1983; Yamaguchi and others, 1990). From ~1830 to 1857 Goat Rocks dome grew at midlevel on the north flank. Many travelers and early residents witnessed eruptions or ashfalls, especially in 1842–47 (fig. 14). Small hot collapses of the growing dome built a large, coarse fan downslope. Lahars descended some flanks as late as 1885 (Yamaguchi and Hoblitt, 1995).

1980 Eruption

After another 123-year pause, small earthquakes began beneath Mount St. Helens between 16 and 20 March 1980. They increased in size and frequency on 25 March and average energy remained high on 27 March when a small phreatic eruption burst from the summit. From then till mid-May the number of earthquakes per day decreased but mean magnitude increased. Many phreatic eruptions took place 28 to 30 March. Their frequency and duration then decreased till ceasing 22 April. Another interval of strong to weak phreatic explosions came 7 to 15 May.

Meanwhile the upper north flank fractured and swelled outward an average 1.5 m per day (Moore and Albee, 1981; Lipman and others, 1981)—a huge bulge growing ever more

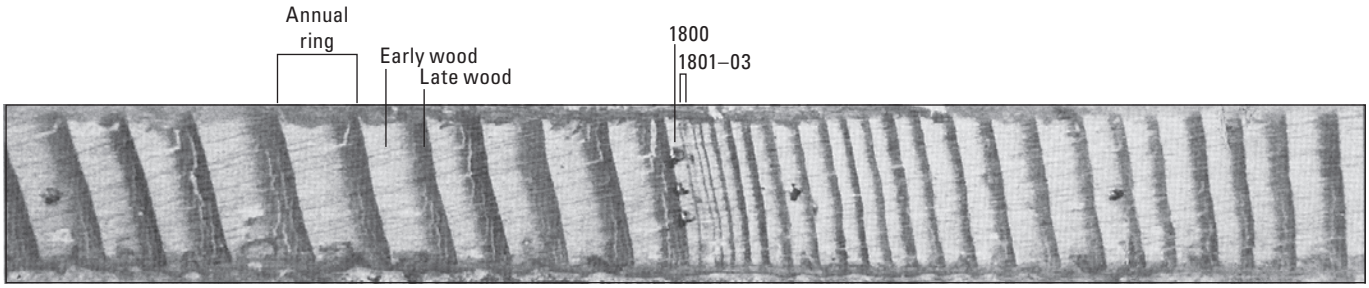

Figure 13. Segment of a sanded and polished core from Douglas fir (*Pseudotsuga menziesii*) northeast of Mount St. Helens showing growth years 1790 to 1825 C.E. (Yamaguchi, 1983). Heavy fall of tephra layer T traumatized the tree (three tiny dots) causing suddenly narrow and even missing (1801–03) annual growth rings. Referencing across many trees allowed dendrochronologist David Yamaguchi to pick various "index" rings precisely. By such cross-correlations Yamaguchi (1983) and Yamaguchi and others (1990) infer that the eruption occurred some time between end of 1799 and beginning of 1800 growth seasons—sometime between September and May. From Pringle (2002, fig. 58).

Figure 14. Paul Kane painting in Royal Ontario Museum showing eruption from Goat Rocks dome at midlevel north flank. The field scene took place 26 March 1847 (see Waitt [2015, p. 15], adapted from Kane [1968]). Kane took much artistic license painting the image. The foreground scene is on Columbia River from the west-southwest, where Mount St. Helens's midflank and north sides are hidden. The Goat Rocks details are as if viewed from north of Toledo—from northwest of the volcano. © Royal Ontario Museum, published with permission of the Royal Ontario Museum.

obvious. An intruding dacite cryptodome apparently caused the earthquakes, bulging, surface fracturing, and phreatic eruptions.

At 8:32 a.m. PDT 18 May 1980, a magnitude-5.2 earthquake accompanied the start of a gigantic landslide from the bulged north flank. One enormous slideblock, then immediately another, together removed 1 km^3 of rock that had contained the cryptodome.

Suddenly depressured, the intruded magma and surrounding hydrothermal system exploded up and north (Voight, 1981). From these explosions a hot gas-rock mixture swept north, accelerating down the volcano to more than 600 km/hr. The swelling ashcloud and current soon enshrouded not only the volcano's north flank but most of the mountain. The hot density current poured north, east, and west across the mountainous landscape.

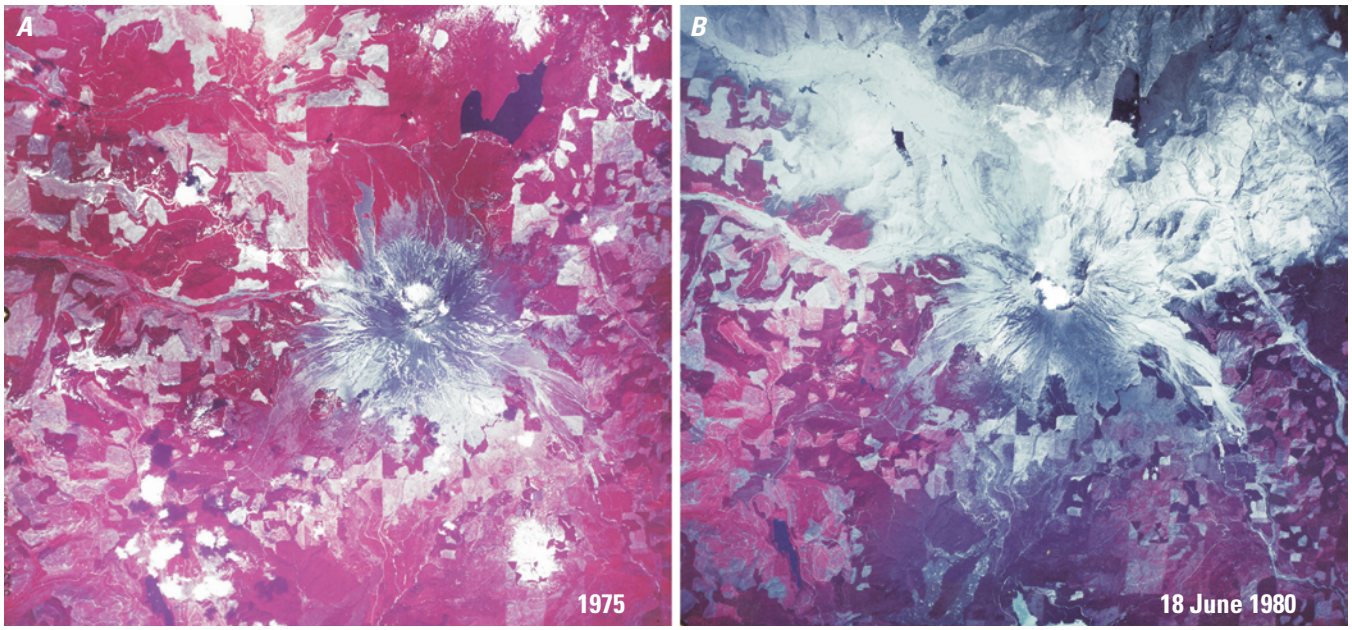

Figure 15. High-altitude infrared vertical aerial photographs of Mount St. Helens area in 1975 and June 1980, Spirit Lake in upper right. Living forest shows as red. In posteruption image former forests are gone—trees laid down, thus canopy gone, the area covered in ash. Photo from USGS EROS Data Center ~1987.

A second magnitude-5 earthquake came two minutes after the first (Endo and others, 1981; Kanamori and others, 1984). A witness on the south saw a series of three tan-cloud explosions burst east to west across the 2,600-m level altitude (Waitt, 2015, p. 236). Photographs from the south and west show an odd ring of white clouds bursting from about the 2,600-m level—seemingly water vapor jetting up the plane of a third huge slideblock that took the summit. A second series of explosions formed into another surge that swept out to overtake the first (Hoblitt, 2000).

The combined surge sped across mountains and valleys. Witnesses watched a sharp-fronted cloud 300–500 m thick hugging the landscape spread out west, north, and east. By 6 minutes after the first earthquake, the surges had flowed 16 to 28 km north, east, and west, leveling forests across 600 km^2 of high-relief terrain (fig. 15).

The hot current gradually slowed as it flowed out. Dropping its freight of gravel and much of its sand, it grew buoyant. It lifted off and rose to the stratosphere in 6 minutes. More of the surge-carried sand fell from the outside of the rising column—even beyond the surge margin. In the stratosphere the top of the column spread laterally, and by 9:00 a mushroom-shaped cloud, now up 30 km, had spread far out (fig. 16) (Sparks and others, 1986). From it fine sand and silt fell for more than an hour. Winds pushed the high cloud east-northeast. It swept across Washington, Idaho, and beyond (fig. 17), turning day to night.

Hidden beneath the surge cloud, the three giant slideblocks—together at 2.8 km^3 Earth's largest terrestrial landslide in historical time—merged into an enormous debris avalanche that flowed down the North Fork Toutle (Voight and others, 1981; Glicken, 1996). Its east edge sped into Spirit Lake, thrusting giant water waves as high as 265 m above lake level (Waitt and others, 2014). It dammed a new lake 63 m above its old level. Seismic records show the avalanche flowed 28 km down the upper North Fork in 10–12 minutes. Its hummocky deposit is as thick as 200 m, average ~50 m, its local relief up to 100 m (Glicken, 1996).

Photo by Marshall Huntting

Figure 16. Mushroom cloud of 1980 eruption early in its development, as viewed from the northwest at Silver Creek in Cowlitz valley. Mount St. Helens is covered by right edge of cloud. Beginning 5 minutes or so after the eruption's start, the cloud rose from the hot-surge area—not from central vent that later issued the sustained plinian plume.

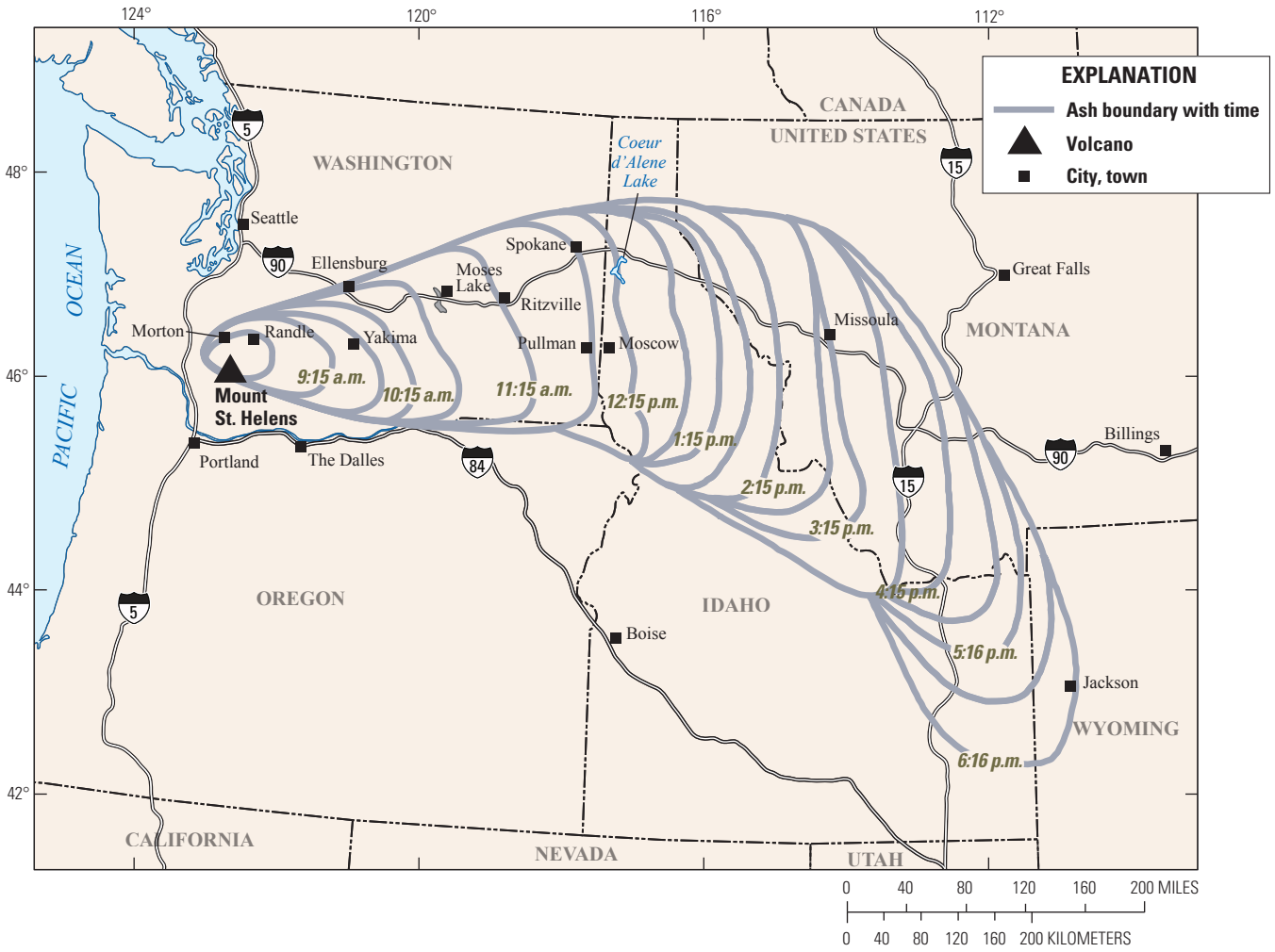

Figure 17. Map showing dispersal of ashcloud of 18 May 1980, its advancing front timed (Pacific Daylight Time) from National Oceanographic and Atmospheric Administration satellite photographs. The first photograph (8:45 a.m.) shows the huge head of the mushroom cloud offset north from Mount St. Helens and already drifting east-northeast. Modified from Sarna-Wojcicki and others (1981, fig. 322).

The hot surge churning down the volcano swiftly melted snow and firn. Before-and-after measurements show the surge stripped about 6 m off Shoestring Glacier (Brugman and Post, 1981; Brugman and Meier, 1981). Slushy, muddy floods poured east and west into valley heads. Huge lahars raced down South Fork Toutle (fig. 18), Smith Creek, Muddy River, and Pine Creek (Janda and others, 1981; Pierson, 1985; Fairchild, 1987; Scott, 1988a; Brantley and Waitt, 1988; Waitt, 1989).

But the biggest lahar issued not directly from the mountain but from the debris avalanche in the North Fork Toutle. The water was mostly the volcano's heated groundwater that the landslides had carried off. This water gushed from the avalanche for hours. Entraining much sediment, it formed a dense lahar as deep as 17 m in valley narrows and 9 m in broad reaches. It peaked 5–15 hours after eruption's start. Dense with sand and gravel, the lahar devoured trees, houses, many bridges and roads, logging camps and heavy equipment. It ran 120 km downvalley and into the Columbia River. Its immense load of sediment filled Cowlitz and Columbia valleys by several meters.

Just after the landslides and explosions, a feeble ash plume angled up from the crater (Criswell, 1987). The plume increased—by 9:00 to a weak vertical column and by 9:25 to a strong Plinian one. This black column jetted fiercely nearly 3 hours. About 12:15 p.m. the column grew much wider, paler gray, and far more turbulent. A pumiceous ashflow raced down the north flank across the debris avalanche.

The turbulent, pale ashy column and intermittent ashflows continued all afternoon, though the column weakened. The ashflows ceased about 4:30 p.m. But the vertical eruption again increased (Criswell, 1987) and peaked about 5:15. It declined rapidly and by 6:15 was down to a weak plume. A weak ashy plume drifted east-northeast all night and next day. Figure 19 summarizes these 18 May 1980 events.

Figure 18. Aerial oblique photograph of the first 18 May flood (via South Fork Toutle River) in the lower Toutle River valley passing beneath Pacific Highway bridge and approaching I-5 bridge. Stopped I-5 traffic in upper left corner. Photograph by Chuck Rosenfeld, Oregon National Guard, published by permission.

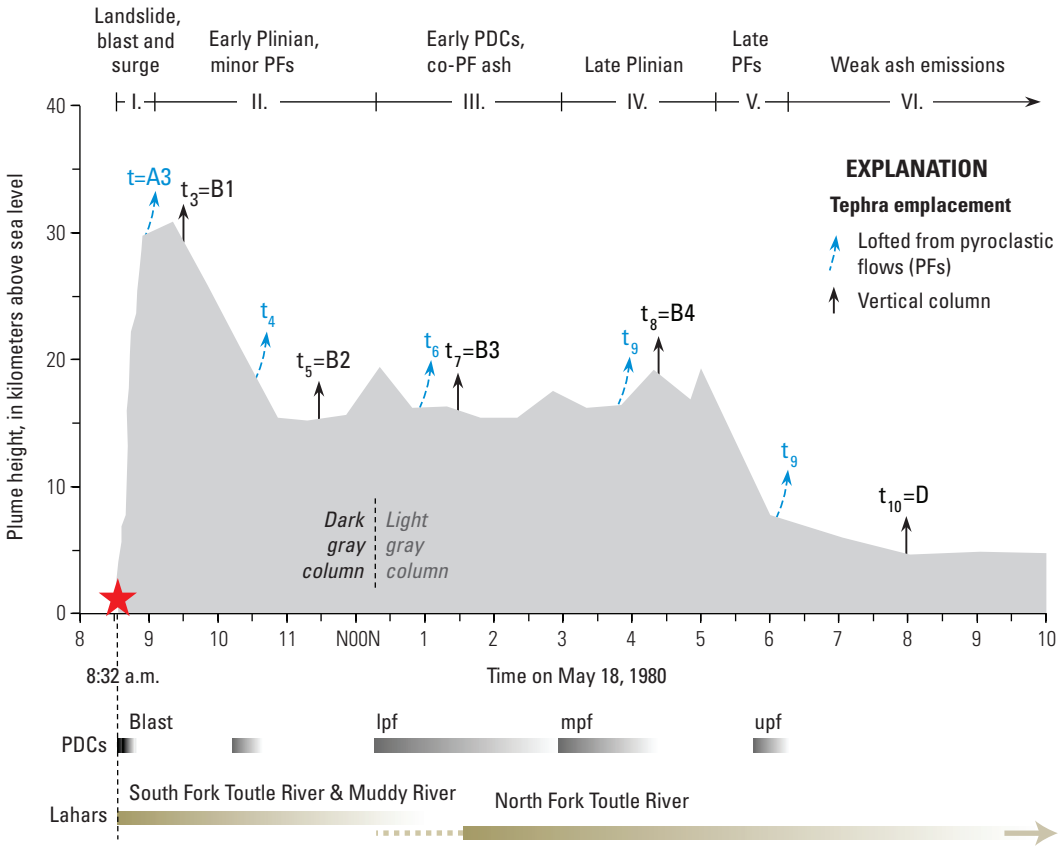

Figure 19. Chronology of events during the climactic eruption 18 May 1980. Maximum plume heights derived from Geostationary Orbiting Environmental Satellite (GOES) (Sparks and others, 1986; Holasek and Self, 1995) and radar (Harris and others, 1981). At top of the graph are the six eruptive phases of Criswell (1987), indicating dominant eruptive processes. Arrows show the origin of each tephra unit—terminology of Criswell ("t" designation) and of Waitt and Dzurisin (1981) (A,B,C,D designations). Lower graphs show the approximate timing of pyroclastic currents and lahars. The pyroclastic density currents (PDCs) represent lower (lpf), middle (mpf), and upper (upf) pyroclastic-flow deposits of Criswell (1987).

May 1980 to October 1986

Smaller explosive eruptions sent up strong plumes on 25 May, 12 June, 22 July, 7 August, and 16-18 October 1980. Each time ash fell downwind and pumiceous ashflows descended the north flank. After the 12 June explosions a dome grew in the vent, but eruptions on 22 July partly blew it out. A new dome grew after 7 August explosions but then blew out 16 October. A third dome emerged 18 October.

Over the next 6 years 17 dome eruptions each added 1 to 6 million m^3 of stiff dacite lava to the crater floor (fig. 20). By late 1986 the dome stood 1,000 m wide and 270 m high—in volume 85 m^3 (Swanson and Holcomb, 1989). Explosions just before some of the 1982–85 extrusions melted snow in the crater and sent sizable lahars down the north flank.

Crater Glacier

Before 1980 Mount St. Helens's cone stood 2,950 m high and held 13 glaciers that covered 5 km^2. The 18 May 1980 eruption took 70 percent of ice volume—all of Loowit and Leschi Glaciers, most of Wishbone, Forsyth, and Nelson Glaciers, much of Shoestring and Ape Glaciers, and the heads of others (Brugman and Post, 1981).

The 1980 landslides left a north-breached crater, its steep rim overlooking the floor 670 m lower. Snow began accumulating in this shaded niche in winters 1981 and 1982. A March 1982 explosion and pumice eruption melted most crater-floor snowpack, but thick snowfans remained around the sides. Each winter snowfall, blowover from the outer flanks, and avalanches off the walls accumulated thicker and thicker in the crater—a third of it rock debris.

By 1994 the persistent snow had compressed into a tiny glacier, and in 1996 a crevasse field revealed a glacier of at least 25 acres (0.1 km^2). The glacier gradually swelled into twin ice arms that wrapped east and west around the dome (Schilling and others, 2004). By September 2001 it had grown to 1 km^2 and 200 m thick and contained 120 million m^3. In 2006 it was formally named Crater Glacier.

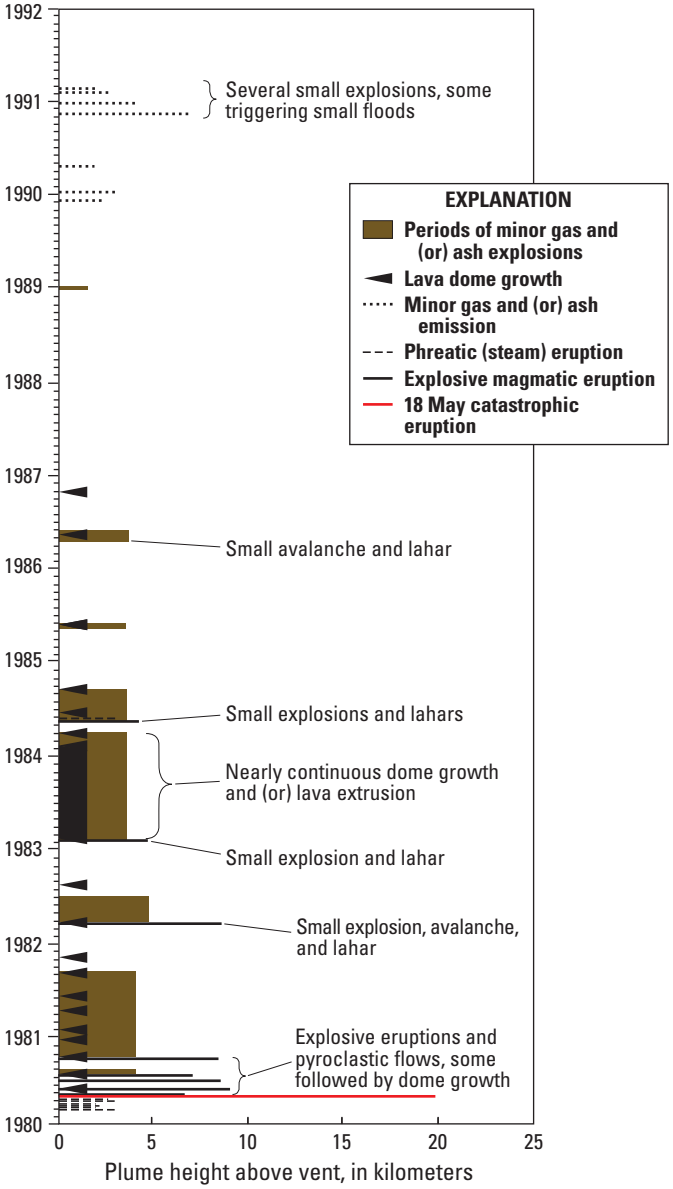

Figure 20. Diagrammatic summary of Mount St. Helens eruptive activity 1980–1991. From Pringle (2002, fig. 5).

Dome Eruptions 2004–2008 and Crater Glacier

A new swarm of earthquakes rattled the volcano in September 2004. Crater Glacier domed and fractured. In October phreatic eruptions burst from south of the 1980s dome, and ash dusted areas 100 km downwind. Dacite lava poked through the glacier and like a great mole pushed 550 m south to the crater wall. In early November 2004 a second extrusion looking like a breaching whale pushed south till it crumbled. A third, more spinelike, emerged later in November, but then crumbled. By early December the new lava in the crater totaled 30 million cubic meters.

In January 2005 a fourth lava spine extruded, then fragmented and collapsed. In June a fifth emerged. The swelling composite dome split Crater Glacier and squeezed its east side against the crater wall. By August 2005 the rubbled dome had grown to 800 m in diameter and 420 m high and held 75 million m^3. Dome growth shifted west in late 2005 and early 2006, shoving Crater Glacier westward. By spring 2006 the crater was a jumble of spent dome lobes (Vallance and others, 2008; Walder and others, 2008). In January 2008 when the eruption had ground to a halt (Dzurisin and others, 2015) the new dome held 95 million m^3. The 1980 south crater floor lay beneath 400 meters of new rock.

Thickened by having been squeezed by the swelling dome, Crater Glacier advanced. Its two arms reached farther north, and then joined north of the 1980s dome. Several years of added snowpack thickened the glacier, and its terminus advanced into the north canyons. By September 2014 it was 2 km long and held about 76 million m^3 (S.P. Schilling, oral commun., 2016). Between 2004 and 2014 the glacier had lost about 44 million m^3—mostly as eruption from the dome vaporized ice into steam.

Crater Glacier is one of only two new glaciers on Earth. The other grew in the caldera of Mount Katmai in Alaska after the 1912 eruption. Both glaciers only replaced larger ones that had mantled much higher cones before they collapsed.

The personal stories of survivors and other participants reveal in exquisite detail all parts of the May 1980 eruption, its prelude, its immediate aftermath (Waitt, 2015). Similar stories about the 1980s dome, Crater Glacier, and the 2000s dome appear in Waitt and others (2016).

Ephemeral Evidence and Surviving Geologic Record

Any large natural event—volcanic eruption, massive river flood, great earthquake, huge tsunami—leaves in its wake evidence by which one may document the extent, speed, and composition of energetic phenomena. But it soon begins to fade. Mud lines wash from trees, stranded wood rots, sand deposits wash from steep slopes. Brush and trees cover the once-bared land, and streams deeply gully once-flat surfaces. Gray deposits oxidize yellow.

One who's watched the landscape and deposits since the May 1980 catastrophes may lament the disappearance of telling evidence. Now more than 37 years after the big event we see landscapes in transition to what will become a longer term geologic record. Today we still see in least overgrown areas many big trees felled in 1980. Decades from now these too will be gone.

A Note on Terminology

A technical term can be imperfect, and over time some concepts change. A new term tries to improve an old—perhaps for a somewhat changed purpose. Some different terms imply only different emphasis. This guide to some extent uses terms preferred by each of the several authors. Yet we cannot just alternate different terms through a section of text. Editing has tried to finesse these differences. The nearby sidebar summarizes some terms and usages.

This guide uses standard grain-size terms for sedimentology in all geologic settings as by Folk (1980). Terms like "gravel" and "sand" and specific versions like "medium sand" define grain size *only*. They imply nothing about genesis or emplacement process. Size terms may be expressed in metric dimensions or in the phi (φ) scale. Elsewhere this guide uses volcanic-specific terms like "lapilli" and "ash" that derive from volcano literature.

Day 1. Prehistoric Tephra Falls and 18 May 1980 Pyroclastic Surge

Along a transect northeast of Mount St. Helens (fig. 21) we contemplate many prehistoric tephra falls, the vanished Spirit Lake communities of the 1920s–1970s. We see the 18 May 1980 eruption through eyewitness stories, deposits of the pyroclastic surge in proximal to distal areas, the downed coniferous forests, the landslides, landslide-induced huge waves at Spirit Lake, and pumiceous pyroclastic flows.

From U.S. Highway 12 at Randle, drive forest road 25 south about 20 miles to forest road 99 toward the Mount St. Helens National Volcanic Monument boundary. Drive road 99 southwest about 4.6 miles to Stop 1.1.

Stop 1.1. Bear Meadow Viewpoint [restrooms] (46.3136° N, 122.0366° W)

May 18th 1980 began clear—only thin high clouds. From this former logging platform Gary Rosenquist and Keith Ronnholm shot iconic photographs of the eruption's start—landslides, eruption cloud, surge front (fig. 22).

Five brief excerpts from eyewitness chronicles (Waitt, 2015) reveal behavior of the surge. From this spot a minute into the eruption:

> Gary Rosenquist: The cloud came over the first ridge, the pace really picking up. The cloud hit a ridge and went up. It continued toward us.

> Joel Harvey: It hit a ridge and went up in the air, but continued out. It hit another ridge and went up. It hit a third ridge and went up. It was like bombs going off—wide divisions between verticals in the cloud top. It came out fast, running low except when going over ridges.

From a ridge north of Green River 17 km northwest of here:

> Don LaPlaunt: The spreading cloud hugged the ground like a D-8 Cat [a large bulldozer]. It came over a hill, then down, following the land tight. The cloud came over a nearer crest and rolled downslope. It came up the next ridgetop then down like a wave, engulfing trees. We looked over the top of this to the cloud piled over the mountain.

And from climbers on Mount Rainier 65 km north-northeast of here:

> John Downing: A distinct flow ran out northwest, and a bit later one east. They were 1,000 to 1,500 feet [300–450 m] thick and hugged the ground. The head of a flow disappeared into a valley, hopped into view over a ridge, and disappeared again into a valley.

> Mike Williamson: Its leading edge flowed like water. It hit a ridge, poured up over, then dropped into the valley. It flowed over the next ridge, and down into the next valley, following the shape of the land. We were 50 miles away, those ridges miles apart, so the clouds really sped.

By these accounts and from deposits (Waitt, 1981) we see that beyond a few kilometers from the summit the great

Sidebar 3. Terminology

Terms used in this field guide to describe the eruptive events and processes at Mount St. Helens on 18 May 1980 include:

Tephra. As first defined, a term for volcanic particles of any size, shape, or composition ejected from volcanoes and fallen through air. Though later expanded to include particles transported by ground-hugging flows or lahars, we use it here to refer to material that fell through air.

Juvenile clast. Pyroclastic rocks derived directly from fresh magma reaching the surface, rather than from pre-existing material (see below). They are typically identified as clean vescicular glass.

Accidental clast. Pre-existing rock fragments disrupted by an eruption and incorporated into the deposit. They include rocks ripped from the vent wall and those entrained from the surface by a flow.

Pyroclastic density current (PDC). Ground-hugging mixture of particles and gas denser than the surrounding atmosphere and moving under the influence of gravity. Individual currents typically exhibit a diversity of flow regimes from dense granular flows (pyroclastic flow) to dilute, turbulent suspensions (pyroclastic surge). Where possible this field guide makes the distinction between "surge" or "flow."

Blast (sensu stricto). Synonymous with explosion, and so by definition its effects at Mount St. Helens are limited to direct effects of explosion. (Used in this sense by senior author.)

Lateral blast (sensu lato). Refers to a high-energy, directed pyroclastic density current. (Used in this sense by many researchers.) At Mount St. Helens others use "blast pyroclastic density current," or blast PDC.

Pyroclastic flow. A dense flowing mixture of pyroclastic materials and gas, usually hot. Typically hugs the topography and remains confined to lower terrain.

Pyroclastic surge. A mobile, low-density, dilute, current. Typically ground-hugging but less controlled by topography than flows and can overtop ridges.

Flowage. A term to encompass all kinds of fragmental flows regardless of origin, including lahars (mudflows and debris flow) and pyroclastic flows and surges.

Debris avalanche. Starting as large landslide—collapse of part of a volcanic edifice—an unsaturated flowing mixture of volcanic particles, water (± ice), and entrained vegetation.

Lahar. Water-saturated flow of volcanic-rock particles and water (± ice) that may entrain woody debris. A lahar having >50 percent solids by volume is termed a "debris flow"; one having roughly 10–50 percent solids by volume is termed a "hyperconcentrated flow." Flow types bear distinguishing textural earmarks, but such flows can evolve with distance along their paths. Depending on initiation mechanism, lahars can contain hot juvenile clasts.

Accretionary lapilli. Spherical aggregates of volcanic ash, commonly having a concentric structure and formed by clumping of moist particles. Sometimes used as a general term for all ash aggregates including structureless ash lumps or pellets.

• • •

Grain-size terms vary with one's scientific training. Some researchers use sedimentological terms of the Wentworth grain-size classification for all sediments including volcanic fragmental deposits (Folk 1980). Others use terms specific to volcaniclastic deposits (White and Houghton, 2006). Grain size terms used in volcanology and sedimentology:

Diameter (metric)	Diameter (phi)[#]	Volcanology term	Sedimentology term
>64 mm	< -6	Blocks, bombs*	Cobbles, boulders
2–64 mm	-6 to -1	Lapilli	Granules, pebbles
<2 mm	> -1	Ash	Sand, silt, clay
<62.5 µm	> 4	Extremely fine ash	Silt, clay

[#] Phi (φ) = $-\log_2 D$, where D is the diameter of the particle in mm.

*Bombs have fluidal morphology

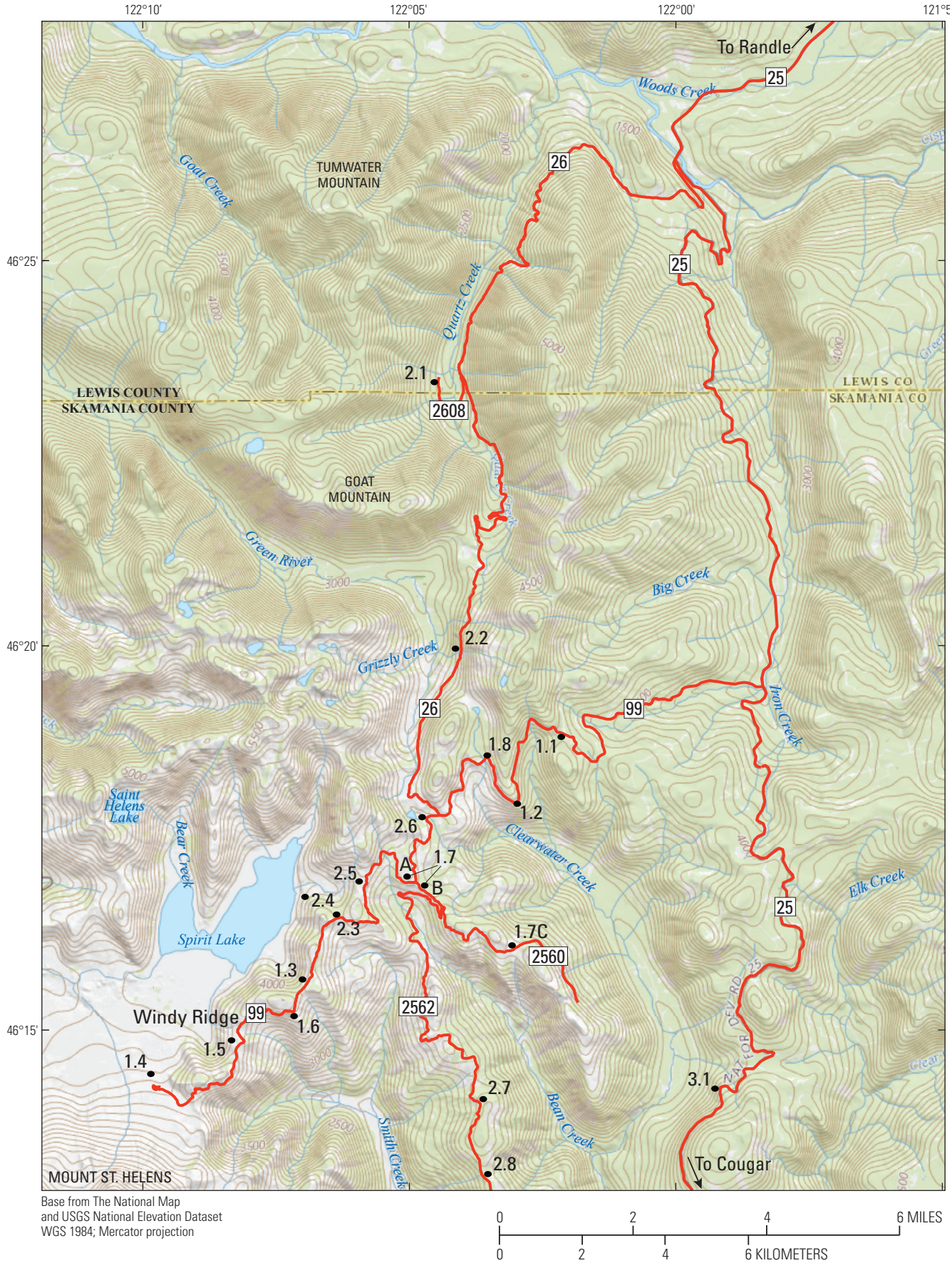

Figure 21. Map showing roads and stops for Days 1 and 2.

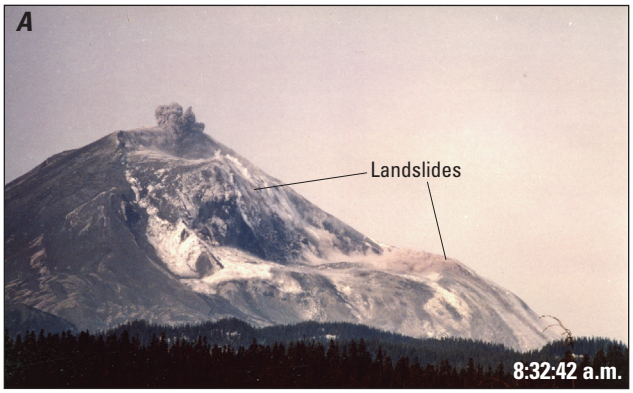

Photos by Gary Rosenquist

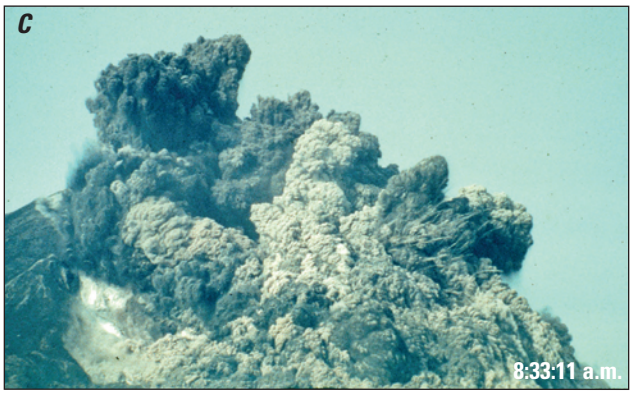

Photos by Keith Ronnholm

Figure 22. Photographs from "Bear Meadow" viewpoint by Gary Rosenquist and by Keith Ronnholm during first 2 minutes of 18 May 1980 eruption of Mount St. Helens. Photographs published by permission.

cloud was no bomb-like explosion spraying the landscape and deserving a term like "blast." Instead it was a hot current that *flowed* out, and it hugged the land.

Drive forest road 99 about 2 miles southeast to Stop 1.2.

Stop 1.2. Surge-Edge Viewpoint: Standing Dead Trees; Tephra Section (46.2990° N, 122.0503° W)

Upper Clearwater valley is gouged out by glaciers that spilled south from the Mount Margaret high country.

Outward from the edge of downed trees lay a zone tens to hundreds of meters wide of trees the 1980 surge had scorched but mostly left standing. The browned needles soon fell off, and over the years so too the bark and most branches. By the mid-2010s even many of the rotting trunks have fallen.

The tall roadcut just north shows several prehistoric coarse pumiceous tephra layers (figs. 7, 23). Overlying east-dipping Oligocene tuff is orangish set J (about 11,000 cal yr B.P.), the bright color perhaps partly from an invisible veneer of Mazama (Crater Lake) silt ash (7,700 cal yr B.P.). Above that is yellowish coarse-pumice Yn (3,300 cal yr B.P.), gray fine-grained set P, and whitish coarse-pumice Wn (1479 cal yr B.P.). Upsection lies coarse-pumice set T (1800 C.E.). Here we are north of the 1980 tephra fall. Most of these beds have been traced tens and even hundreds of kilometers away. Thin darker tephra beds B and X show only in sections close to the mountain.

Drive forest road 99 about 4 miles southwest through downed timber toward the mountain.

Stop 1.3. Donnybrook Viewpoint of Spirit Lake (46.2604° N, 122.1146° W)

Spirit Lake much more than Mount St. Helens had drawn visitors to this area from the 1920s through 1970s (fig. 24). Historical Spirit Lake was smaller in area than present Spirit Lake, and it lay 74 m lower.

By geomorphology, stratigraphy, and lake bathymetry the sequence of catastrophes at Spirit Lake in morning 18 May 1980 is (fig. 25):

1. Front of pyroclastic surge sweeps northeast across lake basin at roughly 400 km/hr, leveling mature coniferous forest and depositing gravel layer A1 (stratigraphic details discussed at stop 1.5).
2. Toe of landslide enters lake at about 250 km/hr and plows northward along both arms.
3. The suddenly displaced lake water runs as huge waves up both arms of lake. From the west arm (Bear Cove) a wave crashes across Eagle Point spur into the east arm.
4. Flowing landslide fills both arms of the basin an average 86 m.
5. Having sloshed up both arms and side valleys as high as 265 m, the water now rushes back. It constitutes a new lake

63 m above old lake level (fig. 26). The new lake averages shallower than the old lake and so is larger in area.

6. Arm of big landslide west of Harrys Ridge meanwhile overrides Johnston Ridge. Part of its east edge drops east off Harrys Ridge into the lake.
7. The continuing surge deposits sandy layer A2 and gradually wanes.
8. Layer A3 (silt) falls 30–90 minutes later, partly from lingering low dust but mainly from the mushroom cloud.
9. Pumiceous tephra (unit B, pebble- to sand-sized) falls late morning to late afternoon.
10. Co-ignimbrite ash clouds deposit tan unit C (very fine sand to silt) in afternoon.

New Spirit Lake had no outlet. Over the next few years its level rose to as much as 81 m above old lake level (and 18 m above the new 18 May 1980 level). In 1985 an engineered tunnel stabilized its outlet about 74 m above the old lake. Recent bathymetry by U.S. Forest Service biologist Charlie Crisafulli shows even the deepest parts of the bottom of new Spirit Lake lie above the surface of old Spirit Lake (fig. 27). The landslide off Mount St. Helens filled the old basin to many meters above the old lake surface. The old lake and the new lake occupy none of the same three-dimensional space. Former landmarks around the old lakeshore— Truman's Mount St. Helens Lodge, the big Duck Bay dock, the Boy Scout, Girl Scout, and YMCA camps—lay not only beneath many meters of water but also beneath tens of meters of landslide rubble.

Drive road 99 about 2 miles southwest to Windy Ridge parking area [restrooms].

Pass south through locked gate (permit via Mount St. Helens National Volcanic Monument). Drive narrow gravel road about 2 miles to its end in small parking area on edge of the Pumice Plain. (This restricted rough road is precarious in some years.)

From parking area walk north down gully about one-third kilometer.

Stop 1.4A. Proximal Surge — Here a "Flow" (46.2331°N, 122.1522°W)

The west bank of gully, 2.5 to 5 m high, exposes thick proximal deposit of the lithic "surge." Unlike the apparently rather dilute surgelike character through most of the vast affected area, the deposit here has much more the character of a dense "flow" whose particles pound each other. The characters include massive texture of gravel and sandy gravel, and only feeble internal bedding. All clasts are lithic—about half of them fragments of the preeruption 1980 cryptodome. Most clasts show evidence of abrasion against each other during flow—their shapes angular to subangular rather than the very angular shapes as in the ridgecrest surge deposit. One west-bank exposure shows fines-depleted vertical pipes— evidently from water or snow trapped at the flow's base that then streamed up through the deposit as fumaroles.

Downgully a 4–5 m exposure shows a fining-up top of one flow overlain by the coarse base of another that is poor in fines (fig. 28). Perhaps three such flow pulses. The surface of this composite deposit slopes north 49 m/km, here one-third kilometer from the steep bluffs to the east. So these seem primary flows directly northward from Mount St. Helens, not secondary ones westward off the bluffs.

Figure 23. Photograph of tephra sequence from sets J to T in roadcut at Stop 1.2.

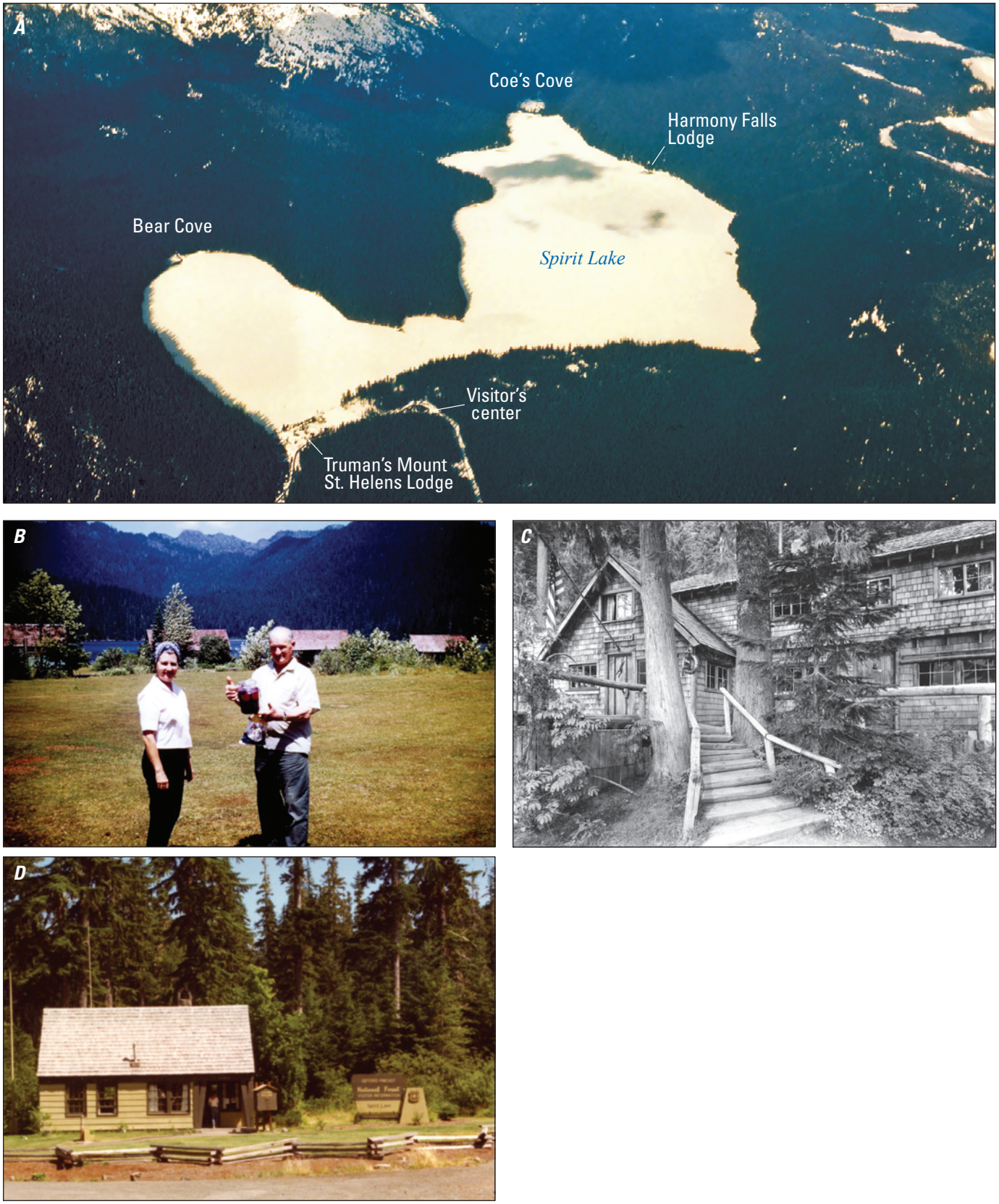

Figure 24. Old Spirit Lake: (*A*) oblique aerial photograph (from 2 April 1980, by R.B. Waitt) shows location of (*B*) Truman's Mount St. Helens Lodge (photograph courtesy Joann and Jack Wolff), (*C*), Harmony Falls Lodge (photograph by Goodwin Harding), and (*D*) U.S. Forest Service visitor's center (photograph from Gifford-Pinchot National Forest).

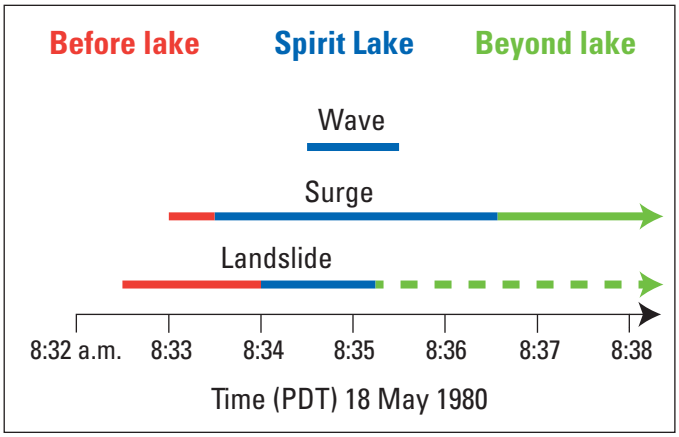

Figure 25. Estimated timing of catastropic events from Mount St. Helens on Spirit Lake in morning 18 May 1980. Colors for a process—for instance surge—approximate its timing from before it reaches lake, while passing over or through the lake, and then running beyond the lake.

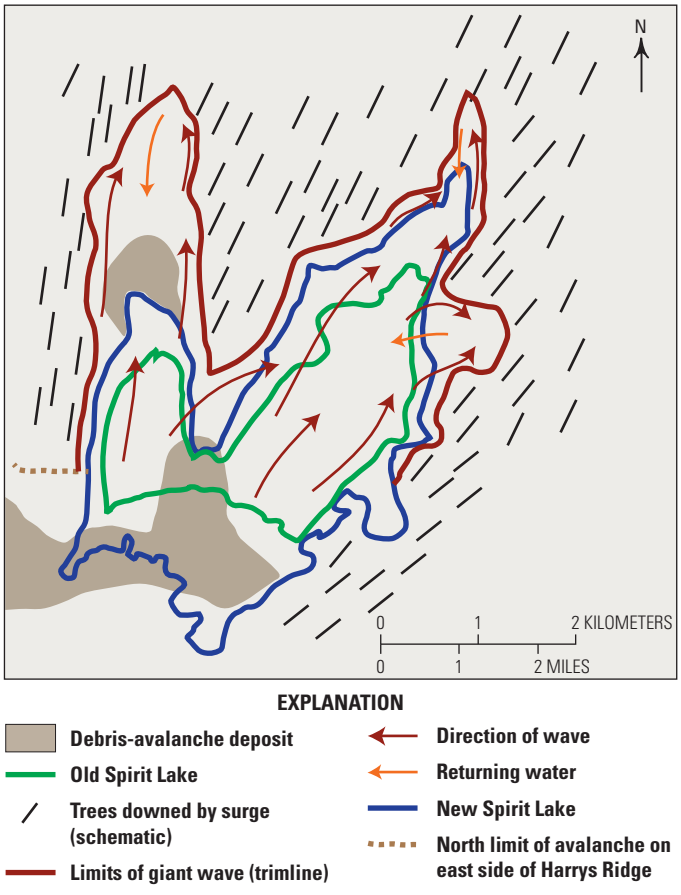

Figure 26. Map of Spirit Lake basin showing distributions of 18 May 1980 debris-avalanche deposits and limits of Spirit Lake water displaced as giant waves.

The top of the lithic coarse bed (layer A1) here is overlain by sandy layer A2, that by silt layer A3, that by 18 May fall deposit (B layers) and that by layer D (fig. 7). The capping scattered pumice pebbles is tephra that fell 22 July 1980.

Exposures like this—layer A1 some 4–5 m thick—didn't exist during seminal 1980–81 field investigations, this area having been an undissected plain. In a few trenches dug in 1980 atop proximal ridgecrests, the surge gravel layer A1 ranged ½ to 1 m thick.

Yet this now-dissected and exposed deposit must be from the same flow that ran across the landscape and leveled the forests and that has mostly the character of a pyroclastic surge. This thick section shows that passing down a low in this most proximal area the process was more a dense pyroclastic flow.

Stop 1.4B. Ancient Tephra Falls (46.2340° N, 122.1527 °W)

East bank of this gully exposes a pre-1980 mound that had accumulated successive tephra falls. Parts of this sequence should look familiar. The dug-out base exposes the top of pumice-gravel set Y (3,300 cal yr B.P.). It is overlain by thick fine-grained set P, and that by dark set B. Conspicuous midway up is the Sugarbowl breccia (layer D, ~1,075 cal yr B.P.). Upsection lies coarse bright pumiceous layer Wn (1479 C.E.), then dark layers X and z, then bright pumice layer T (1800 C.E.). On top lies lithic 1980 surge—but here probably a 'flow' as on the gully's west side (fig. 29).

From parking area drive restricted road about 1.6 miles back northeast. Park by green instrument structure. Hike ridgecrest north about one-third kilometer to a prepared trench on a summit overlooking Windy Ridge area.

Stop 1.5A. Proximal Deposit of Pyroclastic Surge (46.2474° N, 122.1357° W)

The east-dipping bedrock homocline here and in the view north is volcanic and volcaniclastic rocks ~26–24? Ma.

The volcano's north flank displays large effects of the 18 May 1980 eruption: landslides, pyroclastic surge and its leveled forests, pumiceous pyroclastic flows, and ash clouds. Thirty-seven years of erosion and plant growth obscure some former details.

The 18 May deposits on the Pumice Plain are overlain by pumiceous pyroclastic flows from five eruptions between 25 May and 18 October 1980 and by lahar of March 1982 (fig. 30) (Rowley and others, 1981; Waitt and others, 1983; Criswell, 1987). The big hummocks at the head of the west arm of Spirit Lake (Bear Cove) show that the 18 May landslide plowed through the lake and rode up 100 m onto the far shore.

A trench here exposes the 18 May 1980 surge deposit. It contains more than 50 percent juvenile dacite from the spring 1980 cryptodome. This dacite is bimodal: gray and microvesicular low-density fragments, gray-black and nonvesicular

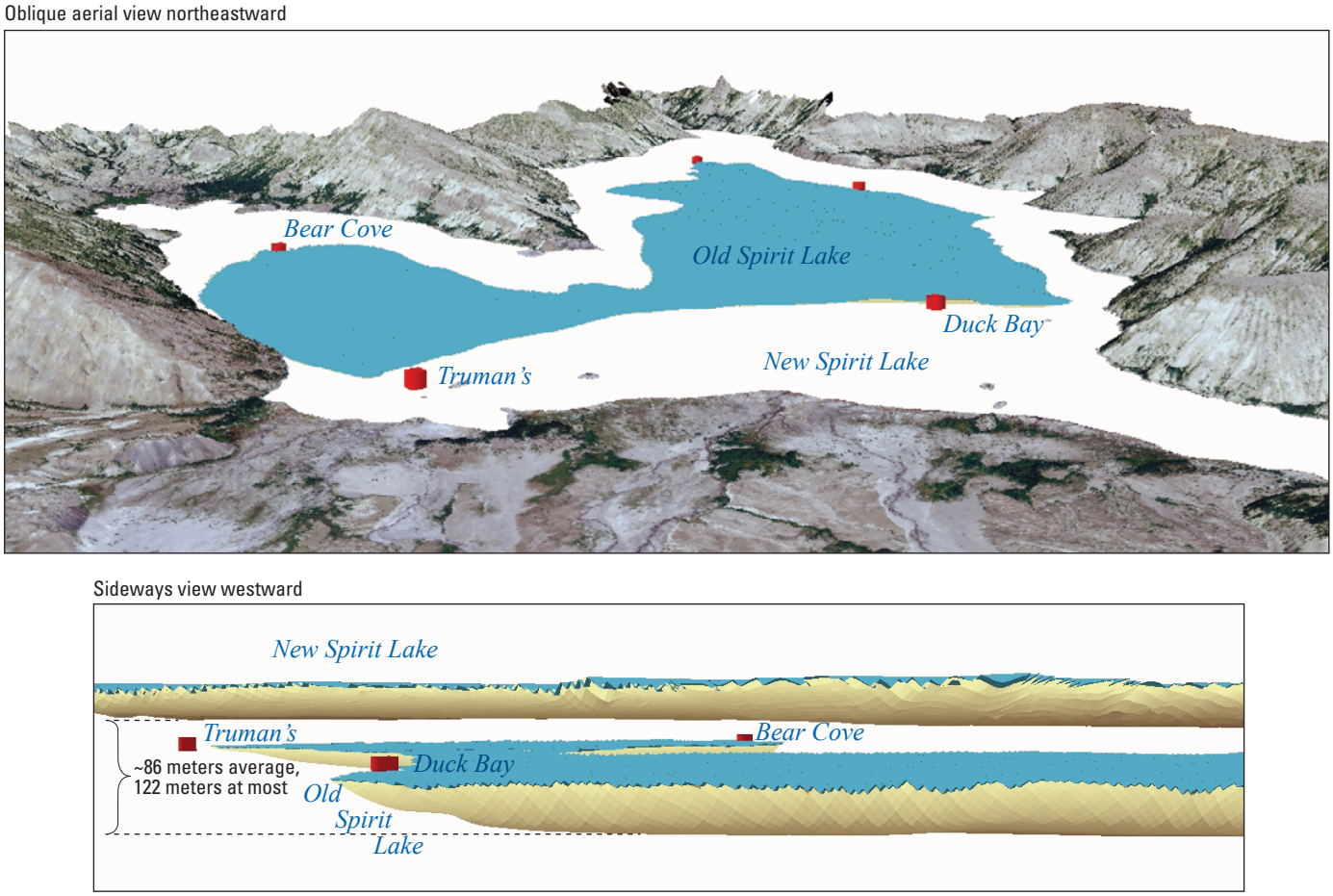

Figure 27. Digital ArcScene images of old and new Spirit Lake. Deepest surveyed spot in *bottom* of new Spirit Lake lies 37 m above *surface* of old Spirit Lake. Brown-yellow depicts lake bottom. Graphic by Adam R. Mosbrucker.

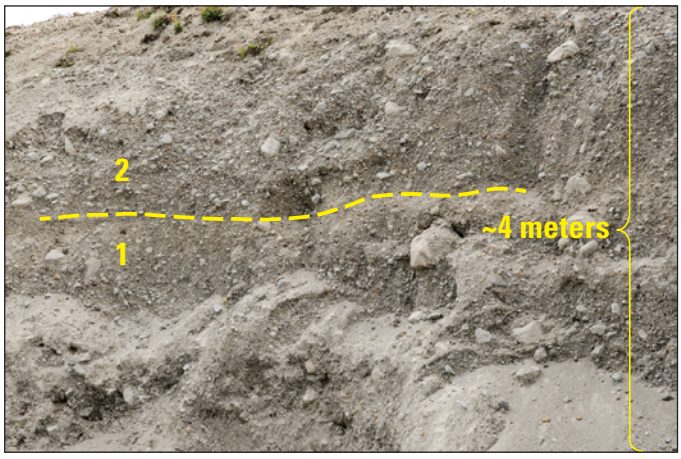

Figure 28. Photograph of thick, massive proximal "surge" deposit—here with characteristics of a "flow." A graded fine-grained bed (dashed lines at its top) suggests the top of one flow ("1"), overlain by a second ("2"). Lower unit is also richer in brownish fines.

high-density ones (Hoblitt, 2000). About a meter thick, the deposit is normally graded from pebble gravel at base to silt at top. In 1980 field terminology this is unit A. Its subdivisions are layer A1 (gravel) 85 cm thick, layer A2 (sand) 14 cm, and layer A3 (silt) 1 cm (fig. 31) (Waitt, 1981).

The lower coarse half of unit A—layer A1—is rich in logs and wood stripped from trees. This organic sublayer, sometimes called Ab, also contains gray dacite and dense lithic clasts as large as 20 cm.

Layer A2 is the fine, graded top of massive layer A1 (the two forming one graded bed). The lower half of A2 is massive granular sand, the upper half laminated sand like classic surge deposits. Layer A3, mainly fall from the mushroom cloud, began accumulating 20 minutes after start of eruption.

Layer A3 is overlain by 18 May fall pumice (unit B) and co-ignimbrite ash (unit C). That is topped by pumice that fell 22 July 1980 (Waitt and others, 1981), now barely visible.

Field investigators in 1980 inferred the devastating flow-age emanated from Mount St. Helens from the initial explosions (Hoblitt and others, 1981; Moore and Sisson, 1981; Waitt, 1981). But interpreting satellite data, Moore and Rice (1984) inferred the main explosion, two minutes after initial explosions, burst out from several kilometers north of the mountain.

Ground data here at Stop 1.5A show instead that the hot tree-felling current emanated from the cone of Mount St. Helens:

1. Mature trees on ridges south and north of us toppled northeastward—away from Mount St. Helens. They lie athwart any hypothetical flow from near Johnston Ridge or Spirit Lake.
2. The south sides of downed logs are much more abraded than north sides. So the sustained, trailing phase of current also came from Mount St. Helens, not from the northwest.
3. The preferred accumulation of surge deposit against the south side of the downed logs also shows the flow was from Mount St. Helens.

Characteristics of the deposits and timber reveal the devastating current was not a high-concentration pyroclastic flow (Walker and McBroome, 1983) but a low-concentration surge (Waitt, 1981, 1984; Moore and Sisson, 1981; Hoblitt and Miller, 1984):

1. Much of the coarse basal half of the deposit is clast supported, poor in fines.
2. Tree trunks lie where they fell. How could a high-concentration flow of lithic clasts not move low-density logs?
3. The surfaces of downed logs above the deposit were far more abraded than the sides and undersides. A high-concentration flow should have abraded the sides more.

Most 1980s and 1990s investigations envisioned a single great surge. Prompted by Moore and Rice's (1984) idea of a second event, Hoblitt (2000) re-analyzed eyewitnesses photographs, satellite imagery, seismic data, and certain stratigraphic data to infer perhaps a second surge that began about 2 minutes after the first and was much larger (fig. 32).

Examining the coarse lower part of the deposit in this pit, one can perhaps see divisions within it that suggest it isn't the deposit of just one event, but maybe two.

Return south about one-third kilometer to a prepared trench by the green instrument structure and antennae.

Stop 1.5B. Two-Layer Base of Proximal Surge Deposit (46.2446° N, 122.1370° W)

A prepared excavation near the instrument container and antennae shows a two-layer stratigraphy near base of unit A, evidence of two depositional pulses. Forest soil developed on pumice tephra (probably T, possibly Wn) underlies 18 May

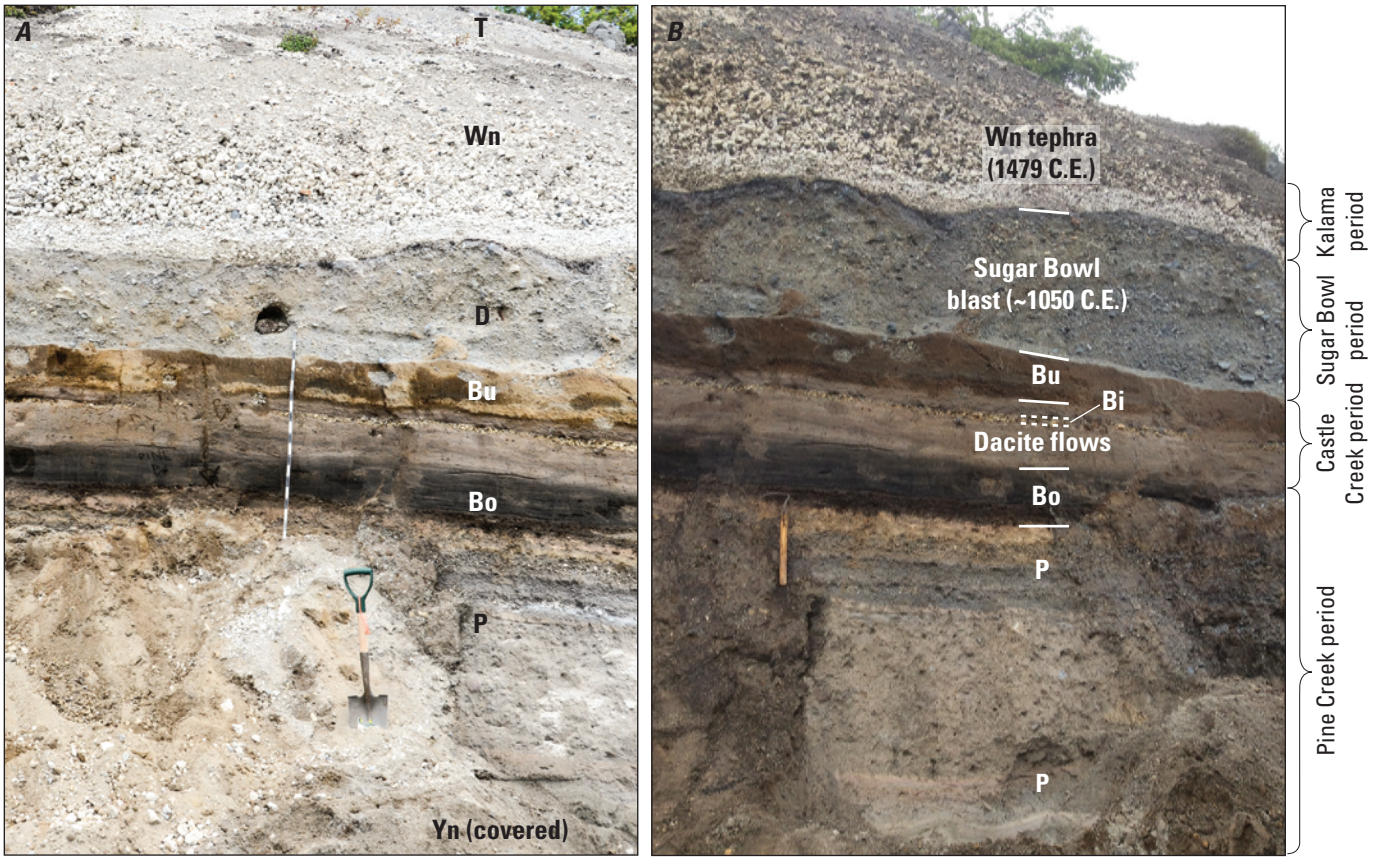

Figure 29. Photographs of tephra sequence at stop 1.4B on northeast flank of Mount St. Helens. *A*, Overall exposure, showing layer T at top. *B*, Detail of section.

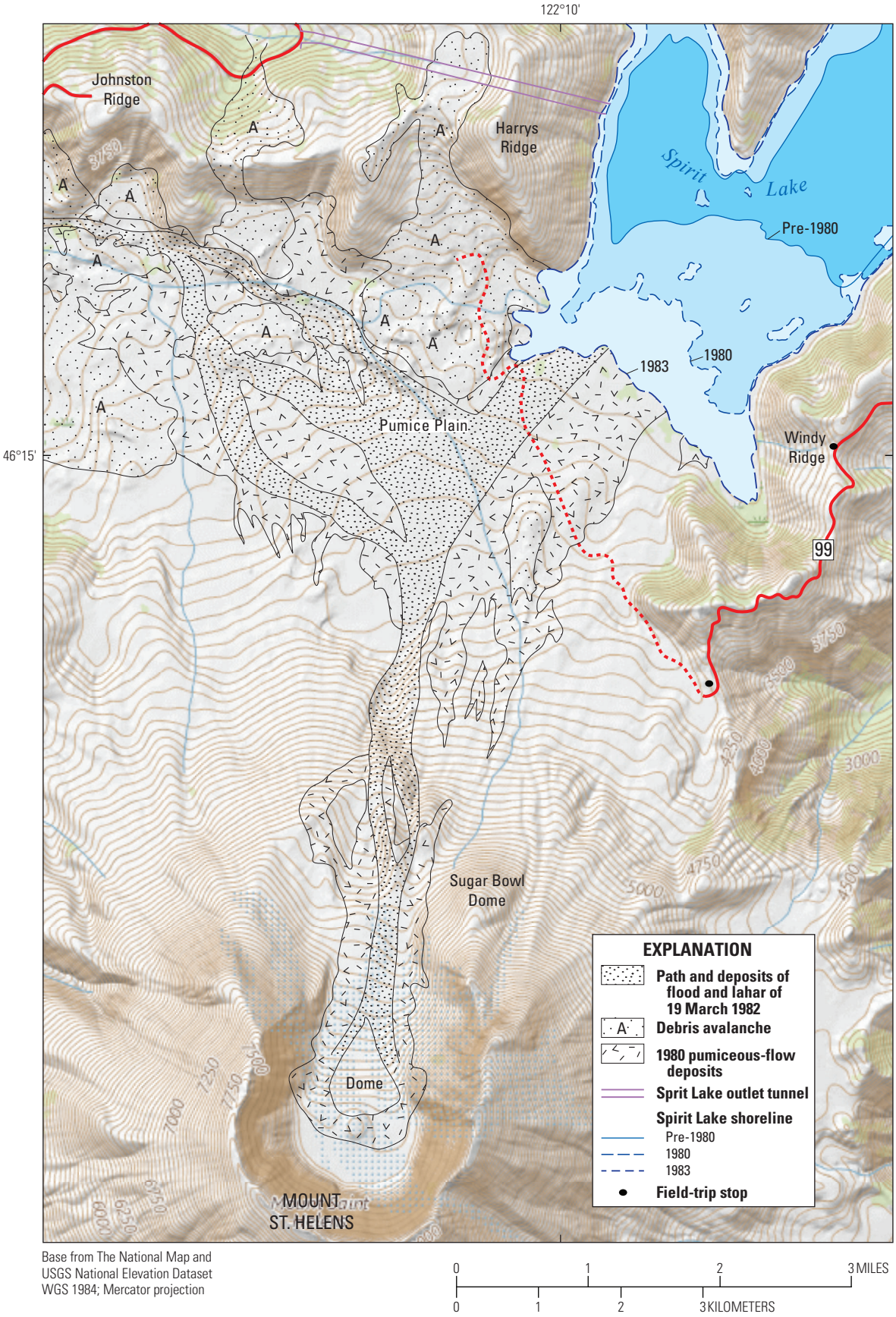

Figure 30. Generalized geologic map of north flank of Mount St. Helens in mid-1980s. A, debris avalanche. Redrawn from Doukas (1990, fig. 26).

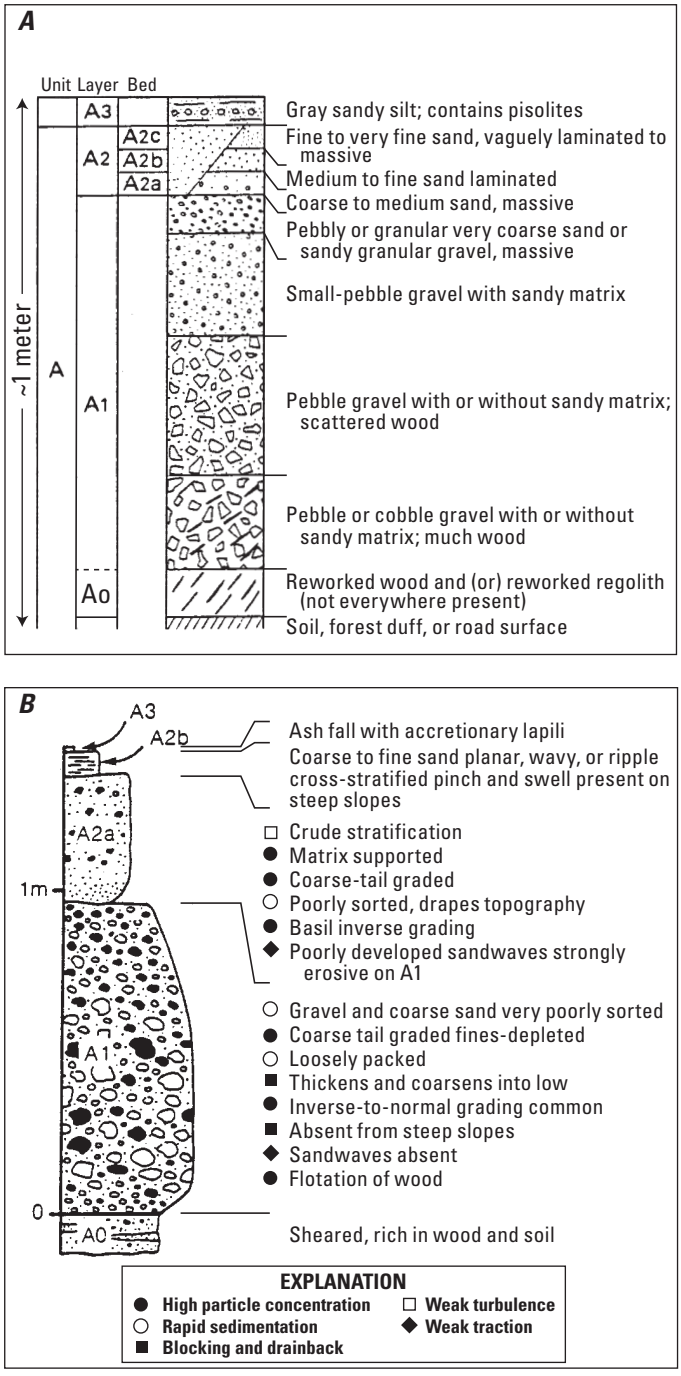

Figure 31. Composite sections depicting deposits of pyroclastic surge of 18 May 1980 from Mount St. Helens. *A*, as portrayed by Waitt (1981, fig. 258) for north and northeast azimuths, and *B*, as portrayed somewhat differently by Druitt (1992, fig. 2) for northeast azimuth.

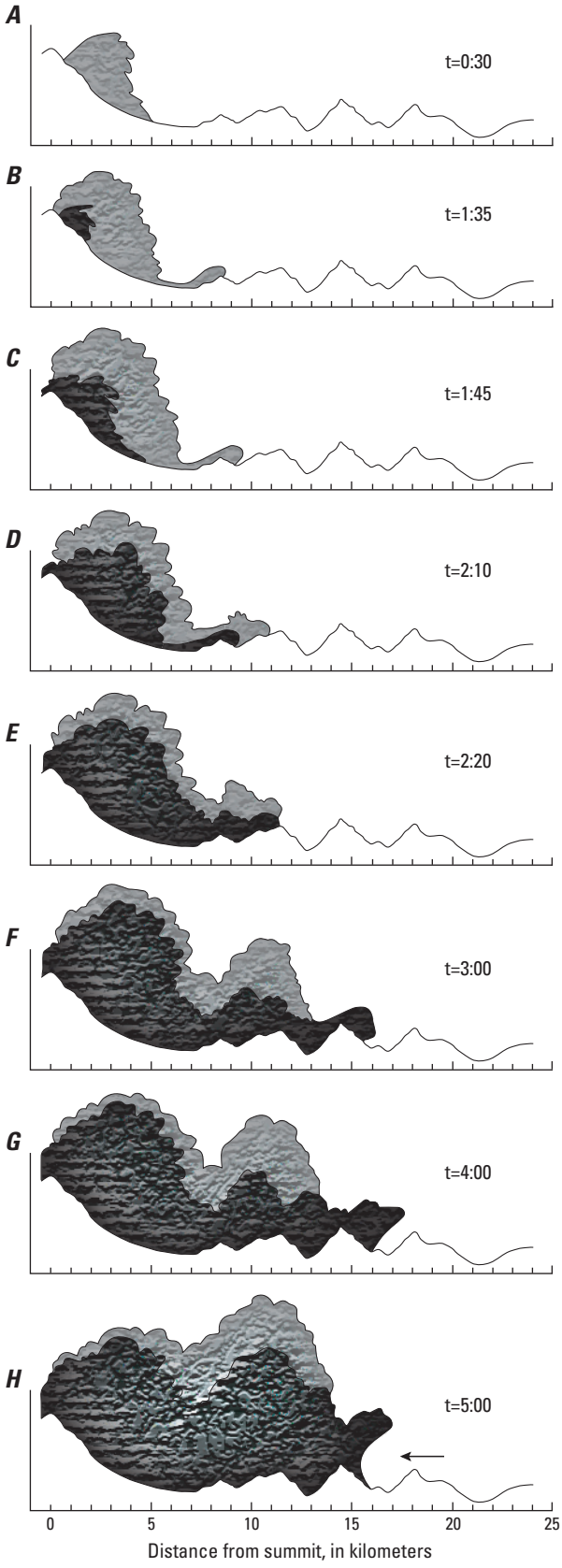

Figure 32. Drawings showing concept of two 18 May 1980 surges (after Hoblitt, 2000). A second surge (dark toned) outruns the first (light toned). Times (t) in minutes and seconds. Arrow at 5 minutes portrays effect of volcano-rushing wind as the surge's heat begins to rise.

1980 deposit. The surge's lowest A1 unit is a fines-poor, grain-supported lens as thick as 20 cm of angular cryptodome dacite. This lens must be from a *first* pulse.

It is overlain by a more cohesive 10-cm coarse layer rich in admixed soil, clasts of pre-1980, and organic material. The 70 cm of A1 material above this layer contains less cryptodome dacite and more altered lithic clasts than the A1 below the soil-rich layer. The soil-rich layer and the A1 material above must be from a *second* large surge pulse (fig. 32) (Hoblitt, 2000; Waitt and Hoblitt, 2017).

Gardner and others (2017) propose a model to explain character of a hypothesized single pyroclastic surge running out the northeast radial. Much of their grain-size data and analyses are compatible with previous studies. But Waitt feels the model hinges considerably on their not taking into account phenomena reported and photographed by 18 May 1980 eyewitnesses and by discounting Hoblitt's (2000) case for two separate surges.

Return on road about 0.4 mile through gate to Windy Ridge parking area (and restrooms). From there drive forest road 99 about 1 mile to a southward cul-de-sac for Stop 1.6.

Stop 1.6. Smith Creek Viewpoint (46.2524° N, 122.1185° W)

The U-shaped head of Smith Creek valley and two tributaries (fig. 6) must have been carved by Pleistocene glaciers. Valley morphology suggests they issued from Plains of Abraham and Mount St. Helens. Yet the volcano then may have been only a dome cluster much lower (thus less a glacial source area) than today's cone (fig. 8) (Clynne and others, 2005).

Standing trunks of large trees in the ridge's lee just east and in the distance to the north show the 18 May 1980 surge lofted off the ridgecrest (fig. 33*A*). The surge debarked many standing trunks, yet many retained bark at their bases and on lee sides. Many small-diameter trees remained upright. These show the flowage was a low-concentration surge. After 37 years only a few of the biggest trunks still stand.

A graded deposit of the surge on a former roadbed (now buried by the parking area) was thinner and its base finer than at nearby Stop 1.5. Decimeters thick on the near-level road, the deposit pinched out on steep slopes above and below (fig. 33*B*). The hot surge was mobile enough to drain off slopes steeper than 25º, though later fall deposits (layers A3, B, and C) stuck.

The Smith Creek valley-floor fill comprises (1) ponded primary pyroclastic surge, (2) laharic debris flow that incorporated much surge material, and (3) secondary ashflows off valley sides (fig. 34) (Brantley and Waitt, 1988).

The paths of meltwater off the east volcano flank were in the 1980s traceable by trimlines and levees from Plains of Abraham down into Smith valley. The laharic floods must have taken several minutes to descend to the valley floor. The dry and hot surge material adsorbed much of the lahar, but the center got wet enough to form a heterogeneous debris flow rich in undigested clasts of the surge that didn't deform much. This constipated, slow mass took some time to move along the valley floor. And so the overlying pyroclastic flows—material first dropped from the surge—were truly secondary.

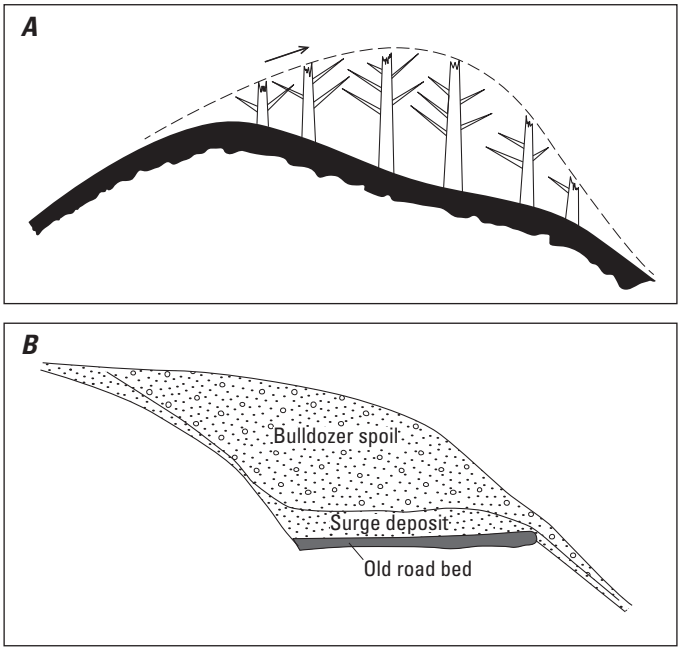

Figure 33. Smith Creek Viewpoint. *A*, sketch showing relation of sheared-off trees to ridgecrests at many places near Mount St. Helens including Stop 1.6. Arrow shows flow direction of 18 May 1980 surge, dashed line its inferred base. *B*, Sketch of surge deposit on flat former roadbed (but now buried) at Stop 1.6 thinning sharply on steep slopes above and below.

Layer A3 caps all these pyroclastic and laharic deposits. So the whole sequence had accumulated and stabilized within 20 minutes.

Drive about 4.4 miles northeast to "Cascade Peaks" station.

Cascade Peaks Interpretive Station [restrooms] (46.2817° N, 122.0813° W)

Stop 1.7. Intermediate-Distance Surge—Clearwater and Bean Valley Heads

Only one of several nearby sites (A, B, or C) about 12 km northeast of Mount St. Helens (fig. 21) will be visited on the fieldtrip.

A. *Drive about 0.15 or 0.3 mile west of Cascade Peaks station and park in wide areas on south side of road (46.2817° N, 122.0836° W).*

Bean Creek heads in an ill-formed glacial cirque. A cut on north side of forest road 99 displays Wn pumice (1479 C.E.) ~1.5 m thick and overlying T pumice (1800 C.E.) separated by dark-gray sand tephra X.

Several pits dug north and south of the road among fir trees reveal 18 May 1980 surge deposit atop pumice-tephra T. Upward the 1980 section is gravel layer A1 (5–10 cm thick),

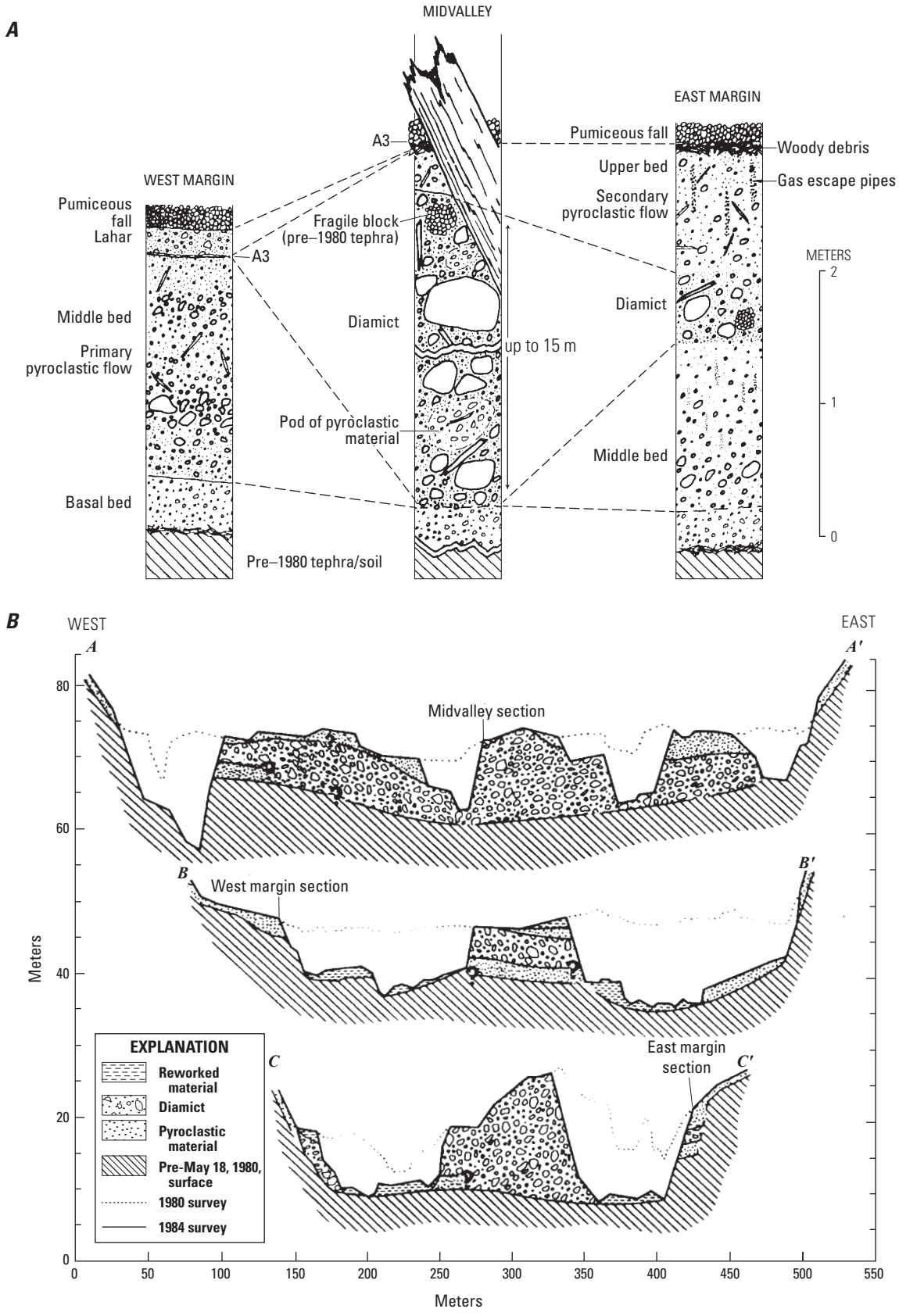

Figure 34. Stratigraphic columns (*A*) and cross sections (*B*) in upper 1.5 km of Smith Creek valley depicting 18 May 1980 diamict emplaced largely as a stiff wet mass. Diamict is underlain by surge deposit and is overlain by secondary pyroclastic flows, and that by mushroom-cloud fall layer A3, and that by main-vent pumiceous fall unit B. Details including locations of stratigraphic columns (sections) in Brantley and Waitt (1988).

sand layer A2 (~5 cm thick), olive-gray sandy-silt layer A3 (1 cm thick), and buff medium-sand layer C (2 cm)—all capped by post-1980 wash or windblown debris (fig. 35).

B. *From Cascade Peaks center turn south onto forest road 2560/2562 (some maps label the 2562 as 380) through gate (need permit). At road intersection 0.6 mile from gate turn left—road 2560.*

Proceed about 40 m down road 2560 (46.2765° N, 122.0728° W). Near here on the low crests north or south of road the basal part of the surge deposit is 17–19 cm thick (layer A1). Above this lies a 4–5 cm diffusely stratified layer (layer A2). This material is capped by 1–2 cm of olive-colored fine ash (layer A3) that fell as aggregates from the mushroom cloud that rose from the surge.

The overlying plinian fall deposits comprise 8 cm of well-sorted pumice from the mid- to late-morning central column (layers B1 and B2). Atop that lies a sequence of pumice fall and fine-grained ash from afternoon 18 May.

The pumice clasts free of fine ash in the lower fall deposits (layers B1 and B2) represent fallout from the dark-gray column jetting from the main vent from about 9:20 a.m. to 12:15 p.m. By 12:20 the eruption column had changed to pale gray and swelled out beyond the crater rim. The first ground-hugging pyroclastic flow rolled down the north flank, and from it co-ignimbrite fine ash drifted northeast at low level—though some ash convected up to broaden the main column. Coarse pumice (>2 mm) continued to jet from the vent but now included abundant pale, fine ash derived both from the column itself and from co-ignimbrite ash rising from the hot flows and drifting downwind. The upper 18 May pumice fall (layers B3 and B4) are coated with fine ash. Some moisture is needed in this process, or the fine ash wouldn't stick to the clasts.

C. *From intersection of roads 2560 and 2562 drive road 2560 southeast 1.7 miles to Mount St. Helens Institute campsite (private; need permission). From tents on northwest edge of open area, hike 5–15 m upslope among fir trees to series of shallow pits (46.2679° N, 122.0518° W).*

The stratigraphy here tells a similar story to stop 1.7B. Notably, the coarse, organic-rich base of the surge deposit grades upward into a finer-grained (lower energy) top. This is capped by the co-surge accretionary lapilli layer A3. Although the accretionary lapilli are poorly preserved at this site, some gentle digging usually reveals a few aggregates ~5 mm diameter. Next, there is a lithic-rich pumice unit that fell during the earliest, vent-clearing plinian column on the morning of 18 May. Coarsening upward points to intensification of the column through mid-morning, and then increasing fine ash after ~12:15 p.m. as the column destabilized and began producing ashflows. The overall 1980 sequence here is underlain by tephra sets T, z, and X.

Return northwest on forest road 2560 through gate to the road 99 intersection near Cascade Peaks Interpretive Station. Drive road 99 north and northeast 1.5 miles to forest road 26 intersection just east of Meta Lake and "miners' car" (see stop 2.6). From road 26 intersection drive forest road 99 northeast another 1.5 miles to a pulloff on north side of a sharp north road bend among standing snags.

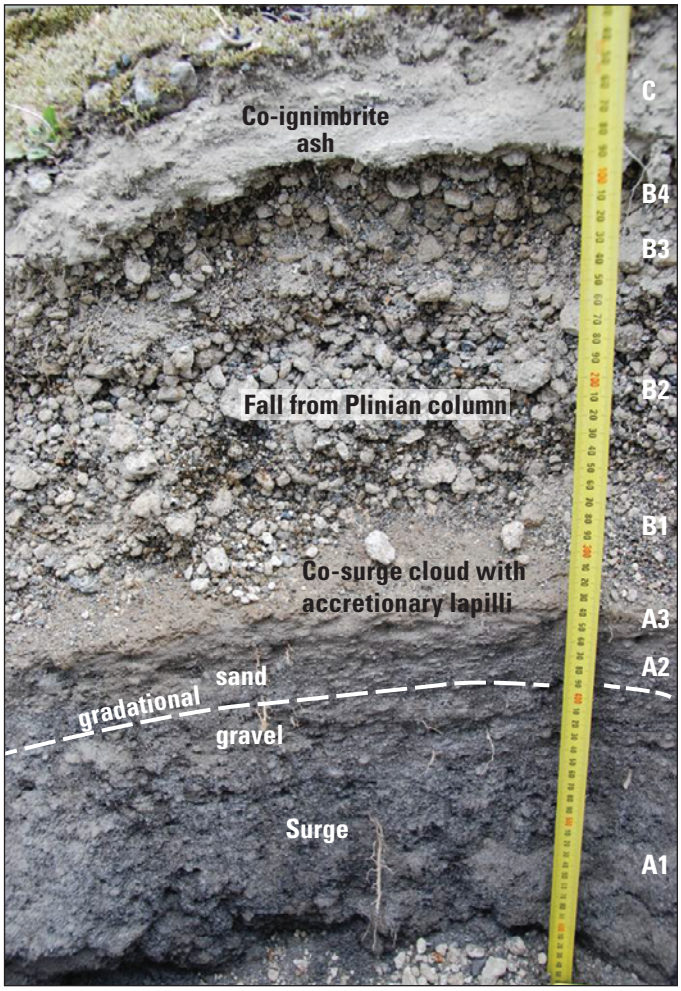

Figure 35. Photograph of pit exposing deposits of the climactic 18 May 1980 eruption at Stop 1.7, site A. Tephra layers labeled on the right with terms of Waitt and Dzurisin (1981). Eruptive processes interpreted in the text.

Stop 1.8. Distal Surge and Scorch Zone (46.3091° N, 122.0594° W)

The outer edge of downed trees merged into a zone tens to hundreds of meters wide where trees were scorched but few fell. The heat-browned needles soon fell off, and over the years most branches. By 2017 many of the big trunks have fallen.

When the surge reached this distal area it had lost lateral momentum and deposited enough of its sediment load to become buoyant and rise. Heat killed these trees, but they remained standing. (On the northwest of the surge area in the North Fork Toutle the hot base of the lofting surge was sharp. The base of scorched fir needles rose outward through the standing snags—from ground level on the proximal [volcano] side to 40 m above the tree base in distal reaches ½ km downvalley.)

The surge deposit hereabouts is only 1–1.5 cm thick. It consists of layer A2 capped by fall layer A3. Sandy A2 extends several kilometers north beyond the scorch zone but gradually thins and pinches out. Eyewitness photographs show some of this sand falling from the outer sheath of the giant column as its hot center rose and spread within the stratosphere as a mushroom cloud. So the uppermost A2 is partly from vertical fall rather than from lateral surge—though in grain size the two are indistinguishable in the field.

Someday these dead trees will have all rotted, the area again lush in forest, and the soil maybe much bioturbated. From a few discontinuous wisps of sand, how would one infer that this event had been lethal? How would you convey this inference to authorities?

End Day 1

Day 2. Pre-Eruption Forest, Pyroclastic Surge, Landslide-Made Wave on Spirit Lake

Forest roads 26 and 99. Old-growth forest. Harmony Falls and Spirit Lake, tephra sections (fig. 21).

(Huge winter-2016 washouts severed access to Stops 2.1, 2.7, and 2.8. Repairs being unlikely before IAVCEI field trip, our intended southward route up road 26 and Stop 2.1 will be discarded. Driving the road and visiting this stop should be possible in the future.)

From Randle as on Day 1, drive forest road 25 south. At about 8.7 miles it crosses Cispus River on a bridge. At about 8.8 miles is turnoff right to forest road 26 (typically no sign). Intended route is up road 26, a curvy one-lane road with turnouts whose former pavement is much broken in repaired sections.

Turnoff right is about 8.3 mi from north end of road 26. This also unsigned road loops clockwise 1¼ mile across the valley to west side and on to parking area and restrooms.

Stop 2.1. Off Road 26, Quartz Creek Big Trees [restrooms] (46.3914° N, 122.0737° W)

From parking area, hike trail through huge Douglas fir, western hemlock, and Pacific silver fir. This is one of the few remaining patches of old-growth forest that before 1980 had surrounded Mount St. Helens in tracts that had escaped forest fires and logging.

Retrace spur road to forest road 26. South on road 26. In another about 4.2 miles is turnoff to Ryan Lake (stay on 26). About 1.5 miles from Ryan Lake turnoff is boundary of Mount St. Helens National Volcanic Monument.

If forest road 26 remains closed by washouts, drive road 26 from road 99 near Meta Lake northward 3.3 miles to Stop 2.2.

Stop 2.2. Monument Boundary—Overview of Downed Forest (46.3359° N, 122.0678° W)

Glaciers flowed out from the Mount Margaret high country during several Pleistocene episodes. Large valley glaciers widened and deepened upper Green valley into its U-shaped cross profile and smooth counterclockwise curve.

The 1980 spectacle becomes muted as alders grow and downed trees rot. Yet one still sees the vast extent of leveled forest. Arms of the surge flowing through different passes and funneled along valleys made fanning patterns here, converging ones there, in the downed trunks.

Logs were salvaged and trees planted outside the monument. On the high north side of Green valley a sharp boundary between old and young trees marks the outer limit of the 18 May 1980 scorch zone. Salvage logging stopped at the outer edge of scorched standing trees, preserving for some time this edge.

Drive forest road 26 south. In 3.3 miles it joins road 99. Drive road 99 southwest. Cascade Peaks center comes in about 1.5 mi, Harmony basin viewpoint and trail in about 4.4 mi.

Stop 2.3. Harmony Basin Viewpoint (46.2744° N, 122.1045° W)

Harmony basin shows effects of the 1980 pyroclastic surge and of a catastrophic wave of lake water displaced by the landslide. Inferred sequence (summary of Stop 1.3) (figs. 25, 26):

1. Surge sweeps northeast, leveling forest and depositing layer A1. Patterns of downed timber show topography channeled a ground-hugging current northeast along Spirit Lake basin. Yet the pattern in downed trees shows that an arm of the surge running east of this ridge crossed the divide where we stand northwestward into Harmony basin.
2. Landslide plowing into Spirit Lake raises catastrophic waves. Its west edge bursts into Harmony basin, washing off the surge deposits and timber up to the trimline 265 m above former lake level.
3. The water drops to the basin floor and flows back west to form new Spirit Lake 63 m above the old. Log rafts strand on the north basin floor, but most wood washes into the lake.
4. Waning pyroclastic surge deposits layer A2.
5. Layer A3 and later tephras accumulate on a stable landscape.
6. For 37 years the logs and branches floating on the lake grind each other to smaller fragments, and much wood sinks. Trees and shrubs reestablish gradually.

Stop 2.4. Harmony Basin Hike

From the trailhead at Stop 2.3, hike 4 km to Spirit Lake and return, total altitude lost and gained 230 m. Purpose is to view effects of the pyroclastic surge and a large wave of Spirit

Lake water (fig. 26). Along the way we pass tuffs and sills of east-dipping Oligocene section that the modern landscape is cut into. The Spirit Lake granodiorite pluton, 23–20 Ma (early Miocene), forms the rugged northwest skyline. It likely fed a surface volcano, now long eroded. Because of narrow trail through alderbrush, discussion is best done in the clear area with view at a high spot of trail just before it drops to Spirit Lake.

U-shaped Harmony Falls basin, a cirque at altitude 1,085 m, hangs 170 m above the former bottom of Spirit Lake, a U-shaped valley with steep truncated spurs—like the one facing the lake just north of Harmony basin. During several glacial maxima a small Harmony glacier must have joined a larger glacier in Spirit Lake basin.

Near the former upper (now only) Harmony Falls the trail drops toward the lake. Here a small moraine of scarcely weathered till overlies striated ~25 Ma welded tuff displaying buff-colored fiamme (flattened pumice). The freshness of the striae indicate they're from the last-glacial Evans Creek stade (~25–20 ka). Their west trend shows that they'd been etched by Harmony glacier—not by the southwest-flowing glacier in Spirit Lake trough. The moraine marks a recessional pause of Harmony glacier in Evans Creek time.

The 18 May 1980 landslide deposits in Spirit Lake and landslide dam on the west raised the lake surface from 975 m to 1,038 m suddenly. By late 1982 stream inflow had further raised lake level to 1,056 m. In 1984 an engineered tunnel spillway lowered lake level to 1,049 m.

West Arm of Spirit Lake

The 400-m height of the debris-avalanche runup over Johnston Ridge (beyond view 3–4 km west) suggests the avalanche entered Spirit Lake around 230–250 km/hr (Stop 5.5 explains the calculation). It pushed a huge wave of displaced water up both arms of the lake, where the upper limit of trimline and logjams is about 265 m above the old lake level, 190 m above present lake level.

Debris-avalanche hummocks at the head of the west arm (Bear Cove, seen from Stop 1.5A) show the avalanche plowed north through the lake and ran more than a kilometer beyond its far shore and up to 80 m above old lake level. The lake's water, hurled high into the valley head, then flooded back across these new avalanche hummocks and jammed logs against their north sides.

Below a sharp line at altitude 1,240 m the valley sides are almost clean of stumps, downed timber, and regolith (fig. 26)—washed off by a wave of displaced water. Long flutes across the sloping spur between the two lake arms (the flutes now obscure) record a wave from the west arm crashing northeast across the spur into lake's east arm.

Coarse layer A1 is as thick as 50 cm above altitude 1,240 m on this middle spur but absent below. On the fluted lower part, fine layer A2 forms the base of the surge deposit. The absence of layer A1 there shows the water wave came near the end of A1 accumulation. The waning surge deposited layer A2. Layer A3 then fell onto stable deposits.

East Arm of Lake and Harmony Falls Basin

We stand above a waterfall that drops over a resistant layer in an east-dipping homocline of Miocene rocks. This is the former upper Harmony Falls—actually a series of several little ones. A 30-m lower Harmony Falls—the big one that made Harmony Falls Lodge at its base so idyllic among tall trees (fig. 24H)—is now 200 m offshore beneath landslide debris that's 40–70 m below lake level.

Bathymetry by Charlie Crisafulli (of the U.S. Forest Service) reveals that the 1980 eruption filled in Spirit Lake's east arm, like its west arm (Gawel and others, 2018). The deepest known spot in the east arm of new Spirit Lake lies 37 m *above the surface* of old Spirit Lake (Waitt and others, 2014). Maximum lake depth in 1974 had been 60 m, mean depth 40 m. Maximum depth in 2011 was 40 m, mean 30 m. So the landslide below present lake level averages 86 m thick (maximum 122 m), its volume more than 425 million m^3.

The trimline of the catastrophic wave along the east arm of the lake rises from about 1,050 m on the south (now alder-obscured) to 1,240 m on the north where the water jammed up the narrowing valley head. Logjams register the 1,240-m level in the north.

Above a sharp trimline at altitude 1,235 m along the north side of Harmony basin, trees lie where felled by the surge. Below that line, water crashing up the basin scraped off timber and surge deposits. The trimline drops east toward the basin head. The subsiding water stranded some timber about the north part of the basin, but most wood washed west in the torrent returning to Spirit Lake.

Shattered stumps on the floor of the south part of Harmony basin were in 1980 circled by horseshoe-shaped scour depressions opening north, a record of sheetflood downslope toward the valley axis (fig. 36). Part of layer A2 and all of layers A3, B, and C overlie the bottoms of the scour depressions cut by water into A1. Much of A1 and part of A2 are missing: the displaced water poured back toward the valley axis while A2 accumulated. This surface remained stable during deposition of A2 (waning surge) and the falls of A3 (morning), B, and C (afternoon).

Sideslope wash, erosion by Harmony Falls Creek, and alder growth have obliterated this sequence. The long-term geologic record of 1980 events here will be muted.

Turn back northeast on forest road 99. Independence Pass parking area and trailhead comes in about 1.3 mile.

Stop 2.5. Independence Pass Trail (46.2821° N, 122.0967° W)

Round-trip trail hike of 2.3 km, altitude gain and loss less ~120 m. From the trailhead hike 0.3 km to ridgecrest (Independence Pass). Continue north ~1 km and return. Along trail we see details of many trees downed by the surge. Visible near Spirit Lake are trimlines and other effects of the water wave when debris avalanche plowed into the lake on 18 May 1980.

The surge deposit here is only about 20 cm thick. Downed trees show diverse effects of a density current. Few or no trees

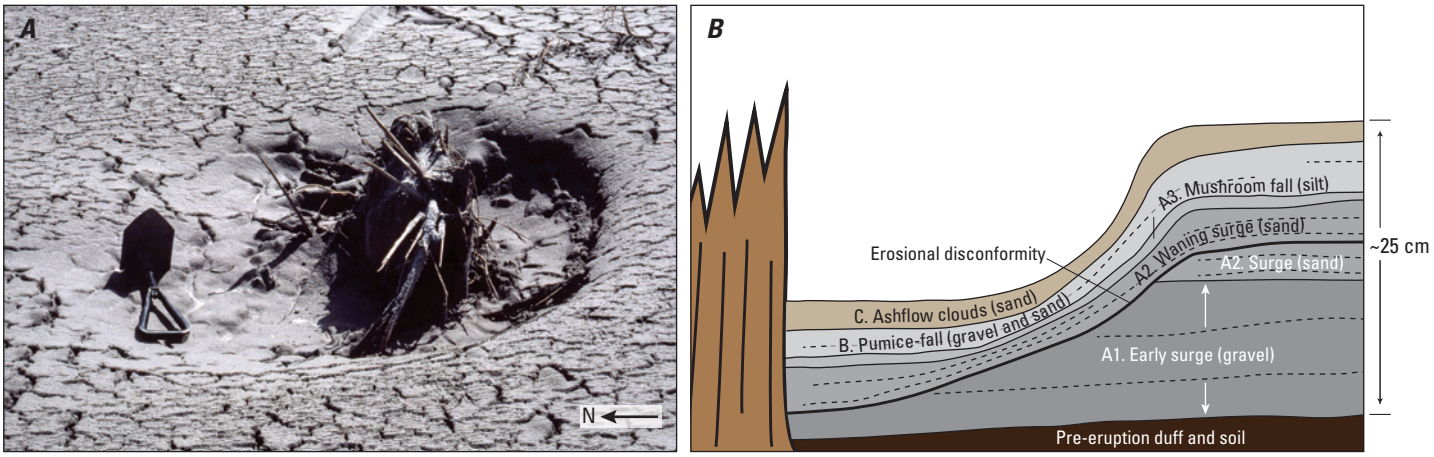

Figure 36. Deposits alternating with flood erosion in Harmony basin. *A*, Stump of tree rooted in flats on south side of Harmony basin. Lake water catastrophically ejected by landslide sloshed high around the basin and then rode the basin floor toward its master creek. Logs in the water bashed stumps to splinters. *B*, Cross section after excavation showing that downslope-running floodwater scoured a horseshoe depression into the just-deposited coarse surge deposit (layer A1). Later surge and fall layers A2 through C mantle the scour subevenly.

were reoriented after they fell. Most of the large (80–150 cm diameter) trees retained their bark, even on top—the volcano side before they fell. And so most trees show that the concentration of the gravel and sand in this flowage was low. The trees must have fallen at the very front of the surge. In reentrants between roots, the undersides of root balls retain bark. They're abraded only a little on protrusions, not at all in reentrants. The undersides of the roots aren't significantly scorched—certainly not charred.

Most (but not all) eyewitnesses who survived being overrun by the surge (Waitt, 2015, chapter 9) reported that the surge grew hotter than it was at its front. The convoluting surge front had entrained much ambient air, and that kept the outer edge less hot than farther back inside the surge.

One sees that topography partly steered the base of the surge. Along the trail high in this northeast part of Harmony basin, trees fell toward azimuth 020. But a large area of the north side of the basin has trees downed toward azimuth 065. So the high area to the north acted as a buttress, the current veering around it clockwise. These two current directions converged farther north along this trail. Standing sheared-off conifer trunks on and behind summit to the north show that the base of the surge lofted over ridges.

Still buried by snow at the time of eruption, some small trees lived. The largest trees here are those survivors. The post-eruption colonizers include noble fir, Douglas fir, Pacific silver fir, western hemlock, alder, and willow.

At the farthest point we hike the trail (46.2875° N, 122.0986° W), a steep bluff exposes Oligocene tuff and tuff breccia. What seems to be bedding dips unusually steeply for this area. Is this really bedding? Or is it flow-foliation? In either case deformed by local tectonic structure?

Return to trailhead. Drive road 99 northeast. In 1.5 mile is "Cascade Peaks" center, and in 2.9 miles the adjacent parking areas for Meta Lake and for "Miners' car."

Stop 2.6. Surge-Wrecked Automobile and Meta Lake (46.2959° N, 122.0784° W)

The surge pushed this once-green 1971 Pontiac Grand Prix a few meters northeast off the road edge, and tree fragments battered it. The trailing hotter part of the current burned off paint and plastic. It has lain outdoors rotting for 37 years. The car's owners died of asphyxia 2 km west-northwest of here, their tracheas clogged with inhaled ash (Eisele and others, 1981; Waitt, 2015).

Hike the trail to the glacial tarn Meta Lake among downed big trees. Once-small trees survived the 1980 surge—having in mid-May 1980 lain beneath still-deep snowpack. Trout survived in the lake that was still ice covered. Life returned fairly rapidly to parts of the surge area where deposits were less than a few decimeters thick.

Return to trailhead. Drive road 99 south. In 1.4 mile is "Cascade Peaks" area.

Cascade Peaks Forest Interpretive Station [restrooms] (46.2817° N, 122.0813° W)

From here turn south onto Smith Creek Butte road (forest roads 2560 and 2562 through gate [need permit]). At road intersection 0.6 mile past the gate, turn right onto road 2562—on some maps labeled NF 380. (Stops 2.7 and 2.8 weren't visited in 2017, for a large washout on road 2562 had severed access to them. Road 2562 will eventually reopen.)

From intersection of roads 2560 and 2562, drive 4.25 miles south on road 2562 to Stop 2.7. At this intersection with a small road east, climb to top of roadcut on the east side of road 2562.

Stop 2.7. 1980 Tephra Sequence (46.23706° N, 122.06306° W)

This site on the axis of 18 May 1980 plinian fall deposits 13 km northeast of Mount St. Helens is 3½ km from the outer edge of 18 May 1980 scorch. These trees were planted after salvage logging.

The pyroclastic-surge deposit, here ~40 cm thick, is divided into coarse layer A1 and upper finer layer A2 (fig. 35). The juvenile component is cryptodome dacite, the accidentals being older eruptive rocks. The capping fall deposit (layer A3—also known as the "blast ashfall") preserves millimeter- to centimeter-sized accretionary lapilli that fell from the 30-km-high mushroom cloud (fig. 37*A*). They are clast supported, indicating they emplaced as a fall deposit with little intervening matrix. And the accretionary lapilli have partly coalesced, indicating that they were moist enough to deform upon impact. For ash to aggregate and grow mud balls like this requires quite a bit of moisture in the plume. Laboratory experiments suggest a water/ash ratio of about 0.2 (Van Eaton and others, 2012).

Where did the moisture come from? The surge itself, convecting up to form the high-level mushroom cloud, must have contained some water. An important source may have been groundwater inside the volcano, which burst out during initial explosions. The surge may have also vaporized glacial ice and seasonal snow from the edifice. Several survivors from the devastated area experienced freezing cold temperatures and ice fragments at the initial onset of the surge (Waitt, 2015, chapters 9, 11, 12). But most witnesses recall scalding hot and dry conditions that resulted in severe burns. There is also no evidence that volcanic ash plastered onto standing trees—as has occurred in some eruptions (Moore and others, 1966) where a surge behaved as a water-rich current. Field evidence in the early 1980s suggested instead that the surge erupted hot and dry (Waitt, 1989). Still, water content in the surge likely varied from place to place and through time. Water may have been initially transported as vapor in the hot surge but later condensed in the rising cloud as it ascended 30 km within ~20 minutes.

Above the surge-related deposits here (layers A1 to A3) lies pumiceous fall tephra from 18 May. The clast-supported lower layers lack an ashy matrix. They represent the Plinian activity from 9:30 a.m. to 12:15 p.m. Above them is an upward transition to ash-coated pumice and lithics. This fine-ash matrix to the upper part of the pumice-fall tephra records a shift in eruption style in early afternoon, when fine ash from pyroclastic flows convected up to enlarge the main column.

But most of this co-ignimbrite ash drifted east at low levels and forms the fine-grained, pale-brown layer C—a process lasting into the evening 18 May (Waitt and Dzurisin, 1981). This unit also contains accretionary lapilli (fig. 37*B*). Contrasting those in layer A3, these lapilli are lighter colored, finer grained, and show delicate concentric laminae. Their local occurrence just downwind from Spirit Lake (but not upwind) suggests the pumiceous flows mixed with sufficient lake water to generate moist, turbulent ash clouds.

Drive south on road 2562 another 1.3 miles.

Stop 2.8. 16,000-Year Tephra Sequence (46.22248° N, 122.06210° W)

In a roadcut (fig. 38) we examine a tall stratigraphic section. At the bottom lie 16,000-year-old tephra set S and 13,000-year-old tephra set J (both Swift Creek eruptive stage). Higher are Smith Creek (set Y), Pine Creek (set P), Castle

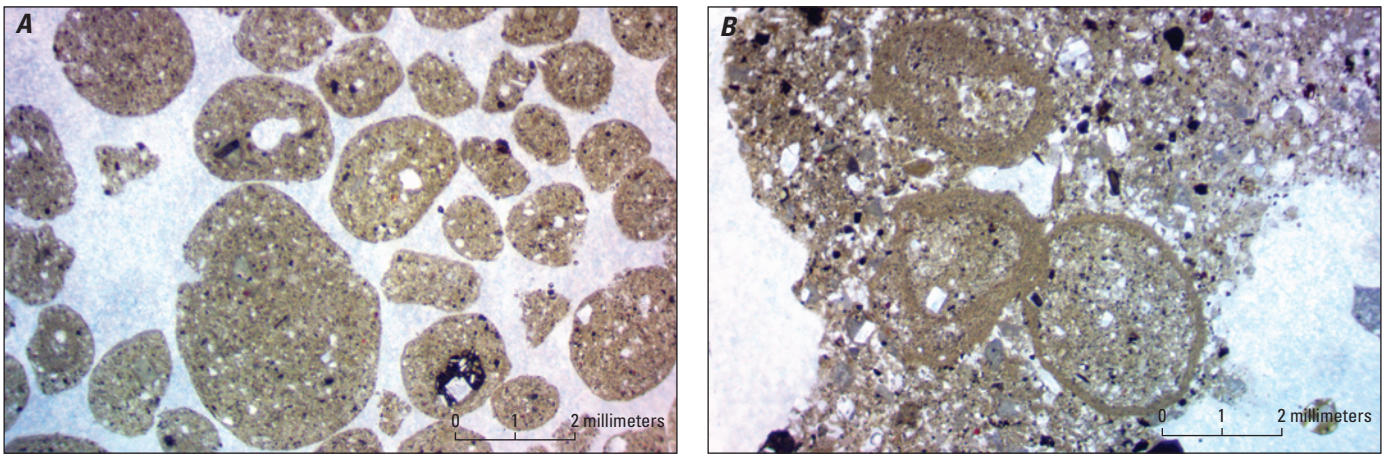

Figure 37. Thin sections of accretionary lapilli from the 18 May 1980 ashfall from the mushroom cloud. *A*, The simple internal structure of these examples indicates they came together fairly quickly and were not recycled into the ash cloud several times. *B*, Recycling in and out of the ash cloud results in concentric layers inside each aggregate.

Creek (set B), Kalama (sets W and X; and bed z), and 1980 surge and fall deposits. We see here fall deposits from each period of the Spirit Lake stage—except Sugar Bowl (layer D) and Goat Rocks (layer T) (fig. 7).

East-side roadcut exposes entire section best (fig. 38). The upper part of the section (Castle Creek set B, and Kalama sets W and X and bed z) shows at north end of the bluff.

Here we are in a sector through which the surge flowed east off the mountain—well south of any direct effects of a northward so-called "directed blast." A section of the 1980 surge deposit atop the bluff on the south shows the divisions of Waitt (1981) seen at Stop 1.5: basal zone (layer Ab) of mixed cryptodome dacite and translocated soil, duff, bark, and wood; overlain by normally graded, fines-depleted dacitic gravel (A1) rich in charred wood; overlain by bedded sand (A2); capped by sandy silt (A3), mostly fall from the mushroom cloud.

End Day 2.

Day 3. Prehistoric Falls and Flows on Mount St. Helens's Southeast and South Flanks

This route explores the east, southeast, and south volcano flanks by forest roads 25, 90, and 83. Stops include Clearwater Creek; eyewitness accounts; 1980 flood on Muddy River; Cedar Flats oldgrowth trees; Pine Creek-age and Cougar-age debris avalanche, pyroclastic flows, and lahars; tephra stratigraphy; Lava canyon (Castle Creek age); glaciated valleys and diverted rivers (figs. 21, 39).

From Randle drive forest road 25 south. From turnoff to road 99 it's about 4 mi up to Elk Pass (altitude 1244 m). From Elk Pass it's about 6 mi to Clearwater overlook (at display signs).

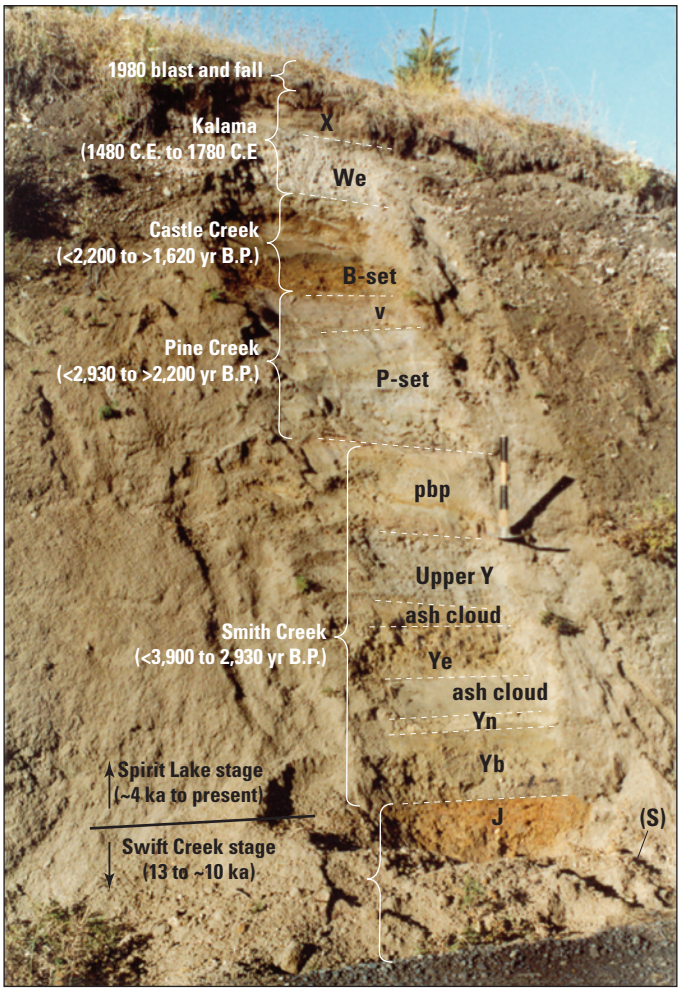

Figure 38. Photograph of tephra section at stop 2.8. Photo by John Pallister ~2003. Shovel handle at unit pbp is ~40 cm long, color divisions 10 cm. Units pbp and v are widespread ash beds discussed by Mullineaux (1996) that separate the set-P tephras from underlying and overlying units.

Stop 3.1. Clearwater Overlook (46.2378° N, 121.9861° W)

Glaciers of Hayden Creek age (150–140 ka) and probably earlier glaciations molded upper Clearwater valley to its U shape with faceted spurs. The 18 May 1980 surge laid down the forest across upper reaches of the valley. In 1980 through 1982 loggers harvested these accessible downed or standing-dead trees. New forestry practices left many standing snags as habitat for owls and other birds. They planted mainly Douglas fir but along Clearwater Creek cottonwood and willow to stabilize banks, provide habitat, cool the water, and so speed plant recovery.

Physical effects of the surge on the east and southeast flanks—downed forests, sandy deposits—are similar to those on the northeast but didn't reach nearly as far. The initial explosions helped propel the surge far out northwest, north, and northeast (fig. 22B, C). These same explosions also directed material *up* that within 80 seconds had piled a cloud of hot particles and gas high atop the mountain (fig. 22D). From this cloud a pyroclastic surge swept down the southwest, south, and southeast—opposite to any "directed" explosion. The fairly low and steep front seems driven mainly by gravity (figs. 22D, 40)—a density flow, not an explosion nor explosion-driven "blast." Yet these deposits on the east and west are identical to those on the northeast and north.

On the inside curve of road 25 a sill or dike of porphyritic basaltic andesite ~7 m thick dips 35° west-southwest, its columnar jointing perpendicular to cooling surfaces. Bedrock here is earliest Miocene, around 23 Ma (Evarts and Ashley, 1993a).

Continue south on forest road 25. It's about 11 curvy miles through trees and down into Muddy valley to Muddy River bridge and parking area.

Base from The National Map and USGS National Elevation Dataset. WGS 1984 Mercator projection.

Figure 39. Map showing route and stops for Day 3. Roads in red. Stop 3.1 (northeast off map) is on figure 21. Trails lead from parking areas to stops 3.7 and 3.8.

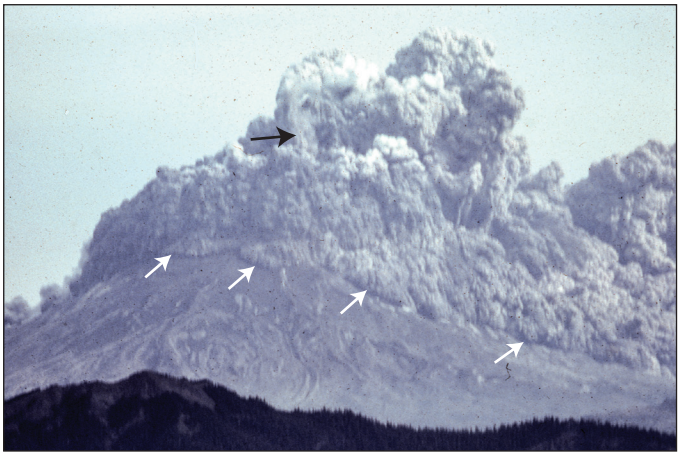

Figure 40. Photograph from the southeast showing ground-hugging hot flow off volcano's east and south sides—opposite direction from a directed "lateral blast." Note the low front of flows (white arrows) off the south and southeast flanks. Lingering vertical white wispy plume strand (black arrow) registers site of Mount St. Helens crater just north of summit. Photograph by Ken Siebert, used by permission.

Stop 3.2. Muddy River Bridge and Lahars [restrooms] (46.1225° N, 122.0152° W)

This reach of Muddy River was a spectacle after a large 18 May 1980 lahar from Ape Canyon and Muddy River, the upper limit of inundation 3 m above pavement level. The large yellowish boulders in the river bed swept down from Tertiary bedrock, the largest boulder—10.4 by 6.0 by 4.6 m—lies 2 km upvalley where lahar depth was 4 m (Pierson, 1985).

From east side of bridge hike ~170 m downstream partly through trees to north end of a continuous high exposure on east bank of Muddy River.

This site exposes three lahars—two thick prehistoric (probably Kalama age) ones and a thin 1980 one on top. The lower Kalama(?) lahar, ~2.5 m thick, is at its base massive pebble gravel enclosing cobbles and boulders up to 70 cm—the character of a debris flow. Near the base is an unusual bed of sorted, well-rounded pebbles of a type that in other lahars Scott (1988a, p. 32–34) descriptively calls a "ball-bearing" bed. Scott (1988b, p. 33–34) infers such extreme rounding by clast-to-clast abrasion owes to intense and sustained shear at a flow's base when it flows deeply down a channel.

This lower lahar grades up to slightly stratified sandy lahar, probably a hyperconcentrated flow. The upper Kalama(?) lahar, ~1.2 m thick, is massive, buff colored, and contains many pumice clasts. Atop this is a wood mat (fig. 41).

Above the wood mat a massive, lithic pebbly-sand lahar is from 18 May 1980 (fig. 41). Two lahars descended Muddy River that day—a big morning one full of lithic clasts including large boulders, and a much smaller afternoon lahar mostly of rounded pumice clasts (Pierson, 1985). People saw some of the energy and violence of this morning lahar (Waitt, 2015, p. 229–231). Yet how puny its deposit seems compared to the underlying ones!

Some investigators have surmised that water in lahars down the east and west flanks had come from the surge itself—that the surge itself had either erupted wet or became wet, as by entraining snow and ice (Pierson, 1985; Scott, 1988a). The water-rich components then supposedly dropped from the surge into a high-density water-saturated basal flow—the surge "transformed" into lahars.

Waitt (1989) disagrees with these speculations that lack field evidence. Surely the surge initiated the lahars, but the characteristics of the surge deposit in 1980 show it had been hot and dry (Waitt, 1981). It didn't stick to vertical tree snags as surge material had plastered onto trees during the 1965 Taal eruption—that surge wet by erupting up through a lake (Moore and others, 1966). Contacts between the surge and the slightly later morning lahars at Mount St. Helens were sharp. Most survivors of the surge emphasize that it was hot and dry (Waitt, 2015). The water in the lahars apparently came from snow and firn and maybe a little ice swiftly melted by the hot and highly turbulent surge (fig. 40) but did not become part of the surge (Fairchild, 1987; Brantley and Waitt, 1988; Waitt, 1989). Such melting stripped 6 m of surface snow and firn off Shoestring Glacier (Brugman and Post, 1981).

Figure 41. Photograph of Kalama (?)-age lahar overlain by 18 May 1980 lahar along east bank of lower Muddy River. USGS photograph by T.C. Pierson.

A pumiceous lahar (not seen in this exposure) originated by swift snowmelt at the base of a pyroclastic flow down Shoestring Glacier observed from aircraft from 3:48 to 3:55 p.m. (Waitt, 2015, p. 249–253).

Continue south on forest road 25. It's about one-half mile to Cedar Flats parking area on the left (unsigned).

Stop 3.3. Cedar Flats Big Trees Trail (46.1130° N, 122.0183° W)

Walk the trail through a stand of huge oldgrowth western redcedar, Douglas fir, and western hemlock. This area was barely touched by the 18 May 1980 eruption—well beyond the edges of the surge, most of it high enough that lahars down Muddy River and Pine Creek skirted it.

Continue south on road 25. It's about 3 miles to unsigned gravel road on east (left) just before Pine Creek bridge that leads up into private rock quarry.

Stop 3.4. Pine-Creek-Age (3,000–2,500 cal yr B.P.) Lahars (46.0742° N, 122.0742° W)

A gravel pit exposes the stratigraphy of planar, massive lahars interbedded with lenticular fluvial coarse sand to openwork cobble-boulder gravel (fig. 42). Largest boulder measures 4 m. Most gravel clasts are dacite, a few andesite. This and other nearby deposits are younger than tephra Ye and older than tephra B—thus Pine Creek age, about 3,000 to 2,500 cal yr B.P. (Crandell and Mullineaux, 1973; Crandell, 1987). The process meanings of the large differences in clast sizes and textures of different layers haven't been studied in detail.

Continue south on road 25 about one-eighth mile to parking area for Pine Creek boulder just across the bridge.

Stop 3.5. Lahar and Big Boulder at Pine Creek (46.07249° N, 122.01818° W)

The Pine Creek lahar was a west distributary of the 18 May 1980 lahar down Muddy River canyon (Stops 3.7, 3.8). It took 28 minutes for the flow to travel 24 km from the volcano's cone down Pine Creek to here near its confluence with Lewis River—its average speed 10 m/s (Pierson, 1985, fig. 9). Its peak stage past the bridge was nearly 10 m, registered by mudlines visible on trees for several years.

A plagioclase-porphyritic andesite boulder measuring 5 by 3.7 by 3 m and weighing about 33 metric tons sloshed up on a bend and came to rest on the road bed 10 m above the creek bed but in only 1 m of lahar deposit. A bulldozer pushed it a few meters to its present spot.

Hike down trail south 80 m to Lewis River for lunch.

Downstream 300 m from here the tall bank exposes Pine-Creek-age lahars similar to those in the gravel pit at Stop 3.4.

Continue southwest on road 25. In 0.7 mile in a straight stretch, road 25 ends and pavement merges with forest road 90. In another one-quarter mile (or about 1 mile from Pine Creek parking) is a Forest Service station.

Pine Creek Information Station [restrooms] (46.0626° N, 122.0293° W)

Drive forest road 90 west, a sinuous course along Swift Reservoir. It's 11 miles to high bridge over Swift Creek and 11¾ miles to intersection with forest road 83.

Turn right onto road 83. Drive north 1.2 mile to parking area at boundary of Mount St. Helens National Volcanic Monument.

Hike the road ~115 m south, then at a blaze on a tree scramble ~65 m east though woods to overlook of canyon head on its southwest side.

Figure 42. Photograph of east wall of rock pit at stop 3.4. Planar lahar and lenticular fluvial gravel interbedded intimately but irregularly, hard to distinguish contacts. Height of exposure about 6 m.

Stop 3.6. Cougar-Age Two-Pumice Pyroclastic Flow Atop Debris Avalanche (46.0901° N, 122.2105° W)

This site is potentially dangerous. Stay back from the actively slumping edge. The top in places is only overhung tree roots. First bump is 40 m down!

Section in canyon head mostly exposes Cougar-age pumiceous pyroclastic flows (fig. 43) that contain two distinct pumice types. The flows underlie tephra sets M and K and yield a radiocarbon age of 20,350 ± 350 cal yr B.P. (Crandell, 1987). The pumice types are white to gray crystal-poor hypersthene-hornblende dacite (66.5 percent SiO_2) and tan to dark brown crystal-rich augite-hypersthene-hornblende dacite (63.5 percent SiO_2). The white pumice dominates at most sites. The brown is present everywhere, dominant in places. The flows include rare pumice blocks as large as 5 m. In Swift Creek's headwaters the upper flow unit contains blocks of brown lava from dome-collapse avalanches—evidence that domes were growing near the end of the explosive phase of eruption.

These pyroclastic flows, as thick as 100–250 m, cover most of a huge debris avalanche. For a time they dammed Lewis River. These flows are 100 m thick in lower Swift Creek above Swift Dam. The volume for the two-pumice flows is at least 0.5 km^3. Contacts between the several flows are sharp: the thick section likely accumulated during closely spaced eruptions. The two-pumice flows seem to underlie the Swift Creek lava flow ($^{40}Ar/^{39}Ar$ age 17.0 ± 3.2 ka) and directly overlie the debris avalanche, both Cougar age. That contact is sharp, and there's no soil on the avalanche—thus apparently little time between the related deposits. And the two most common rock types in the flows are the same two dacite rock types that compose the avalanche.

Magma intruding a dome complex may have caused the avalanche. It was the largest collapse in the volcano's history before 1980. The Cougar eruptive stage marks the beginning of the growth of the edifice we now see as Mount St. Helens.

Continue on forest road 83 northeast across south flank of Mount St. Helens. From parking area at monument boundary it's 1.8 mile to road 81 intersection and 10.3 miles across several bridges to parking area on north (left) side of road 83 for Stop 3.7.

Figure 43. Photograph looking east at pumiceous pyroclastic flows at Stop 3.6. Tephras sets K and M would lie at the soil. Below the soil the three pumiceous pyrocastic Cougar-age flows are about 2.5, 10, and >15 m thick (downsectionward), tops marked by concentrations of coarse pumice blocks.

Prehistoric Tephra Falls and Lava Flow

We are on the edge of the bouldery, vegetation-stripped path of an 18 May 1980 lahar down the Pine Creek fan from Mount St. Helens's southeast flank. The lahar descended this part of the fan about 10–12 min after the start of the eruption—judged from Pierson's (1985, fig. 9) inference that the lahar reached Swift Reservoir in half an hour.

From parking area on forest road 83, hike 150 m north across Pine Creek to tall layered outcrop along Muddy River and another 150 m to farther north outcrop.

Stop 3.7. Sequence of Ancient Tephra Falls (46.16436° N, 122.09147° W)

Erosion by the 1980 lahar exposed several nearby stratigraphic sections of tephra (fig. 44). The tephras include pumice tephra set S (about 15,800 cal yr B.P.) overlain by one or two lahars. These lahars are overlain by oxidized set J (about 13,500 cal yr B.P.), layer Ye (3,300 cal yr B.P.), fine-grained set P, and layer We (1482 C.E.). Section contains a few intercalated lahar and surge deposits. Near the top, lahars lie below and above tephra set X (about 1680 C.E.). At the very top lies the 1980 lahar.

Return to parking area. On forest road 83 continue northeast across Muddy River bridge to parking lot at end of road in 0.4 mile. From parking area this "stop" is a trail loop. Hike ~0.7 km east, cross bridge, then hike back, along opposite side of Muddy River.

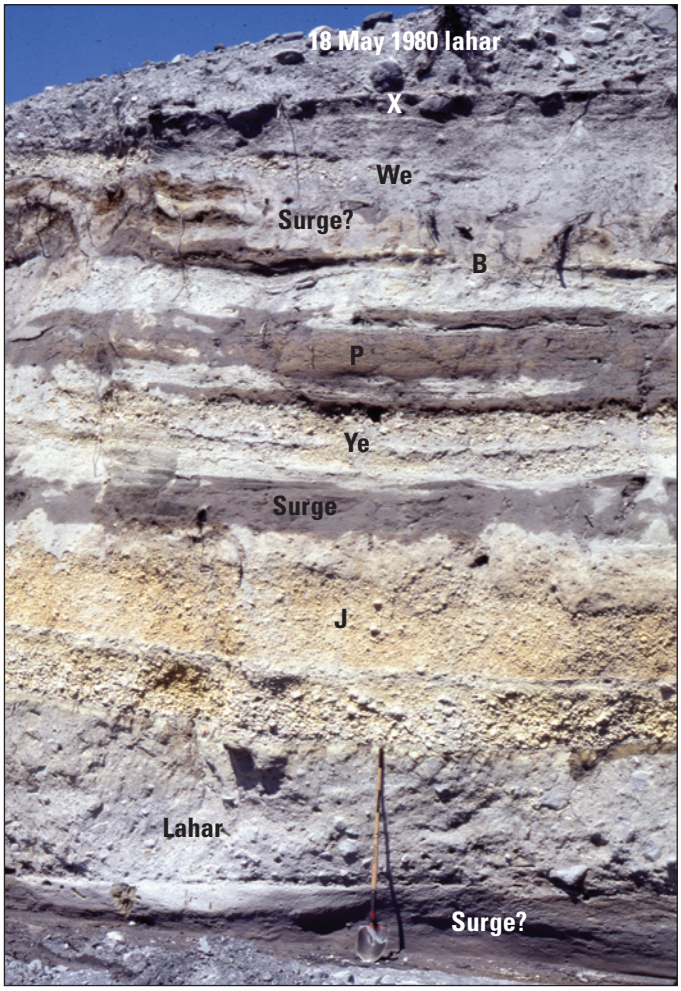

Figure 44. Photograph of stratigraphic section at Stop 3.7—one of several nearby exposures. Set S tephra lies below the base of this outcrop. Lahar and surge deposits alternate with fall tephra—from set S at or below base to set X near top. A lava flow of Castle Creek age (stratigraphically equivalent to tephra B) lies beneath the stream channel—and is our next stop. USGS photograph August 1981 by R.B. Waitt.

Stop 3.8. Intracanyon Lava Flow (46.16839° N, 122.08311° W)

The 18 May 1980 lahar reamed out this canyon and bared an intracanyon andesite lava flow of Castle Creek period (~1,800 cal yr B.P.). About 16 m thick, the lava flow shows two styles of jointing: lower well-formed columns (colonnade) about 8 m thick formed by slow cooling up from the flow's base, and an upper set of small, irregular columns (entablature) formed by faster cooling down from the top.

Hike to the steep part of the canyon, where Muddy River falls over the lava flow and reveals the contact of lava overlying oxidized late Oligocene rocks (about 25? Ma). Shear at the flow's margin may have caused platy jointing near the lava flow's base.

Return southwest on forest road 83 to road 90. On road 90 southwest it's 6.6 miles to the village of Cougar. From Cougar on State Route 503 spur it's 5¼ miles to intersection of throughgoing State Route 503.

Drive SR 503 west. This is lower Speelyai valley.

Lower Speelyai Valley

Lewis River lies 3 km to the south in a tight canyon of a glacier-molded valley (fig. 5). The hills 1 km south and north of us bear topographic marks of former glaciers: whaleback erosional forms, ice-marginal channels.

The open valley here is the preglacial valley of Lewis River. Lower Speelyai Creek is grossly underfit for this valley. A large glacier down the valley during Hayden Creek and older glaciations apparently pushed Lewis River south. Upon glacier retreat the river became superposed in a bedrock course there. Farther south beyond view, the hills in places are molded into drumlin and subglacial-channel forms up to 600 m above the valley floor. During full glaciations Lewis River had been shoved as far as 7 km south. Some of this glacier-blocked drainage overflowed into valleys 10 km even farther south (Mundorff, 1984; Evarts, 2005).

Overlying the old till exposed on valley margins, thick lahars partly fill this valley. We visit them at Stop 3.9.

From the intersection of SR 503 spur, drive main SR 503 west 2.2 miles to turnoff south (left) to Speelyai Bay. Drive this road 1 mile south to abandoned sand-gravel pit at entrance to recreation area.

Stop 3.9. Lahars of Cougar Stage (45.9844° N, 122.4176° W)

A former gravel pit in the bay of lower Speelyai Creek partly exposes a 10-m-thick pebbly lahar that came down Lewis River during Cougar stage time (Major and Scott, 1988, fig. 7; Evarts, 2005). An underlying sand lahar is barely exposed at north end of the outcrop. This deposit, 50 m above the lahar-infilled floor of the valley and 1–2 km wide at this level, shows that massive lahars have passed down Lewis River. Evarts (2005) mapped these deposits to infill lower Speelyai and Lewis valleys at least 70 m thick. They trace as map units 22 km farther down Lewis valley (Evarts, 2004a, b). Charcoal upsection in these deposits dates to 27,479±3,090 cal yr B.P. (Major and Scott, 1988).

As thick as these and other Mount St. Helens deposits are in Lewis valley, they only infilled existing valleys (Hyde, 1975; Evarts, 2005). To have overwhelmed and eroded down the divide south of lower Speelyai valley enough to capture Lewis river into its present course required larger forces over more time. Two or more extensive pre-Wisconsin glaciations—glacier surfaces 450–500 m above the lahar tops here—seem the cause of drainage diversions. Yet this story isn't entirely known.

End Day 3.

Day 4. The Kalama Eruptive Episode and Some Older Features, Southwest and South Flanks

On Day 4 we examine Kalama-age deposits on Mount St. Helens's southwest flanks (fig. 45). The Kalama period may be divided into three phases by the chemistry of eruptive products: early Kalama dacites, middle Kalama andesites, late Kalama dacites. A few stops on the south flank examine pre-Kalama deposits. A hard hat may be prudent for Stop 4.3.

Tree-ring dates constrain the emplacement dates for the various Kalama-age deposits. Age brackets for the three phases overlap (Yamaguchi and Hoblitt, 1995).

Early Kalama Dacites

After an apparent repose of 400–500 years (Hoblitt and others, 1980; Crandell, 1987; Clynne and others, 2008), activity commenced with the large eruption of Wn tephra in late 1479 C.E. (Yamaguchi and Hoblitt, 1995; Yamaguchi, 1983; Mullineaux, 1996). After Wn, the most voluminous of the early Kalama tephras, came tephra layers Wa, Wb, We, and Wd. Tephra We erupted in 1482 C.E. (table 1) (Yamaguchi, 1985). All these consist of dacite pumice and subordinate lithic clasts. Winds dispersed them mainly northeast and east. Early dacite pyroclastic flows and lahars descended southwest to Kalama valley. Calendric tree-ring dates for pyroclastic-flow deposits range from 1482 to 1489 C.E. (table 1). There's little overlap between areas of the tephras and flowage deposits, their relative timings poorly constrained. Tephra and flowage deposits are known to be in contact at only one site, where a pyroclastic-flow deposit overlies tephra We.

Most flowage deposits consist mainly of dense, slightly vesiculated dacite, likely from collapse of a summit dome. These flows are intercalated with less voluminous pumiceous flows, surges, and lahars from explosive eruptions. The origin of many flows is not evident from field criteria alone, but paleomagnetic determination of minimum emplacement temperatures helps resolve ambiguity. The whole-rock SiO_2 content of the early Kalama dacites ranges between 64 and 66.5 percent (fig. 46). By tree-ring dating, the early Kalama dacite phase ended sometime between 1489 and 1510 C.E. (Yamaguchi and Hoblitt, 1995).

These extensive Kalama-age deposits in Kalama River headwaters dammed several tributaries that since have held shallow water bodies including Blue Lake, McBride Lake, and Goat Marsh.

Middle Kalama Andesites

Sometime between 1489 and 1510 C.E.—10 to 31 years after the start of Kalama activity—the early Kalama dacitic eruptions gave way to eruptions of middle Kalama andesitic tephras with a bulk SiO_2 content of about 58 percent (fig. 46). The andesitic set X tephras comprise many beds abundant to the northeast and east but lie also on other flanks. The pattern suggests the tephras erupted over months to years. They were succeeded by many blocky andesite lava flows (SiO_2 content 57–58 percent) on all volcano flanks, especially southeast and east. Pyroclastic-flow deposits of identical chemistry and mineralogy overlie these lava flows in places. The ages of trees rooted in andesitic pyroclastic-flow deposits in Kalama valley indicate they were emplaced by 1566 C.E., within 87 years of the start of the Kalama period (Yamaguchi and Hoblitt, 1995). The middle Kalama dates are bracketed by a limiting start date of 1489 C.E. and a limiting end date of 1566 C.E. (Yamaguchi and Hoblitt, 1995).

Late Kalama Dacites

The eruptive style and magma chemistry changed again sometime between a limiting tree-ring date of 1489 C.E. and a calendric tree-ring date of 1647 C.E.—10 to 168 years after the Kalama eruptive period began. A new dacitic summit dome (SiO_2 about 61 percent) (fig. 46) began to shed nonvesicular debris down the volcano flanks, at first mainly west and northwest. In 1647 C.E. (Yamaguchi, 1986) one or more explosions at the dome sent pyroclastic flows of vesicular dacite debris west and west-northwest into the South Fork Toutle and Castle Creek valleys. The summit dome then shed nonvesicular dacite debris (62–64 percent SiO_2) until the end of the Kalama eruptive period.

The youngest nonvesicular summit-dome debris of the late Kalama phase has a silica content of 63–64 percent. The only tephra associated with the growth of this summit dome is z (Mullineaux, 1986, 1996). The tephra is sandwiched between late Kalama dacite pyroclastic flow deposits. Its wide azimuthal distribution suggests an extended eruption period. The z tephra contains scattered lapilli of vesicular summit-dome dacite.

Figure 46 shows the silica contents from 38 sequential Kalama stratigraphic units. The abrupt change from early dacites to andesites seems due to mixing of dacitic and basaltic magmas (Pallister, and others, 1992; Gardner and others, 1995b; Smith and Leeman, 1987, 1993).

A limiting date for hot debris emplaced on the volcano's east flank constrains the end of the Kalama eruptive period to before 1750 C.E. Limiting tree-ring dates of 1489 and 1750 C.E. bracket the late Kalama dacitic phase (Yamaguchi and Hoblitt, 1995). The late Kalama summit dome slid off the volcano at the start of the 18 May 1980 eruption.

The eruption of the T tephra in 1800 C.E. defines the start of the Goat Rocks eruptive period.

Day 4 Road and Trail Stops

From Woodland, drive SR 503 east about 23 miles and SR 503 spur about 6 mi to turnoff north onto forest road 81 toward Merrill Lake. Drive forest road 81 north. At 4 to 5.6 miles road passes Merrill Lake downslope to the west.

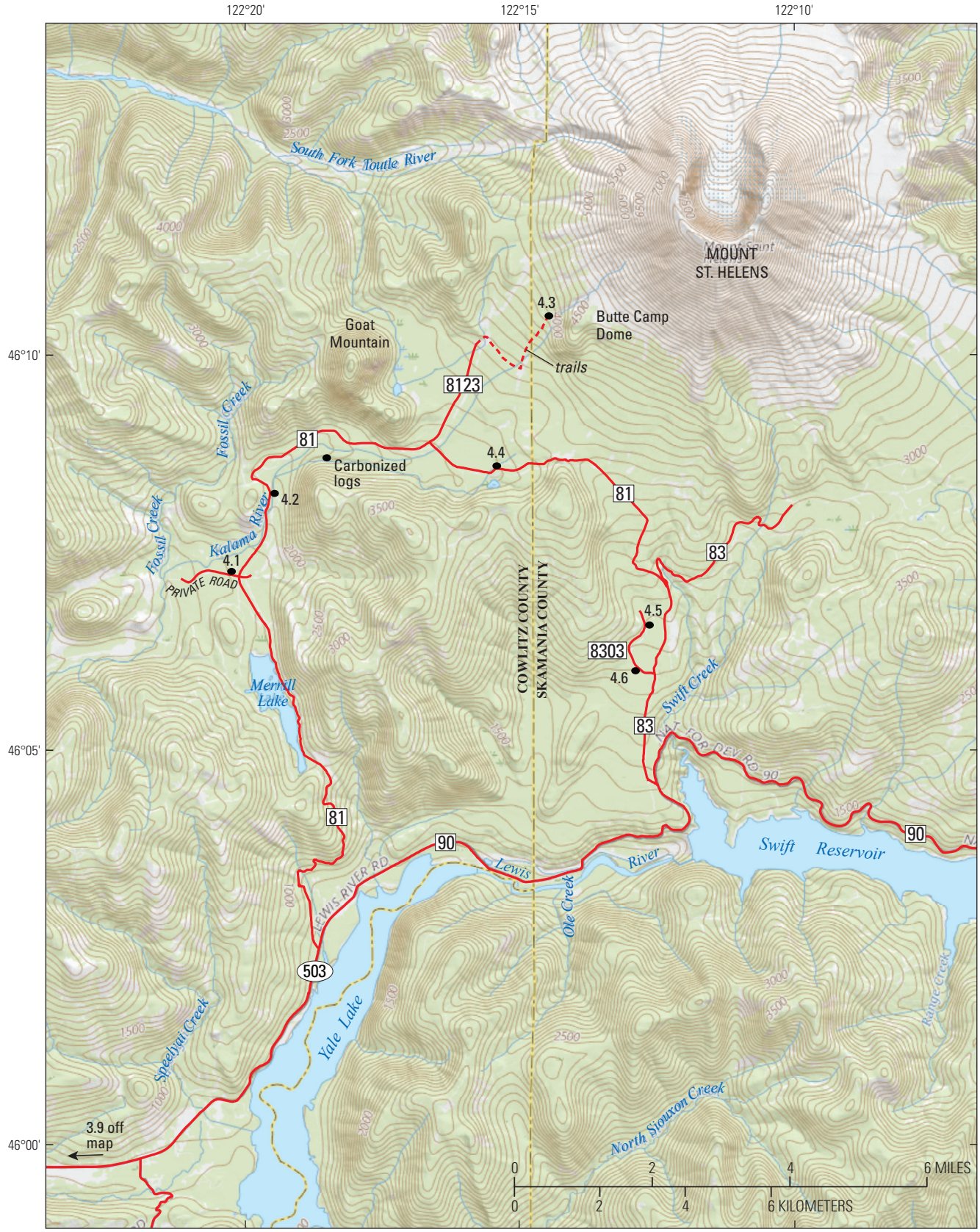

Base from The National Map and USGS National Elevation Dataset
WGS 1984; Mercator projection

Figure 45. Index map for route and stops of Day 4.

Table 1. Dates or limiting dates for eruptive periods and volcanic deposits emplaced at Mount St. Helens since 1479 C.E.

[Modified from Yamaguchi and Hoblitt, 1995. N.A., not applicable]

Eruptive period (phase or subphase)	Emplacement date or bracketing interval[1]	Deposit type and rock type	Drainage or flank of volcano	Evidence of heat or contemporaneous
Most recent eruptive period	1980–2009	Various	Various	Various
Dormant Interval	1945	Lahar (dacite)	Blue Lake	None
	1885	Lahar (dacite)	South Fork Toutle River	None
Goat Rocks eruptive period				
	1857	Eruption column	N.A.	Witnessed
	1844	Lahar (dacite)	South Fork Toutle River	See discussion
	1842–43	1842 tephra (dacite)[2], dome (dacite)[2]	North-northwest	Eruptions witnessed, trees singed
	1800	Floating Island lava flow	North	Postdates tephra T
	1800	Tephra layer T (dacite)[2]		
Kalama eruptive period				
Late Kalama phase, upper subphase	Before 1837	Lahar (dacite) (?)[3]	Pine Creek	None
	Before 1772	Lahars (dacite)[3]	Blue Lake	Contains summit dome rock
	Before 1750	Hot lahar (dacite)[2]	Pine Creek	Blocks prismatically jointed; paleomagnetic data
	1722	Lahar (dacite)[3]	Muddy River	Contains summit dome rock
	Before 1694	Lahars[3]	Pine Creek	None
	Before 1722	Tephra bed z complete (dacite)[2]	Northeast to southeast	N.A.
	Before 1694	Tephra bed z start (dacite)[2]	Northeast to southeast	N.A.
	1667	Lahar (dacite)[3]	South Fork Toutle River	Contains summit dome rock
Middle subphase, lower subphase	1647	Pyroclastic flow (dacite)[2]	South Fork Toutle River	
	1489–1647	Lithic summit dome (dacite)[2]	N.A.	N.A.
Middle Kalama phase	1489–1566	Pyroclastic flow (black andesite)[2]	Kalama River	Breadcrusted rocks; paleomagnetic data
	1489–1566	Lava flows (andesite)[2]	Most flanks	N.A.
	Before 1566	Tephra set X complete (?) (andesite)[2]	All	N.A.
	1489–1510	Tephra set X start (andesite)[2]	All	N.A.
Early Kalama phase	1489	Pyroclastic flow (dacite)[2]	Kalama River	Carbonized logs
	1482	Pyroclastic flow (dacite)[2]	Kalama River	Carbonized logs
	?	Tephra layer Wd	Northeast to southeast	N.A.
	1482	Tephra layer We[2]	East	N.A.
	?	Tephra layer Wb[2]	East-northeast	N.A.
	?	Tephra layer Wa[2]	East-northeast	N.A.
	1479	Tephra layer Wn[2]	Northeast	N.A.
Dormant				

[1]Underlined dates limit eruptive periods or phases. Previously reported calendric dates are included for completeness.

[2]Deposits unequivocally generated by eruptions on the basis of deposit type (domes tephras) or evidence for elevated emplacement temperatures.

[3]Deposits probably generated by hot avalanches from growing summit dome (unmarked lahars were probably climatically induced).

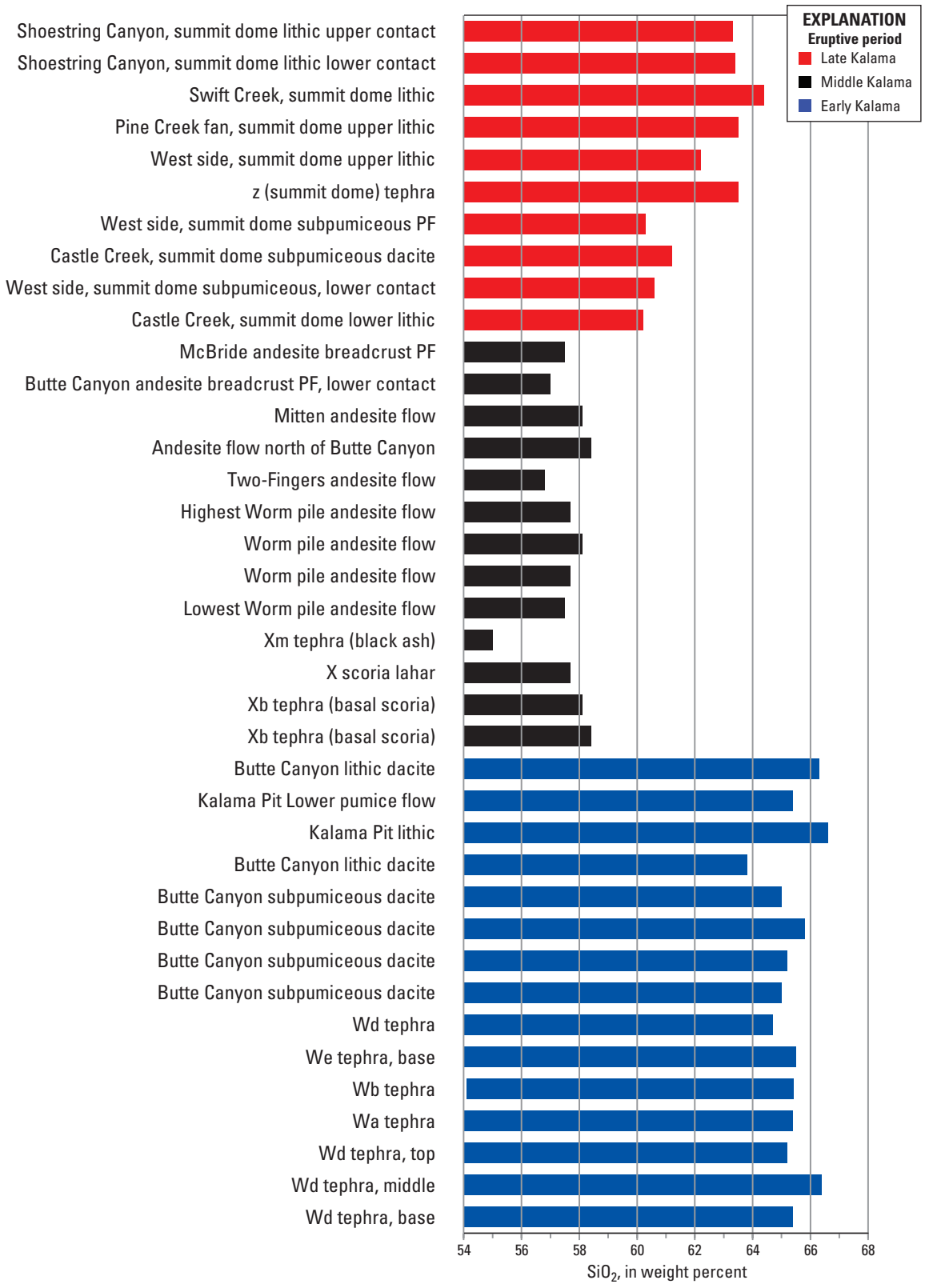

Figure 46. Plot of SiO_2 weight percent content of Kalama-age eruptive rocks and tephra, made by R.P. Hoblitt. Specific units identified in stratigraphic order. SiO_2 analyzed by whole-rock X-ray fluorescence in USGS labs in Denver in the 1970s and 1980s. Plot quantifies the sequence dacite to andesite to dacite from early to late Kalama times.

Merrill Lake (Along Forest Road 81)

Merrill Lake occupies a north-draining tributary of Kalama River. A lava flow down Kalama valley dammed this tributary and formed the lake. This flow is contemporaneous with the Cave Basalt flows south of Mount St. Helens emplaced about 1,895 cal. yr B.P. (Crandell, 1987; M.A. Clynne, unpub. data 2016). This flow cropping out along road 81 by the lake is nearly 13 km long but exposed mainly in its terminal 5 km, the rest covered by younger Kalama deposits. Drill holes indicate the lava is 20 m thick near the lake's north end. Merrill Lake has no surface outlet: it must drain through fractures in the basalt and fragmental deposits beneath.

Continue north on forest road 81 to the intersection of a small road 6.8 miles from the roadhead on SR 503 spur, or about 1.2 miles beyond north end of Merrill Lake. Park on wide shoulders here.

Hike gated road 150 m west and at road crossing hike 200 m north into old gravel pit.

Stop 4.1. Alluvium From Early Kalama Pyroclastic-Flow Deposits (46.1221° N, 122.3357° W)

The aggregate quarry exposes alluvium shed from early Kalama pyroclastic flows that terminate 1.5 km north. Kalama River deposited this debris while rapidly incising the new pyroclastic flows. Lack of silt and clay and the loose texture of even the most massive beds indicates a streamflow rather than debris-flow environment.

Return to vehicles. Continue north on forest road 81.

Road 81 (46.1309° N, 122.3251° W)

Break in slope on road 81 about 0.9 mi north of intersection near Stop 4.1 marks the terminus of the early Kalama pyroclastic-flow deposits.

Continue north on forest road 81. At about 1.4 mi from intersection near Stop 4.1 and ½ mile north of the break in slope, turn east (right) into old sand-gravel pit.

Stop 4.2. Early Kalama Flowage Deposits (46.1381° N, 122.3242° W)

We visit an aggregate quarry on east side of Kalama River near road 81 river crossing. The quarry's north face exposes two of the longest early Kalama pyroclastic flows—13.5 km from the pre-1980 summit and 0.6 km from their termini. The lower unit consists of angular to subangular clasts in a friable matrix of gray ash. Most clasts are slightly vesiculated hypersthene-hornblende dacite, but 20 percent are basalt and hypersthene-hornblende pumice. These excavations revealed that this unit is thicker than 13 m. Clasts from the lower unit were analyzed paleomagnetically (Hoblitt, 1978; Hoblitt and Kellogg, 1979). Half were emplaced above their maximum blocking temperatures of 400–450 °C and half below 450 but above 300 °C. These data suggest emplacement by a pyroclastic flow but don't exclude laharic origin.

The upper unit consists of lapilli and blocks of pumice and lithic debris in a matrix of moderately cohesive ash. The pumice is pale yellow, rounded, and inversely graded. The lithic debris is mainly early Kalama dacite but includes pre-Kalama accidental clasts. Gray at the base, the deposit grades up to grayish pink, which we infer is a pyroclastic-flow deposit. It is capped by a few tens of centimeters of alluvium.

Continue north on forest road 81 for ½ mile to Kalama Horse Camp on the southeast (right).

Carbonized Logs

Erosion and slumping in 2006 or 2015 has made this site (fig. 45) no longer feasible. Nor could we find the earlier-described outcrops (Hoblitt, 1989). We retain the description for what it reveals. A new route leads to the approximate location.

From Kalama Horse Camp (46.1427° N, 122.3270° W) follow Kalama Horse Camp entrance road to Toutle Trail trailhead (46.1429° N, 122.3236° W). Take Toutle trail to its intersection with Cinnamon Trail (46.1424° N, 122.3232° W). Follow Cinnamon Trail to 46.1438° N, 122.3069° W on the south side of Kalama valley; leave the trail and descend the steep valley side to 46.1445° N, 122.3075° W near the south bank of the Kalama River.

Before flooding changed things, carbonized tree stumps in growth position stood near here. A nearby carbonized log-jam had been exhumed by river erosion from an early Kalama pyroclastic-flow deposit. The unit containing the logjam was probably the first early Kalama flow into this part of Kalama valley. Dendrochronological analysis of carbonized growth-position stumps indicates the trees died in 1489 C.E. (Yamaguchi and Hoblitt, 1995).

From Kalama Horse Camp turnoff, continue northeast on forest road 81. In 2.6 mi lies intersection of forest road 8123. Drive road 8123 upslope north 1.5 miles to road's current end at a washout, now also the Blue Lake trailhead.

Stop 4.3. Kalama Stratigraphy in "Butte Canyon"

Blue Lake Trailhead (46.1665° N, 122.2621° W)

From forest road 8123, follow Blue Lake trail upslope northeast 0.5 km through coniferous forest. At trail intersection (46.1687° N, 122.2560° W) take Toutle trail (#238) southeast for 1.3 km. Trails cross Kalama-age andesitic "breadcrust" pyroclastic flows scattered with large scoriaceous bombs. At intersection with Blue Horse trail #237 (46.1676° N, 122.2561° W), continue southeast on Toutle trail #238.

Trail descends steeply into a gully (46.1674° N, 122.2463° W) informally called "Butte Canyon," which drains the north side of Butte Camp Dome. 18 May 1980 lahars destroyed vegetation near the gully; the new lahar deposits and

the surrounding area were mantled by tephras on 25 May and 12 June 1980. Conifers soon colonized the new surfaces. Erosion has continued in the gully since 1980.

Hike upgully 0.2 km to the first Kalama-age outcrop (46.1694° N, 122.2438° W). Most of this outcrop is composed of early Kalama dacitic pyroclastic flows and lahars. The contact between the early Kalama deposits and the middle Kalama scoriaceous andesite pyroclastic flow lies near top of section.

Continue upgully ~0.8 km past many Kalama-age exposures on both sides. Most are early Kalama dacitic flowage deposits overlain by the scoriaceous middle Kalama andesitic pyroclastic-flow deposit, which is overlain by lahar deposits emplaced at different times. The uppermost lahar is from 18 May 1980. Clasts of late Kalama summit dome dacite lie within all these lahar deposits.

About 1 km from where you entered it, the gully is flanked closely by middle Kalama lava flows to the northwest and by Butte Camp dome (120–110 ka) to the southeast. Here (46.1742° N, 122.2394° W) on the northwest gully side, early Kalama dacitic flowage deposits are overlain by a thin layer of middle Kalama andesitic set-X tephras, in turn overlain by rubble from Middle Kalama andesitic lava flows (see measured section). The section measured in July 1983 was many meters out from the current wall. ***Take care near the unstable outcrop.***

The early Kalama deposits are underlain by Smith Creek-age deposits (about 4,000 to 3,300 yr B.P.) that rest on even older deposits. Paleomagnetic analysis of each early Kalama dacitic unit in the section revealed both lahar and pyroclastic-flow deposits. The distinction is difficult or impossible from visual criteria alone.

Hike back down the gully and climb its northwest side onto the bench adjacent to the lava flow. In summer 2016 this could be done at 46.1723° N, 122.2405° W. (If this route is impassable, see "Alternate route" below.) Climb to top of the bench. Follow this surface northeast through the forest to the overlook at the east edge of the bench (46.1743° N, 122.2396° W) above the measured section. ***The slope below the overlook is steep: beware of the edge***. Upstream the gully becomes a tall rock canyon.

The orange-brown outcrop upcanyon toward Mount St. Helens exposes the same scoriaceous andesitic pyroclastic flow deposits we crossed on the entrance trail and encountered in outcrops in the gully. Before the canyon formed, these scoriaceous flows ponded in a low between the middle Kalama lava flows and Butte Camp dome. These pyroclastic-flow deposits also overlie the lava flows. The canyon formed between the dome and the lava flow, and it dissected the ponded scoriaceous flows. The early canyon that had cut into the scoriaceous pyroclastic flow was then partly filled with lahars, mainly of late Kalama dacites. This fill—the light-colored material left of the orange-brown outcrop—was in turn dissected as the canyon deepened.

Erosion in this canyon increased markedly since 18 May 1980, the canyon now more than 5 m deeper. The early Kalama section is now better exposed but steeper. Sediment eroded from this canyon has now filled in McBride Lake.

Hike southwest ~230 m downslope to the bench along the lava-flow margin. Early Kalama flowage deposits, the middle Kalama scoriaceous pyroclastic-flow deposit, and lahar deposits are locally exposed here. Some of the lahar deposits contain late Kalama summit-dome dacite clasts. A prismatically jointed summit-dome dacite boulder lies in a probable lahar levee (46.1727° N, 122.2415° W). Descend southwest ~585 m to near the terminus of the middle Kalama andesite lava flow (46.1691° N, 122.2470° W). The lava flow evidently followed a channel eroded in early Kalama flowage deposits. You now stand at the base of one bank of the paleochannel. The lava flow is mantled by the scoriaceous pyroclastic flow. Atop that lie spotty lahar deposits, some of them containing late Kalama summit-dome dacite clasts.

Hike ~90 m west to the Toutle Trail (46.1691° N, 122.2482° W) and return by Toutle trail and Blue Lake trail to the parking area.

Alternate route.—If the specified route onto the bench along the margin of the lava flow is impassable, continue down the gully until you find an acceptable route onto the bench. Then follow the instructions for the specific route. Or descend the gully to the Toutle trail and follow it northwest. Leave the trail at 46.1691° N, 122.2482° W and hike through the woods about 0.1 km east to 46.1691° N, 122.2470° W. You are now at the base of the bench. Follow the instructions for the specified route.

Return to parking area of forest road 8123. Drive road 8123 1.5 mile to forest road 81. Drive road 81 east. The former McBride Lake is just south of road at 1.0 mile. Roadcut is just beyond on left at 1.1 mile.

Stop 4.4. Relation of Early Kalama Flowage Deposits to Early Kalama Tephras (46.14192° N, 122.2549° W)

McBride Lake—now filled with sediment from Butte Canyon—lies south of the road. The roadcut across from the lake is capped by a friable gray early Kalama pyroclastic-flow deposit that contains charcoal. This flow overlies scattered lapilli of early Kalama hypersthene-hornblende dacite pumice that is part of the We tephra erupted in 1482 C.E. (table 1). This relation establishes that part of the early Kalama tephras predate part of the early Kalama flowage deposits.

Continue on forest road 81 uphill east. Redrock Pass is in 1 mile. The small parking area is for the trail up to Butte Camp.

Redrock Pass (46.1437° N, 122.2351° W)

Oxidized rubble of an early Castle Creek andesite lava flow, probably ~2,000 yr B.P., is overlain by the Cave Basalt of middle Castle Creek time ~1,895 yr B.P. (M.A. Clynne, unpub. data, 2016).

Here is the trail north up to Butte Camp and the southwest flank of Mount St. Helens. In the late 19th century and early 20th century before roads and when some climbs were

Kalama stratigraphy, measured section on northwest side of "Butte canyon," Stop 4.3 (46.1742° N, 122.2394° W)

Unit	Thickness	Description
		Late dacite
21	0–4 m	Lahar: granules to boulders supported in matrix of cohesive, light pink-brown, silty fine sand; clasts are lithic, angular to subangular, gray and pink dacite of Kalama summit dome; pinches out against lateral flow rubble of unit 20.
		Andesite
20	>10 m	Marginal rubble of andesite lava flow: large angular blocks of andesite, grain supported.
19	0–30 cm	Set-X tephra: dust and ash, bedded, brown, yellowish brown and black; beds are faulted and contorted from loading by overlying flow rubble of andesite flow.
		Early dacite
18C	~1.4 m	Pyroclastic surge(?): dust and ash (lower 50 cm), planar and cross-bedded, gray and pink-gray; grades up into 0.7 m of lapilli and small blocks supported in a matrix of massive gray-brown ash; grades up into 20 cm of planar and cross-bedded, gray-brown to pink-brown dust and ash.
18B	~5–40 cm	Pyroclastic surge(?): lapilli of early Kalama dacite supported in matrix of friable gray ash; massive; gradational contact with unit 18A.
18A	~5–30 cm	Pyroclastic flow or surge(?): coarse ash, lapilli, and small blocks; massive, grain-supported, friable; blocks consist mainly of lithic, gray early Kalama dacite, subordinate pink early Kalama dacite, white pumice and dark-colored pre-Kalama accidental clasts; gradational contact with unit 18B.
17	0–35 cm	Pyroclastic surge: dust and ash, pumiceous, planar and cross-bedded, gray, pink-gray, and tan.
16	1–2 m	Pyroclastic flow: lapilli to large blocks of mainly gray angular to subrounded, lithic to subpumiceous early Kalama dacite, subordinate pink early Kalama dacite, white pumice, and dark pre-Kalama accidental clasts supported in matrix of pink-brown cohesive ash; zone of friable coarse ash along lower contact; many angular clasts prismatically jointed.
15	2.5–3 m	Pyroclastic flow: lapilli to large blocks, grain-supported, subangular to subrounded, dominantly lithic to subpumiceous, early Kalama dacite, subordinate pink early Kalama dacite and dark pre-Kalama accidental clasts; matrix of cohesive, gray-brown ash; many gas-escape structures.
14	10–50 cm	Pyroclastic flow(?): lapilli and scattered small blocks of dominantly gray and pink, subangular lithic to subpumiceous, early Kalama dacite, and subordinate white pumice and dark pre-Kalama accidental clasts in matrix of cohesive brown-gray ash; contact with overlying unit marked only by texture change; may be a fine-grained facies of overlying unit.
13	~2.4 m	Lahar: cobbles, grain-supported, subangular to subrounded, dominantly gray subpumiceous early Kalama dacite, subordinate pink dacite and dark pre-Kalama accidental lithologies; interstices filled with lapilli of cobble lithologies in a matrix of cohesive pink-gray ash; scattered boulders along upper contact.
12	~2.5 m	Pyroclastic flow: lapilli, blocks, and large blocks of dominantly gray subpumiceous early Kalama dacite, normally graded, grain-supported along basal contact; grades upward to matrix supported; matrix consists of friable gray ash; subordinate proportion of pre-Kalama accidental clasts and gray and pink early Kalama lithic clasts.
11	0.8–1 m	Lahar: granules, gravels, and cobbles of white pumice and light-gray subpumiceous early Kalama dacite, concentrated along lower contact, in matrix of gray fine to coarse sand; grades up into a zone dominated by gravel of pink and gray lithic and subpumiceous early Kalama dacite and dark-colored pre-Kalama accidental clasts, in matrix like that of the pumice-rich zone; upper part of unit locally cut and filled by small lahars.
10	1–10 cm	Pyroclastic surge(?): ash, planar-bedded, gray to pink-gray.
9	0–70 cm	Pyroclastic flow: lapilli to blocks of dominantly subpumiceous gray early Kalama dacite supported in a matrix of cohesive, pink-gray ash; dacite clasts are subangular; small proportion of pre-Kalama accidental clasts.
8	0–15 cm	Pyroclastic surge(?): dust and ash, planar and cross-bedded, gray and pink-gray, no oxidation; may be genetically related to unit 9.
Kalama/pre-Kalama contact		
7	~35 cm	Tephra(?): Many beds of ash and dust; various shades of pink, gray, and brown, faint yellow oxidation.
6	1 m	Pyroclastic flow and stream-reworked equivalent: lapilli and blocks of light yellow, cummingtonite-hornblende pumice and gray subpumiceous dacite supported in matrix of pumiceous ash; massive, moderately cohesive; abundant carbonized and incipiently carbonized limbs and wood fragments; upper part fluvially reworked, maximum thickness of undisturbed pyroclastic-flow deposit is 40 cm; faint yellow oxidation throughout.
5	10–20 cm	Set-Y tephra: multiple beds of ash and (or) small lapilli; lapilli are dominantly light yellow, cummingtonite-hornblende pumice, subordinate proportion of lithic lapilli; tephra beds are variably eroded and distorted by overlying unit.
4	1–80 mm	Organic-rich alluvium: organic matter, 1–4 mm, brown, uncharred; locally interbedded with as much as 8 cm of gray silt.
3	0–5 cm	Alluvium(?): silty sand; brown; contains abundant small charcoal fragments.
2	0–7 cm	Tephra(?): ash and small lapilli of pumice and lithic clasts; ash is pink-gray; lapilli are light gray; lapilli are angular to subangular; discontinuous.
1	>1 m	Dome rubble: large blocks of Butte Camp Dome dacite 120–110 ka, grain-supported; interstices filled with silty sand (ash ?); soil developed on top, charcoal fragments and discontinuous bright orange lenses of Mazama ash in soil.
~18 m total thickness		

led by George Merrill and L.A. McBride, the usual hiking trail to Mount St. Helens lay roughly where forest road 81 now lies from near Cougar past Merrill Lake and McBride Lake to here (Waitt, 2015, chapter 2). The trail upslope is the surviving remnant of that old trail.

Continue east and southeast on forest road 81, now downslope. In 2.9 miles lies intersection of Road 83 (our route latter part of Day 3. Follow road 83 downslope south 1.3 mile and turn right northwest onto road 8303. In 0.9 mile on the 8303 turn into parking lot for Ape Cave.

Stop 4.5: Ape Cave (46.1081° N, 122.2117° W)

Ape Cave is the longest known (3,400 m) uncollapsed lava-tube segment in the world (Greeley and Hyde, 1972). This beautifully formed tube is one of many lava tubes within the Cave Basalt (~1,895 years old). This most extensive part of the Cave Basalt flowed south down a stream channel cut into dacitic pyroclastic flow and lahar deposits of Swift Creek age (16–10 ka) (Crandell, 1987; M.A. Clynne, written commun., 2016). The lava flow—its volume ~0.25 km^3—reached Lewis River 14 km from the presumed flank vent at about 1,600-m altitude on the volcano.

Dress warmly: the cave is cool and damp. You provide your own illumination. A flashlight is adequate, a lantern superior, a backup recommended. Descend stairway to cave floor. The reach of cave downhill of the entrance has little rubble from roof collapses. Many large rubble piles clutter uphill reaches. Explore downhill part as time and interest permit.

Return south on forest road 8303. In 0.7 mile turn into parking area for Trail of Two Forests.

Stop 4.6. Lava Cast Area ("Trail of Two Forests") (46.0995° N, 122.2126° W)

Trails lead to numerous tree molds—some upright, some horizontal—all surrounded by and thus within the Cave Basalt (about 1,895 cal yr B.P.) They show details of how a thin lava flow may engulf a standing coniferous forest.

Follow forest road 8303 east ¼ mile to forest road 83. Drive road 83 downslope south 1.7 mile to intersection of forest road 90. On road 90 continue downslope south 0.9 mile to Swift Dam overlook.

Swift Dam Overlook (46.0666° N, 122.1996° W)

This overlook is on a Cougar-age fan (20 to 18 ka) that once blocked Lewis River. (View is now so overgrown we won't stop.) Other remnants of the fan lie to the east just beyond Swift Creek and to the southwest on the south side of Lewis River 70 m lower than the overlook. A large debris avalanche overlain by pyroclastic flows (seen at Stop 3.6), lahars, and tephras compose the fan (Hyde, 1975; Crandell, 1987; Clynne and others, 2008).

End Day 4.

Day 5. Modern and Ancient Volcaniclastic Sedimentation in Toutle Valley

In Toutle River valley (fig. 47) we examine prehistoric lahar deposits, effects of the 1980 eruption, and later geomorphic and biologic changes. Lahars have flooded the Toutle many times in the past 50,000 years, and it is the watershed most affected by the 1980 eruption.

This leg of field trip proceeds east up highway 504 (State Route 504). All stops but 5.2 and 5.8 are along or just off the highway at signed sites. Directions are mainly by approximate milepost on SR 504. The miles are highway distance east from Interstate 5.

Stop 5.1. Mount St. Helens Visitor's Center at Silver Lake (SR 504, mile 5.3, 46.2945° N, 122.8211° W)

First operated by the U.S. Forest Service and now by Washington State Parks, the Mount St. Helens Visitor's Center on Silver Lake (fig. 5) has displays, movies, maps, and books about the 1980 eruption. Mount St. Helens is visible here in good weather.

Silver Lake formed about 2,500 years ago when large lahars dammed Toutle River tributary Outlet Creek. Four lahars swept down Toutle valley during the Pine Creek period (fig. 7), the largest exceeding 1 km^3 in volume and 260,000 m^3/s in peak discharge. Sudden dambreak release of an ancestral Spirit Lake is the only plausible source of so much water.

Two debris avalanches off Mount St. Helens's north flank date to ~2,560 cal yr B.P. (Hausback and Swanson, 1990). They must have dammed ancestral Spirit Lake to a then-new higher level. The lake then gradually rose until it overtoped this debris dam. This overflow downcut swiftly, releasing much lake water catastrophically.

In its 2,500 or so years, Silver Lake has undergone a natural succession from open water to a lilypad marsh now only 3 m deep.

Stop 5.2. Pine-Creek-age lahars on Outlet Creek (46.3241° N, 122.7281° W)

SR 504 to Toutle; southeast [right] on S. Toutle Road; in 230 m turn left into Toutle transfer station.

This stop is along Outlet Creek at the southeast end of the Toutle transfer station. (Please check with site manager for permission to park and access the site. Do not obstruct station operations.) From the southeast corner of the station site, walk through semi-open brush down to the creek and 30 meters downstream along Outlet Creek.

The outcrop (fig. 48) exposes two 2–3-m-thick Pine Creek-age lahar deposits that overlie a soil dated to 3,520±30 cal yr B.P. developed on older lahar deposits. The older Pine Creek deposit is

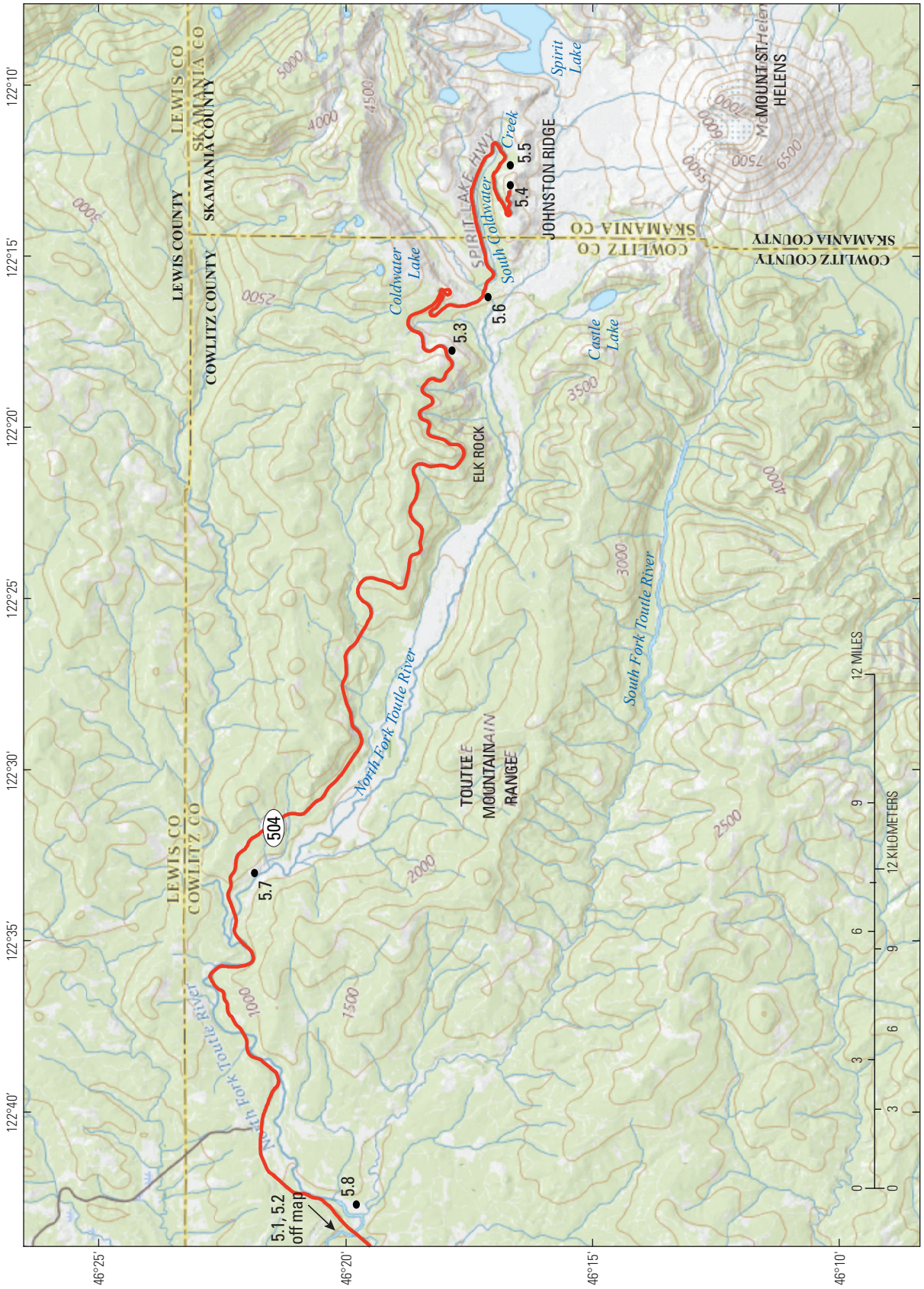

Base from The National Map and USGS National Elevation Dataset WGS 1984 Mercator projection

Figure 47. Index map for route and stops of Day 5. Stops 5.1 and 5.2 on figure 49.

Figure 48. Lahar deposits of Pine Creek age (~2650 cal yr B.P.) in Toutle River valley near confluence of the North Fork Toutle and South Fork Toutle. These deposits formed from breakouts of an ancestral Spirit Lake dammed by debris avalanche(s) from an eruption of Mount St. Helens approximately 2900–2500 years ago. Here they overlie soil developed on older lahar deposit (also see Scott, 1988b, 1989). PC1, the largest of four lahars, had a volume of 10^9 m^3 (Scott, 1988b). Dashed line highlights a clast of debris-avalanche deposit entrained by the lahar. Geologists stand 5–10 m above present river level, similar to river level when these lahars passed. USGS photograph by Jon Major.

dated to 2,560±200 cal yr B.P. (Scott, 1989). The gray Pine Creek deposits are massive and poorly sorted, composed mainly of subrounded to rounded dacite gravel in a sandy matrix. The deposits are inversely graded near their bases, normally graded near their tops. The older Pine Creek-age deposit contains rare megaclasts to 1-m diameter of pinkish-gray poorly sorted diamict.

On Mount St. Helens's north flank lie two Pine Creek-age debris-avalanche deposits, each smaller than the 1980 one (Hausback and Swanson, 1990). The base of the younger deposit contains uncharred logs dated to 2,640±290 cal yr B.P. The Pine Creek-age lahar deposits here have classic debris-flow texture yet contain dominantly fluvial gravel. They must originate by breachings of an ancestral Spirit Lake that had been dammed by one or both of the avalanches. The enclosed megaclasts are likely pieces of the debris avalanches. Scott (1988b) infers that these lahars as sediment-rich flows that began as watery floods.

Stop 5.3. Castle Lake Viewpoint (SR 504, mile 41, 46.2966° N, 122.2993° W)

Bedrock in this area is andesite lava flows and fragmental volcanic rocks of late Eocene and early Oligocene ages (~35–27 Ma). In this east-dipping homocline we are downsection of similar rocks east of Mount St. Helens (seen on Days 1 and 2) as young as earliest Miocene (25–20 Ma) (Evarts and others, 1987). The higher country to the northeast is carved in the early Miocene Spirit Lake granodiorite pluton, dated 22 Ma (Evarts and others, 1994).

From time to time Pleistocene glaciers formed in the high country to the northeast and probably also on Mount St. Helens. A trunk glacier filled Toutle valley here and reached downvalley to Hoffstadt bluffs. Several moraines of Hayden Creek age and older (probably ~140 ka and older) lie along both valley sides west of Elk Rock (fig. 11) (Crandell, 1987; Burk and others, 1989). Glacial erosion beveled the steep slopes at the south end of this ridge and at Elk Rock downvalley. Before 1980 the valley floor had partly filled by lahars and pyroclastic flows from Mount St. Helens eruptions during Ape Canyon (40–35 ka) and Swift Creek (16–13 ka) stages, and during Smith Creek (3,900–3,000 cal yr B.P.) and Pine Creek (3,000–2,550 cal. yr B.P.) periods.

This would have been an unhealthy spot at 8:35–8:40 a.m. on 18 May 1980 when the surge from Mount St. Helens swept this ridge 13.5 km from the crater.

We see here large effects of the 18 May 1980 eruption (fig. 49): 1980 crater, remnant trees knocked down by the surge, huge debris avalanche, many ponds filling lows among avalanche hummocks, and lakes dammed in tributaries at avalanche margins. Natural revegetation within Mount St. Helens National Volcanic Monument contrasts with planted nowsizable firs on state and private timberlands just west.

The landslide came as three blocks (fig. 50), the first two showing on eyewitness photographs (fig. 22). Slide block III went unseen beneath the swelling eruption cloud. Slide block I remained fairly intact as it slid north, depositing debris in Spirit Lake and on and near Johnston Ridge. Part of slide block I flowed west down Toutle valley, forming the margins of the debris-avalanche deposit. Johnston Ridge steered most of slide block II and all of slide block III west, and they became a flowing debris avalanche down the valley center. Avalanche deposit in the upper North Fork Toutle covers 60 km^2 to average depth 45 m.

This hummocky landslide deposit blocked several tributary valleys and it dammed lakes. About 0.4 km^3 of the avalanche inundated Spirit Lake and blocked its outlet. The avalanche's left margin dammed Castle Lake to the south (figs. 5, 51), and the right margin Coldwater Lake to the east. An avalanche trimline once marking the walls of South Coldwater valley fades

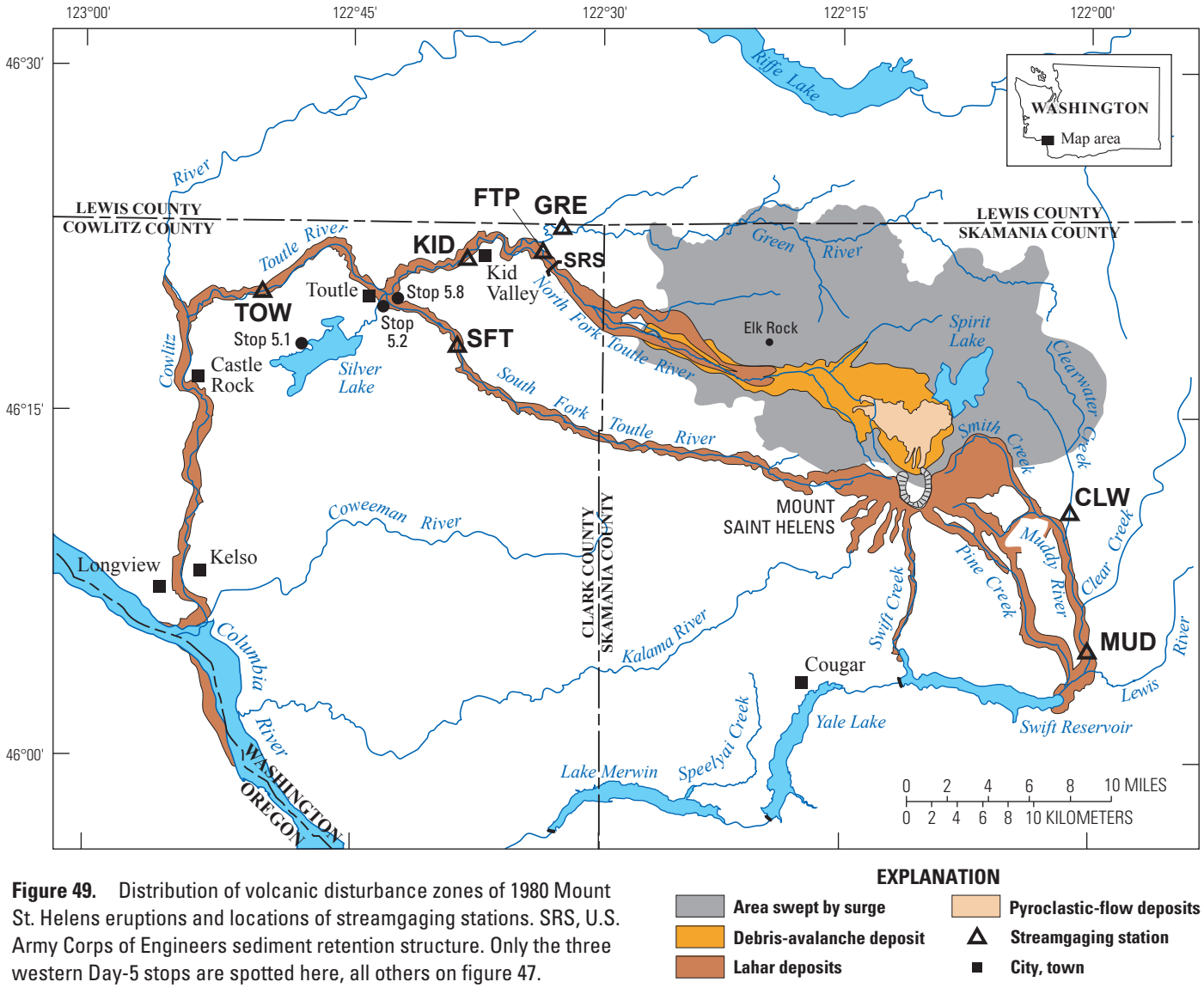

Figure 49. Distribution of volcanic disturbance zones of 1980 Mount St. Helens eruptions and locations of streamgaging stations. SRS, U.S. Army Corps of Engineers sediment retention structure. Only the three western Day-5 stops are spotted here, all others on figure 47.

with the passing years. The many terraces along the North Fork were cut in just a few years as the river incised the avalanche.

Outlets engineered at Coldwater, Castle, and Spirit Lakes prevent uncontrolled breaches of the sort that dammed Silver Lake in Pine Creek time (Stops 5.1 and 5.2). Several wells monitor groundwater levels within the Castle Lake blockage. A 2.6-km tunnel drilled through bedrock to South Coldwater Creek drains Spirit Lake.

The mountain's groundwater carried off in the landslide began to leak from the avalanche deposit within two or three hours. Most of it emerged from the reach just upvalley of us. By 12:40 p.m. (18 May 1980) a flood was big enough to be spotted by search-and-rescue helicopters despite thick haze in the reach of valley below us. In two more hours it was ravaging much farther downvalley. Water continued to pour out of the avalanche just above here until after dark. Many firsthand accounts of this flood appear in Waitt (2015, chapters 16 and 19).

Stop 5.4. Johnston Ridge Observatory [a U.S. Forest Service Visitor's Center: includes restrooms] (SR 504, mile 52, 46.2754° N, 122.2168° W)

Johnston Ridge is named for David A. Johnston, U.S. Geological Survey scientist, who a few hundred meters west of here died in the first minutes of the 18 May 1980 eruption. The eruption transformed the landscape before us (fig. 52). Johnston Ridge (Oligocene basalt and fragmental flows) bore the brunt of the explosive 1980 eruption. On the volcano side the surge scoured vegetation and soil down to bedrock and draped the ridgecrest with a meter of gravel and sand. Flowing twice as fast as the avalanche, the surge got here first. Most of its deposit underlies the avalanche. Razed trees on the lee of the ridge fell not north but uphill south—*toward* the volcano. They reveal eddies in the surge as it sped over sharp ridges.

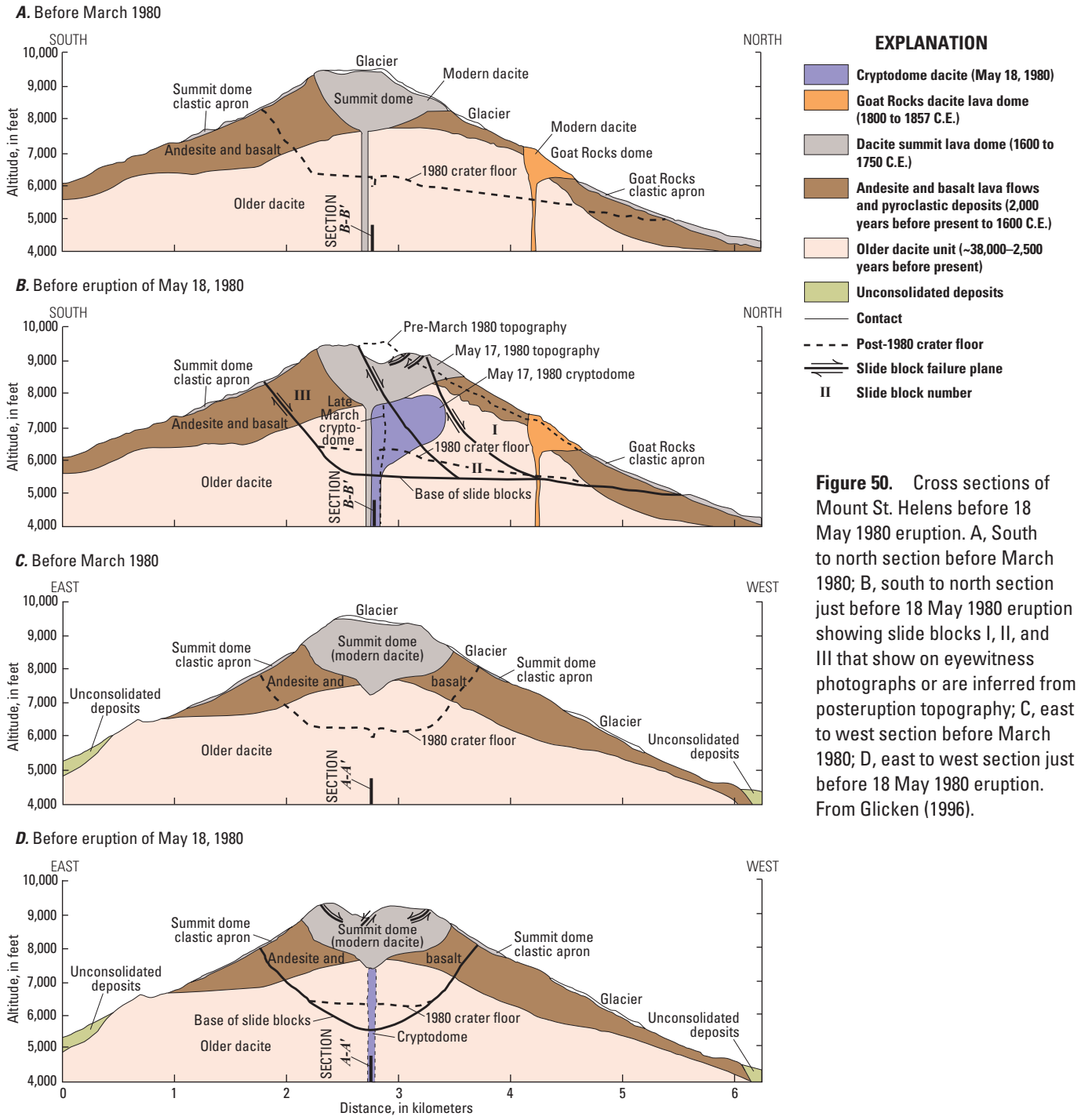

Figure 50. Cross sections of Mount St. Helens before 18 May 1980 eruption. A, South to north section before March 1980; B, south to north section just before 18 May 1980 eruption showing slide blocks I, II, and III that show on eyewitness photographs or are inferred from posteruption topography; C, east to west section before March 1980; D, east to west section just before 18 May 1980 eruption. From Glicken (1996).

The composite debris avalanche slammed into this ridge and mostly turned west down the North Fork. But one arm overrode the ridge and dropped into South Coldwater valley. Its remnants top parts of the ridgecrest east of the observatory.

This splendid view into the 1980 crater shows light-colored dacite in the volcano's core overlain by mafic andesite and basalt of Castle Creek age higher in the crater walls. Kalama-age dacite in turn locally overlies the mafic rocks (fig. 53*A*).

In the crater center the large 2004–08 dome lies just south of the 1980–86 lava dome (fig. 53*B*). The growing 2004–08 lava dome split Crater Glacier and squeezed it against the east and west walls (Walder and others, 2008). The twin arms of the regrown glacier wrap around both domes, join just north, and in recent years the glacier has advanced to the crater's the north edge.

Channels incise through avalanche and overlying pyroclastic-flow deposits. The cleft of Loowit canyon on the

Figure 51. Oblique aerial view to east-southeast of part of upper North Fork Toutle River valley. Castle Lake dammed by left margin of 18 May 1980 debris avalanche. USGS photograph by Steven Brantley, 1992.

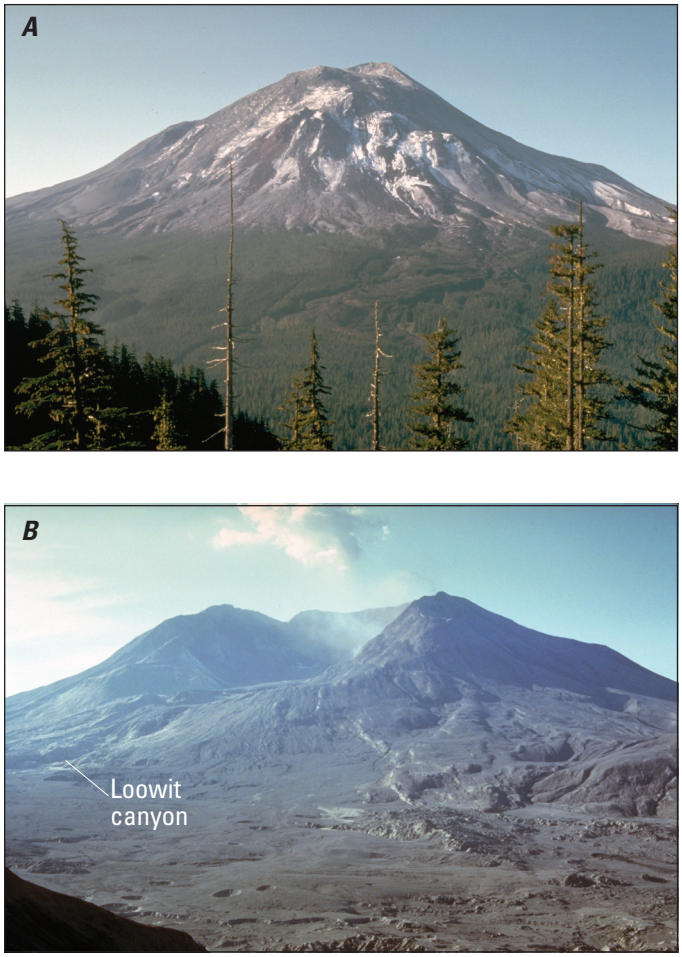

Figure 52. Photographs of Mount St. Helens from Johnston Ridge 10 km northwest of the volcano. *A*, 17 May 1980; *B*, 10 September 1980. Loowit canyon has enlarged greatly since late 1980. USGS photographs by Harry Glicken.

lower north volcano flank also deepened. Most of this erosion occurred in the few years after eruption. In the past 20 years the channels have widened laterally but not further incised (Zheng and others, 2014; Major and others, 2018).

Stop 5.5. Ridgetop Trail—Johnston Ridge Observatory to Avalanche Runover (46.2733° N, 122.2084° W)

From JRO we hike about 1.2 km east on trail and return (about 0.6 km paved, 0.5 km gravel).

Two of the 1980 landslides off Mount St. Helens ran over two saddles on Johnston Ridge—up 390 m from the ridge's pre-eruption base. Hiking the trail east, we cross from higher areas swept only by the surge into a broad saddle overtopped also by landslide (by this distance they're debris avalanches) (fig. 54). What evidence marks our crossing into debris avalanche?

Between two saddles lies a slightly higher "island" not overridden. This contact gives a maximum level the surface of the avalanches reached. An upper limit is also visible 1–1.5 km east in a sharp trimline high on Harrys Ridge. There one finds jams of logs that the landslide bulldozed aside.

Where an avalanche runs up onto an opposite valley side, converting its kinetic energy to altitudinal energy, one measure of its velocity just before runup is the conservation-of-energy relation $v=\sqrt{2gh}$, where v is velocity of flow, g is gravitational acceleration, and h is height or runup.

At a distance of 7.3 km from the former summit of Mount St. Helens, a toe of the 1980 debris avalanche, having crossed a valley floor, rode 390 m up over ridgecrests (fig. 55). Were this debris flowing entirely by its own momentum, a frictionless flow would be moving at least 87 m/s (313 km/hr) to achieve this runup. A tongue of this flow struck Spirit Lake with enough speed and volume to raise waves as high as 265 m on opposite shores.

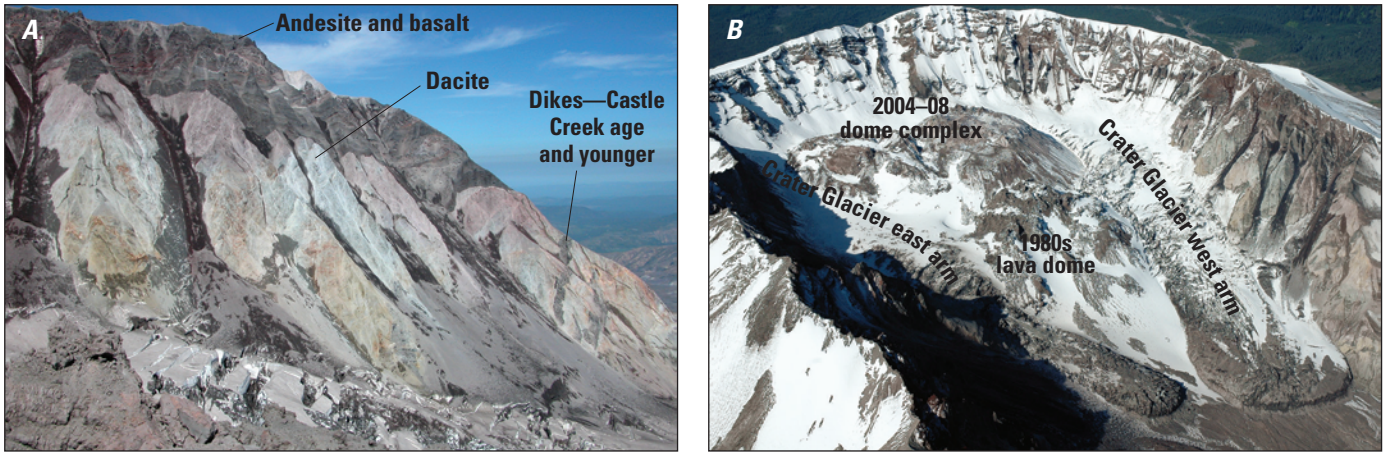

Figure 53. Views of Mount St. Helens crater. *A*, View of west crater wall showing older dacite core of volcano (>2,500 cal yr B.P.) overlain by units of andesite and basalt (≤2,500 cal yr B.P.). Dikes cut through older dacite core. Length of this view ~0.8 km. USGS photograph by D.R. Sherrod 8 July 2008. *B*, Oblique aerial view to southwest of 1980–86 and 2004–08 lava dome complexes and arms of Crater Glacier. Rim to rim, crater is about 1.7 km wide. USGS photograph by J.W. Vallance, 26 June 2007.

Figure 54. View directed northeast of mounds of 18 May 1980 debris-avalanche deposit ramping up south side of Johnston Ridge.

But some rock avalanches, as at Avalanche Lake (Northwest Territories, Canada), clearly achieved high runups by being partly shoved from behind (Evans and others, 1994). If a debris avalanche transfers some momentum from its head to its toe, the simple equation above yields a velocity too high—rather than being a minimum. For the Avalanche Lake slide, Evans and others (1994) apply dynamic simulations that include longitudinal forces—a push from behind. Calculations from centers of mass before and after the slide yield maximum velocity as little as 71 percent of the "minimum" velocity from the $v=\sqrt{2gh}$ relation.

The Avalanche Lake exercise provides an arithmetic means to scale down the high velocities for the Mount St. Helens slides just before runup. If assisted by a push from behind, runup velocity reduces to 61–65 m/s (220–235 km/hr) as it reached the base of the ridge.

Before and after photos of the crater from nearby Harrys Ridge show the changes by growth of lava domes in 1980–86 and in 2004–08 as well by Crater Glacier's growth (fig. 56).

Stop 5.6. Hummocks Trail (SR 504, mile 45, 46.2866° N, 122.2716° W)

The Hummocks Trail is a 3.5-km loop over the debris-avalanche deposit. This fairly easy hike includes 100 m of net altitude loss and then gain over hilly terrain.

The 18 May 1980 eruption began with gigantic mass movements (fig. 50). Three slide blocks—a series of retrogressive slope failures—formed into a composite debris avalanche—all together 2.5 km^3. Glicken (1996) mapped the slide-block distributions by rock type—older dacite, andesite and basalt, modern dacite—that match outcrops in the crater walls. Here we are near the boundary of slide blocks I and II (fig. 57).

Colors and mineralogy in the hummocks reveal rock types (figs. 58, 59). Older dacite is white, gray, or pink hornblende-hypersthene dacite; dark minerals and plagioclase phenocrysts longer than 2 mm make a salt-and-pepper look. Andesite and subordinate basalt is black to dark gray, red where oxidized or otherwise altered. Modern dacite is a gray-pink hornblende-hypersthene dacite with many inclusions and phenocrysts generally smaller than 2 mm.

Glicken's (1996, plate 4B) 1:12,000-scale map shows a pattern: younger black andesite and basalt and modern dacite (units dab, dmd, dwu) at the margins, older dacite (unit dod) in the center, and mixed matrix (unit dmx) in distal reaches. Comparing the pattern of rock types with the old mountain shows where the three fragmenting slideblocks ended (figs. 45, 57–59).

On a high hummock, white hornblende-hypersthene dacite of the "older dacite" unit (pre-Castle Creek, older than 2,500 cal yr B.P.) underlies the "andesite and basalt" unit (fig. 60). This contact is like that in the crater (figs. 50, 53A). So the hummock is a single block, the contact here right-side-up. The debris slid and perhaps turned in map view but didn't tumble.

Besides compositional differences, the avalanche comprises two distinct facies: block facies (pieces of the mountain

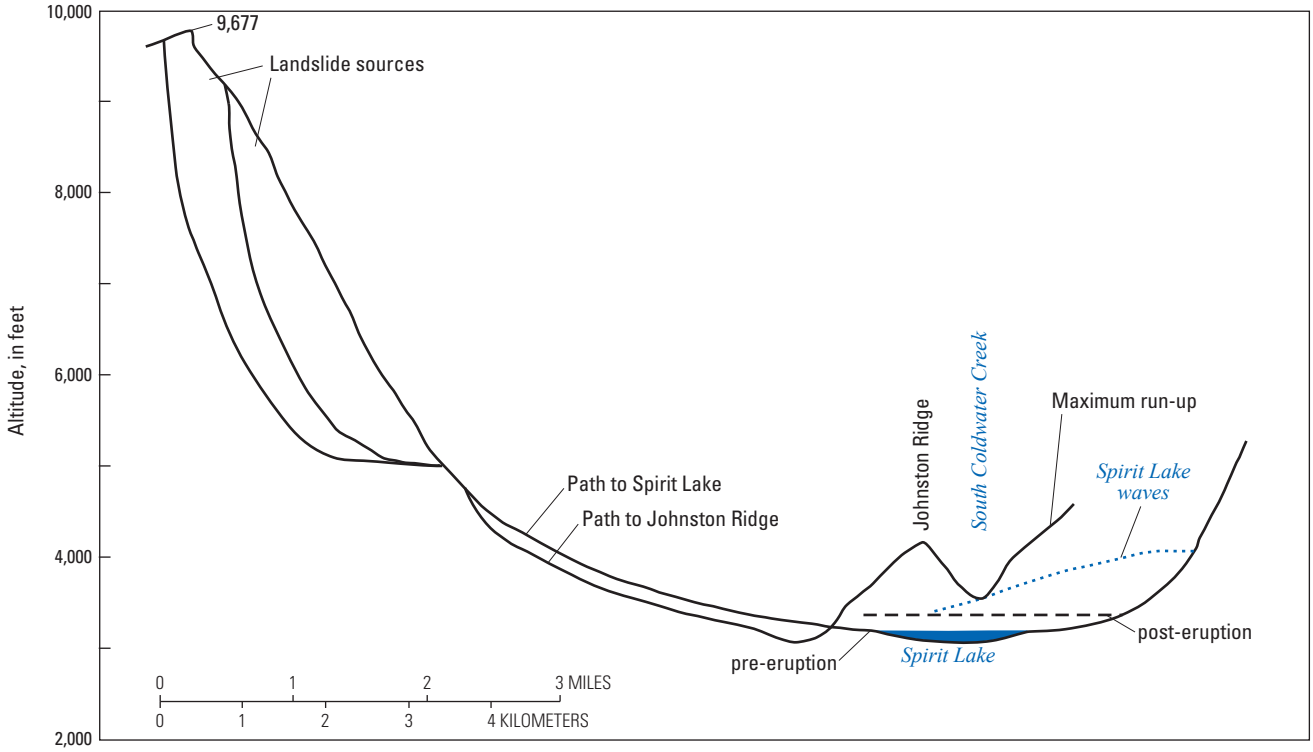

Figure 55. Two profiles of Mount St. Helens 18 May 1980 landslide paths: to South Coldwater Creek runup, and into Spirit Lake. From Waitt and Begét (2009).

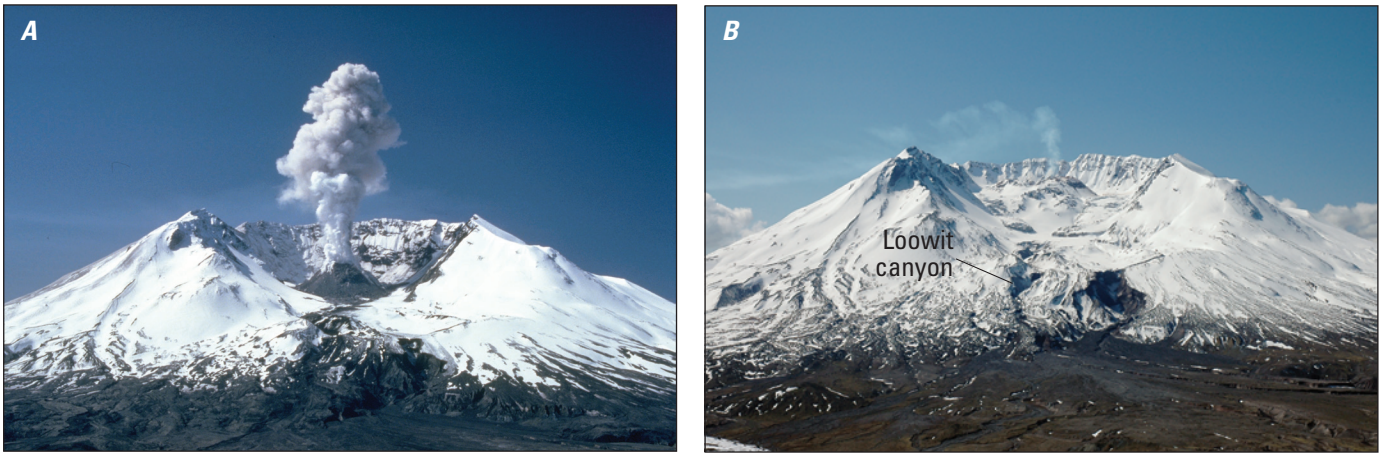

Figure 56. View from Harry's Ridge southward to Mount St. Helens. *A*, 19 May 1982. USGS photograph by L. Topinka. *B*, 20 April 2008. USGS photograph by E. Iwatsubo. Loowit canyon enlarged by runoff from the crater.

moved fairly intact), and matrix facies (disintegrated rocks from the mountain mixed with the 1980 dacite magma) (figs. 58, 59). In the block facies the shattered clasts preserve the mountain's stratigraphy. The matrix facies contains rock types from the mountain thoroughly mixed into unstratified textures. The block facies of proximal areas grades into matrix facies in distal parts.

The hummocks—the most distinctive landform of the debris-avalanche deposit—formed as simple horsts and grabens and by interaction within the avalanche as it decelerated (Glicken, 1996). In laboratory experiments, Paguican and others (2014) show that hundreds of hummocks develop as a landslide in an extensional environment spreads laterally while flowing downvalley—making hundreds of Toreva-like rotation blocks along small normal faults, some separated by small strike-slip faults.

Ponds and wetlands in lows among the hummocks have promoted rapid biological recovery. Plants abound along groundwater-fed brooks, seeps, and ponds on the avalanche surface. But the North Fork Toutle floodplain is repeatedly disturbed. Plants there are sparse and far less diverse. One sees here the voluminous erosion as the North Fork Toutle reestablished across the deposit.

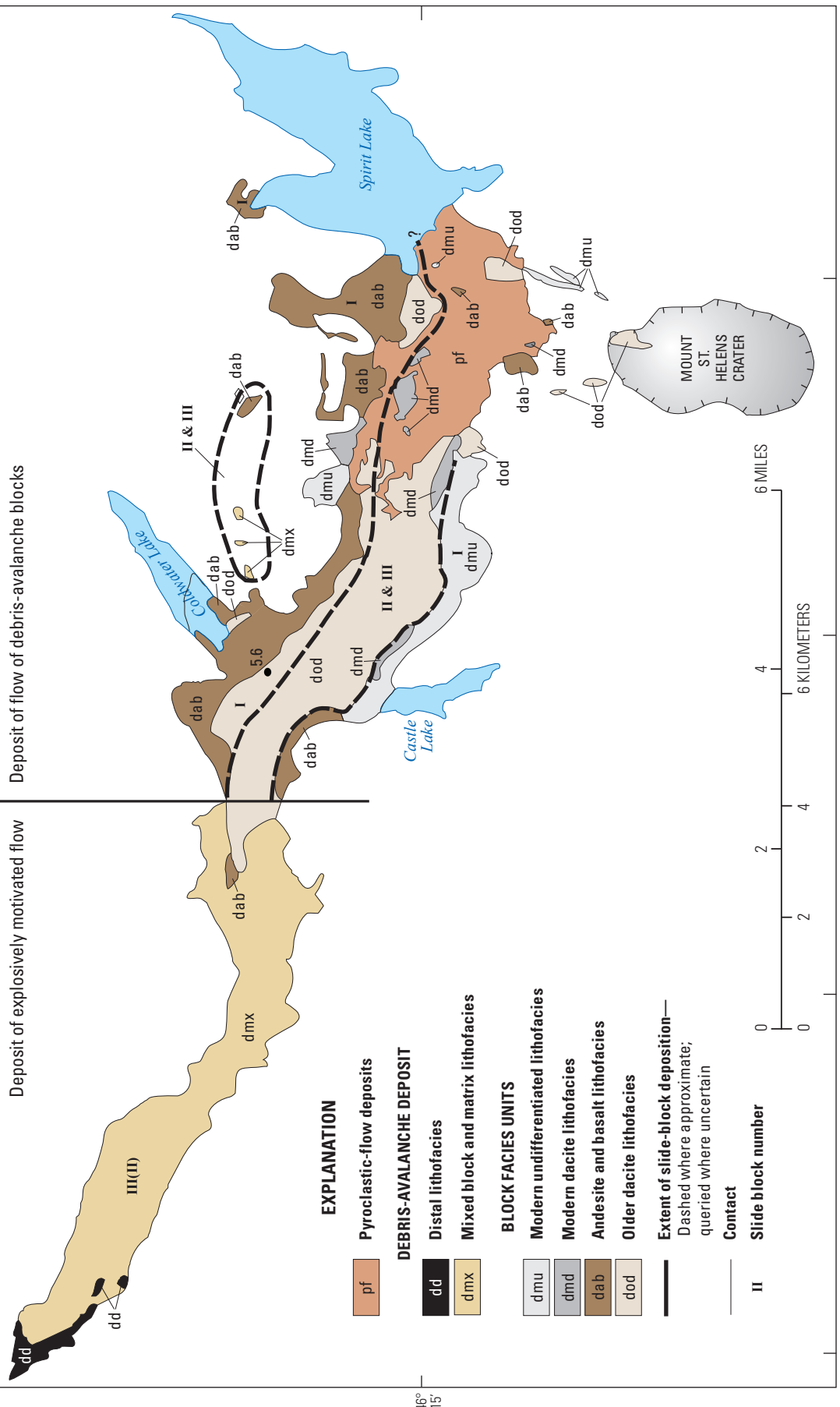

Figure 57. Generalized map of 18 May 1980 debris-avalanche deposit. Roman numerals indicate inferred derivation from the three slide blocks off Mount St. Helens (see fig. 50). From Glicken (1996).

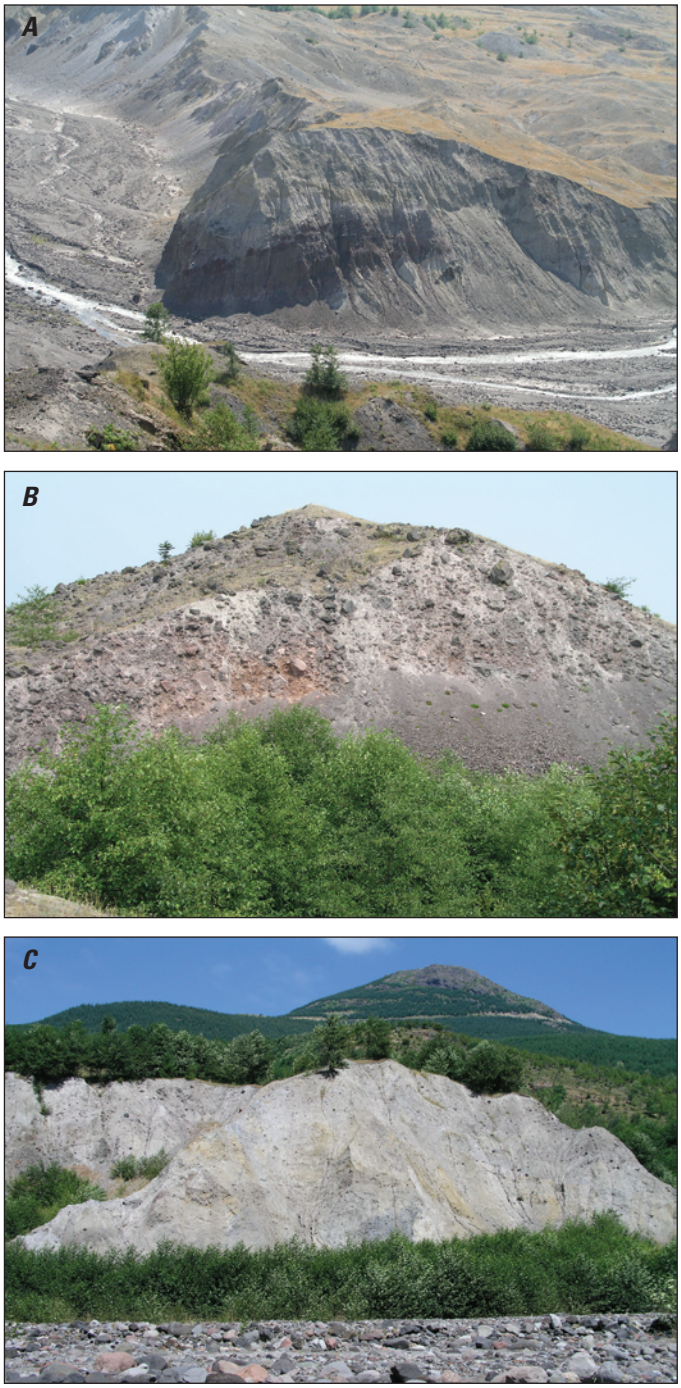

Figure 58. Images of textures of hummocks in 1980 debris-avalanche deposit. Some hummocks retain stratigraphic relations observed in volcano and represent block facies transported more or less intact from volcano to depositional site (*A*). Others partly mix with matrix, but rocks remain fairly large (*B*). Still others represent broad lithologic units from the volcano, but retain no stratigraphic relations and the components are pulverized, called by Glicken (1996) matrix facies (*C*).

Drive 24 miles down SR 504. Just west of big bridge over the river (near milepost 21), turn left onto Sediment Dam road. Follow it east to road's end in 0.9 mile.

Stop 5.7. Sediment Retention Structure (SRS) (off SR 504, mile 21, 46.3632° N, 122.5489° W)

Erosion of the voluminous debris-avalanche and pyroclastic deposits vastly increased the flux of sediment down Toutle valley. In the 37 years since eruption, Toutle River has moved nearly 360 Mt (million metric tons) of suspended sediment past the gaging station Toutle River at Tower Road (informally called TOW; figs. 49, 61, 62) (Major and others, 2000, 2018; U.S. Geological Survey streamgage 14242580, accessed March 27, 2018, at https://waterdata.usgs.gov/wa/nwis/inventory/). This load—including some from the South Fork Toutle—is 14 percent of the total 1980 debris-avalanche volume in the upper North Fork Toutle. Lahars during the eruption moved 300 Mt of

Figure 59. Oblique aerial images of 18 May 1980 debris-avalanche deposit in upper North Fork Toutle River valley. Note the hummocky topography, general texture, and deposit erosion. Broad stratigraphic texture shows mostly in hummocks close to the volcano (*A*), whereas farther downvalley textures are more blended (*B*). Hummock size generally decreases downvalley.

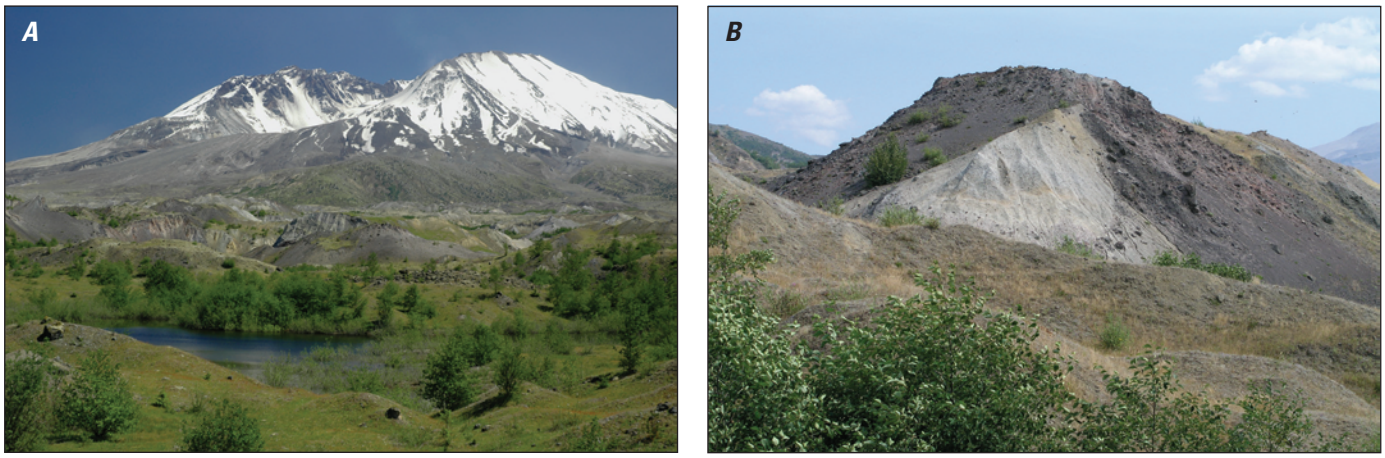

Figure 60. Ground images of 18 May 1980 debris avalanche deposit. *A*, Upstream view of deposit from intersection of Hummocks Trail and Boundary Trail. *B*, Hummock along Hummocks Trail that preserves original stratigraphy: andesite and basalt unit overlie older dacite (compare this dark over light stratigraphy with such stratigraphy in rock in figure 53*A* and with that in distant hummocks in figure 59*A*).

this material (Fairchild and Wigmosta, 1983; Major and others, 2005). A March 1982 lahar contributed ~3 Mt (Dinehart, 1998). Winter storms over the years have moved most of the rest of the material (Major, 2004). Severe storms and runoff in January 1990 and February 1996 moved particularly large volumes of sediment. Such prodigious sediment wreaks havoc downstream in Toutle and Cowlitz Rivers, aggrading their beds and diminishing conveyance. The U.S. Army Corps of Engineers (USACE) spent much time and money in 1980–87 dredging channels (fig. 63). This was unsustainable. So the USACE developed a longer-term plan to manage sediment coming downriver: storing much of the sediment upriver. And so this sediment retention structure (SRS) was built on the lower North Fork Toutle.

The 550-m-long, 56-m-high earth-cored SRS began trapping sediment in November 1987. Stacked rows of culverts in its face allowed sediment to settle but water to pass. As sediment accumulated to the level of lowest culverts, that row was closed and the next higher opened. Ultimately all culverts were closed and flow now passes over the north-end spillway. The structure had by 2007 trapped ~130 Mt of sediment.

Once the SRS began operations, the sediment mass passing KID and TOW gaging stations below the SRS plummeted (figs. 61, 62). Yet the amount of sediment accumulating behind the SRS and the fluxes past TOW indicate sediment flux from the upper North Fork Toutle remains several tens of times that before the 1980 eruption (Major and others, 2018). Lateral erosion rather than vertical incision delivers the persistent sediment (fig. 64).

Sediment filled the SRS to the spillway level by 1998. Sand and finer sediment now bypass the SRS, renewing problems in lower Cowlitz River. In 2007 the USACE again dredged the Cowlitz. They have since constructed grade-building structures (engineered log jams) in the sediment plain and raised the lip of the spillway 2.1 m to induce additional sedimentation. These measures are part of a phased sediment-management strategy of the USACE.

The SRS has no passage for migratory fish. USACE built a fish facility 2 km downstream (McCracken, 1989). Washington Department of Fish and Wildlife collects wild coho salmon and steelhead trout there and releases them in upstream tributaries. Yet a dam is a dam. Conservationists and sport fisherman fret over fish mortality and restricted passage of fish migrating upstream and downstream (Hinson and others, 2007).

Drive SR 504 west to Toutle; turn south (left) on South Toutle Road and in 2.3 km turn left into Harry Gardner Park. Drive to end of turnaround. Walk west to South Fork Toutle River, then north 250 m to exposures along left bank of the North Fork Toutle just upstream of confluence.

Stop 5.8. Lahar Deposits of 18 May 1980 (46.3287° N, 122.7108° W)

Exposed in the riverbank are deposits of two 1980 lahars with contrasting textures (fig. 65). The lower deposit overlies soil where pre-1980 trees are rooted. This first lahar came down South Fork Toutle River. The deposit is composed mainly of granules to small-pebble gravel in a massive sand matrix. This lahar formed when the hot and turbulent surge (or pyroclastic density current) spilled down the west flank of the volcano, melting snow and ice (Fairchild, 1987; Scott, 1988a; Waitt 1989). This lahar ran downvalley more or less as a flash flood—a very rapid rise to its peak, and rapid fall from it. Peak discharge dropped sharply with distance downvalley (Fairchild and Wigmosta, 1983; Fairchild, 1987; Major and others, 2005). About 4 km from the volcano it had peak discharge of about 68,000 m^3/s and volume of about 14 million m^3—but for only 6.5 minutes. By the time flow arrived here at the confluence of the South and North Fork Toutle Rivers, 50 km downstream from the volcano, it had lost most of its coarse load and was in transition to a diluted hyperconcentrated flow. Here its peak discharge was about 4,000 m^3/s, volume about 8 million m^3, and it lasted about an hour.

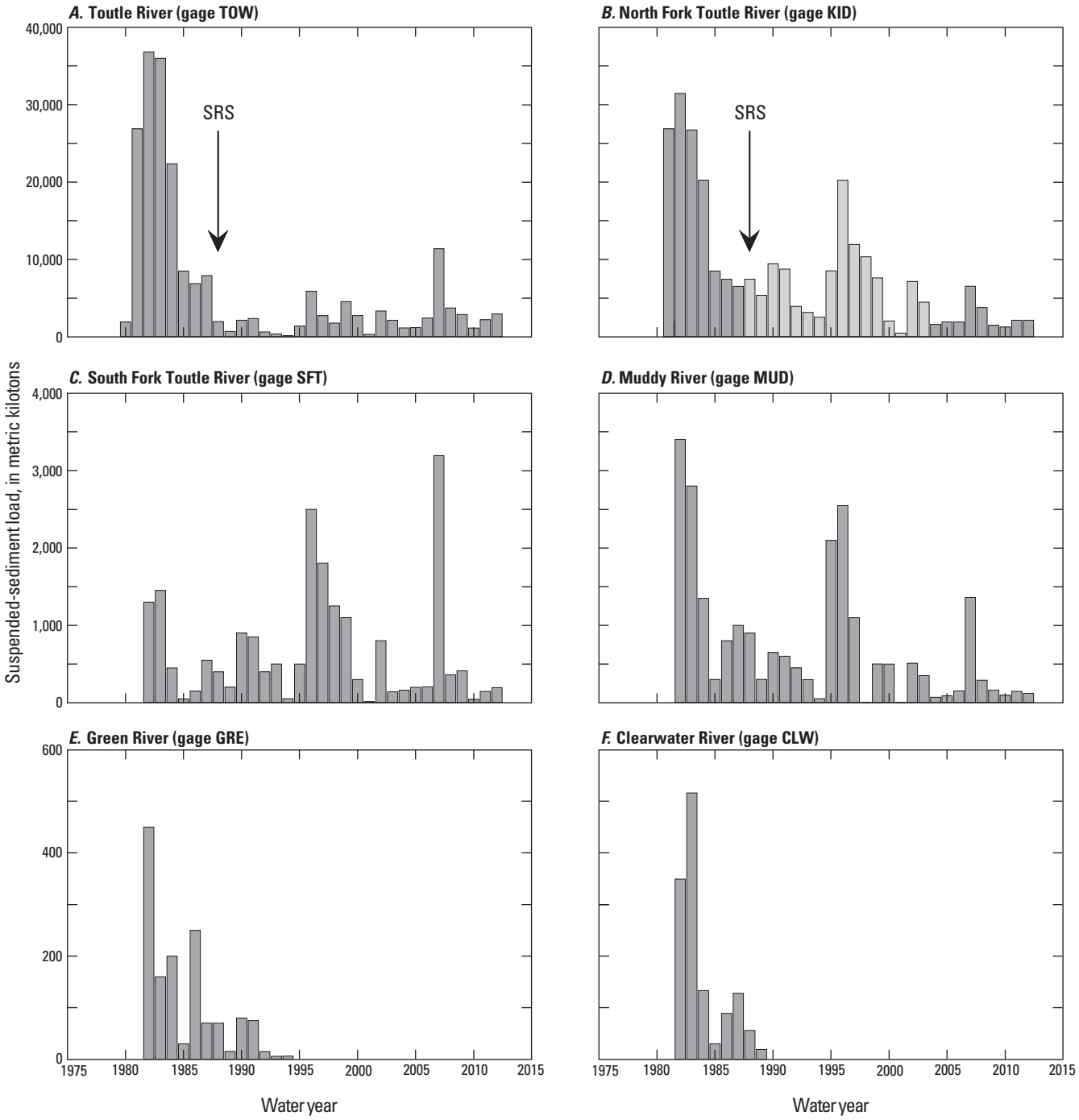

Figure 61. Time series of suspended-sediment loads measured at various streamgaging stations (3-letter codes) at Mount St. Helens. The lightest colored bars for North Fork Toutle River show projected load that would have been measured if sediment retention structure (SRS) had not been built; the darkest bars show loads measured at station FTP just downstream of SRS. Note the approximately order-of-magnitude change in vertical scale for different disturbance zones. See figure 48 for basin disturbances and locations of gaging stations. Modified from Major (2004) and Major and others (2018).

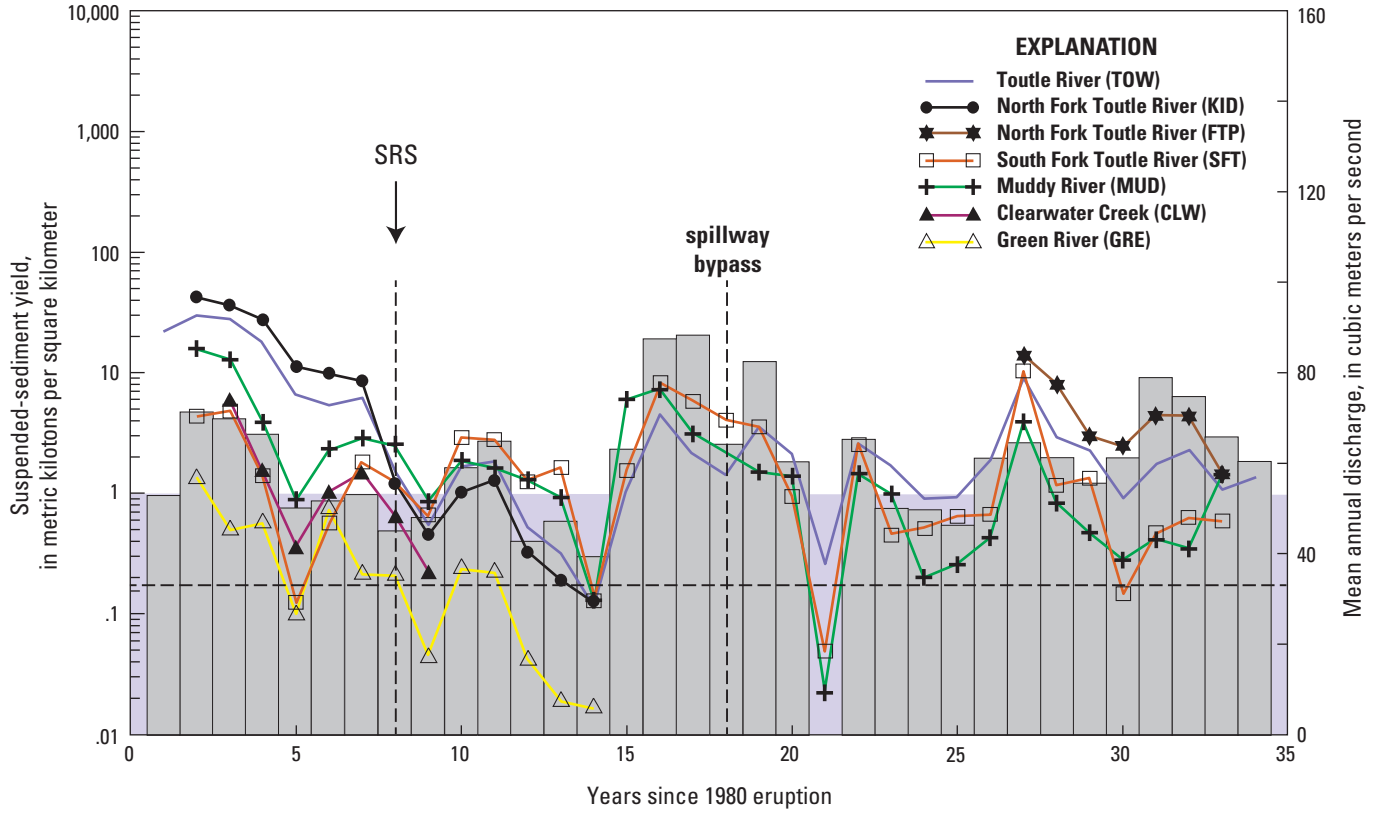

Figure 62. Time-series plot of suspended-sediment yield (load per unit basin area) at Mount St. Helens. See figure 49 for basin-disturbance map and streamgage locations. Background shading (purple) shows average annual yields from several western Cascade Range rivers. Dashed horizontal line is the approximate mean value of that range of average annual yields. Histogram shows mean-annual discharge measured at gage TOW on Toutle River. SRS line marks completion date of sediment retention structure on North Fork Toutle River in 1988. Spillway bypass line indicates when water and sediment began passing over the SRS spillway in 1998. From Major and others (2018).

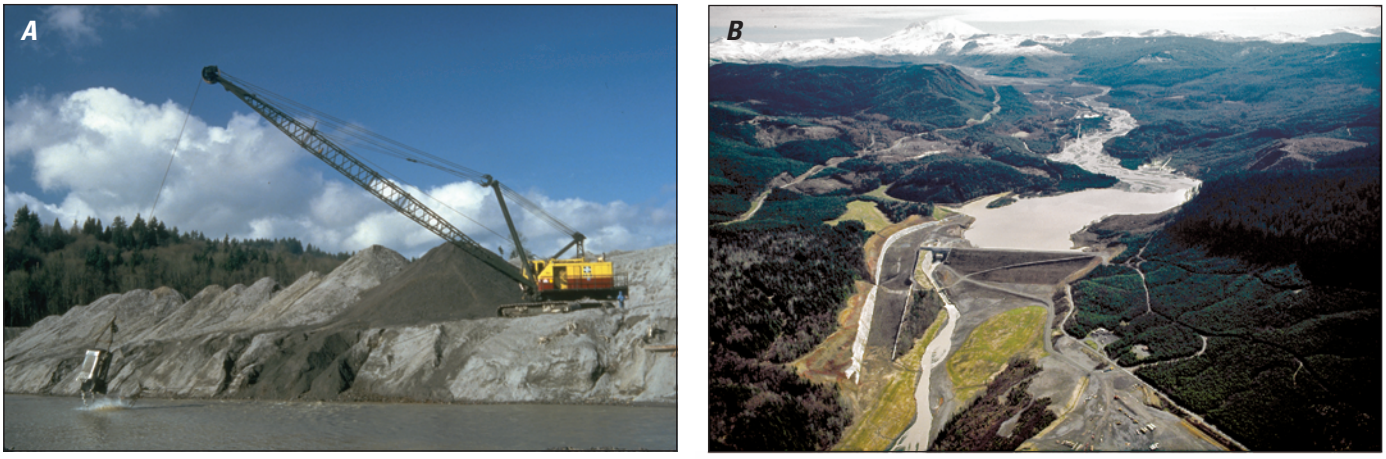

Figure 63. Mitigation of posteruption sediment transport along the Toutle-Cowlitz River system. *A*, Sediment dredging along Cowlitz River. USGS photograph by L. Topinka. *B*, Sediment retention structure built on North Fork Toutle River. U.S. Army Corps of Engineers photograph by B. Johnson. From Major and others (2005).

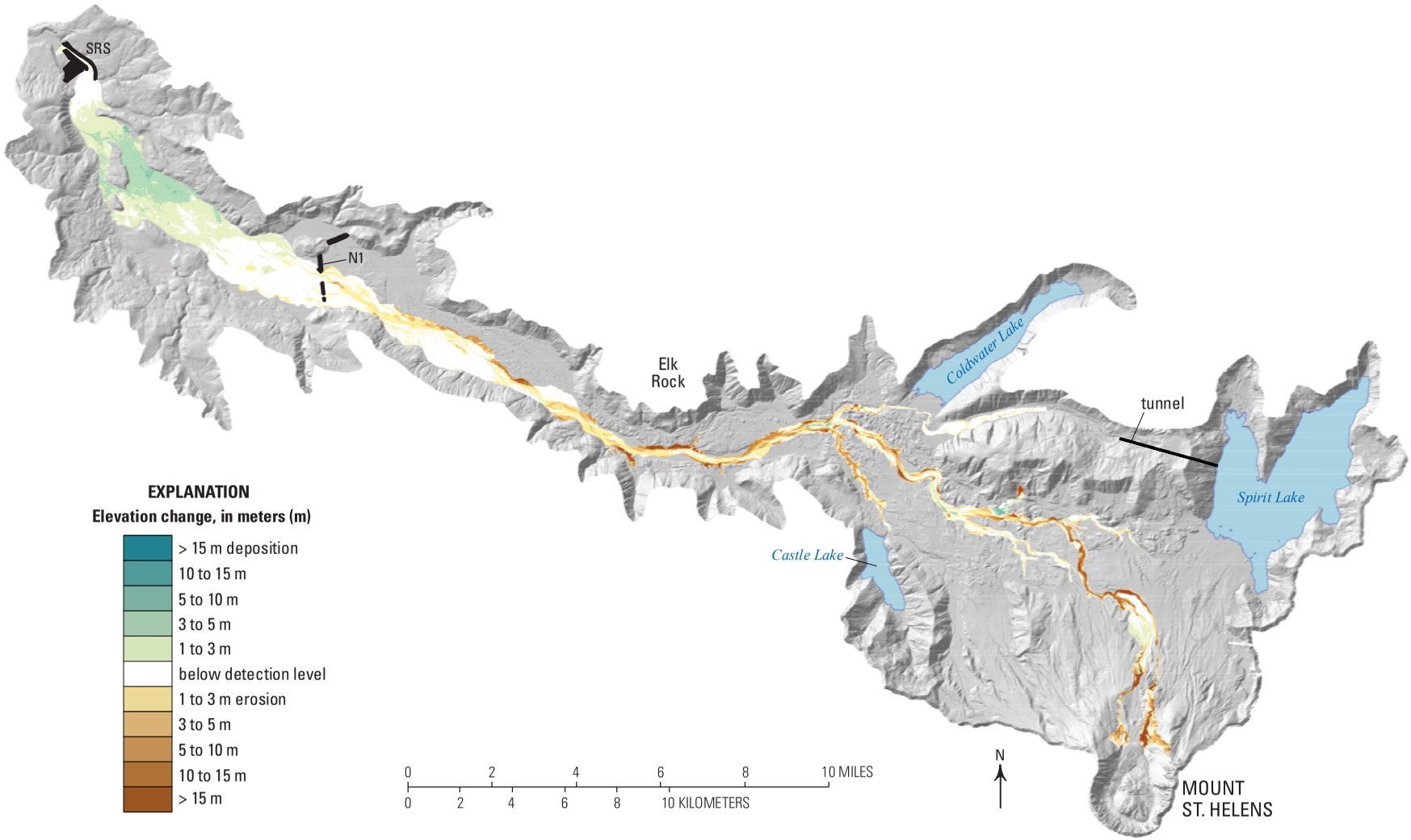

Figure 64. Digital-elevation model of topographic difference (DoD) created by differencing digital elevation models derived from aerial photography in 1999 and an airborne lidar (light detection and ranging) survey in 2009. The DoD is draped over a hill-shaded topographic model derived from the 2009 lidar survey. SRS is the sediment retention structure completed in 1988; N1 is the site of a former small retention structure built in early 1980s. From Major and others (2018).

The 1980 North Fork Toutle lahar was much larger and lasted longer. In contrast to the first lahar deposit, the overlying North Fork lahar deposit is massive, poorly sorted, and contains abundant coarse gravel in a silty sand matrix (Janda and others, 1981). This flow originated through dewatering and erosion of parts of the debris-avalanche deposit for many hours in morning, afternoon, and into evening 18 May—far more prolonged than was the South Fork lahar. Within 4.5 km of its source (about 15 km from the volcano) its volume was about 140 million m^3, and it lasted 8 hours (Fairchild and Wigmosta, 1983; Fairchild, 1987). It rose to peak discharge over more than an hour, remained at its peak of 7,200 m^3/s more than 2 hours, then gradually waned over several hours. Downstream its volume and peak discharge attenuated little. At the mouth of Toutle River 70 km from the volcano, its flow volume (120 million m^3) and peak discharge (6,050 m^3/s) had decreased by only 15 percent, but flow duration had increased to 11 hours and peak discharge lasted about 1 hour (Fairchild and Wigmosta, 1983; Major and others, 2005). The exceptional volume and long duration of this lahar caused extensive damage along Toutle and Cowlitz River valleys.

Drive SR 504 west to I-5, and I-5 south to Portland.

End Day 5

End field trip

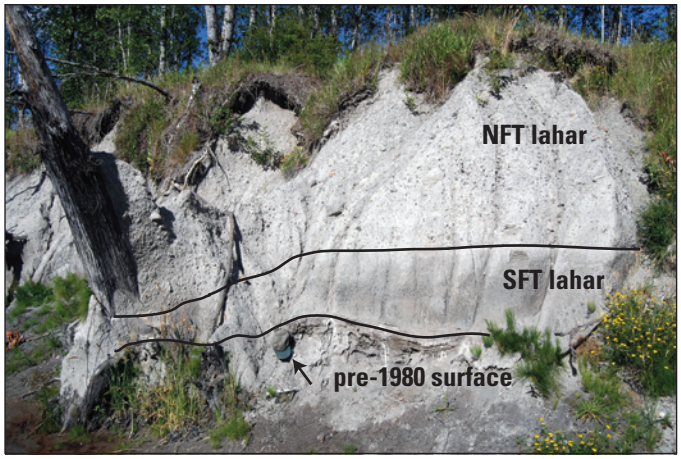

Figure 65. Deposits of lahars that swept down South Fork Toutle River (SFT) and North Fork Toutle River (NFT) on 18 May 1980. Note the differing textures of the lahars, and the location of pre-1980 surface on which buried trees are rooted. Hat for scale (arrow).

References Cited

Anderson, J.L., Tolan, T.L., and Wells, R.E., 2013, Strike-slip faults in the western Columbia River flood basalt province, Oregon and Washington *in* Reidel, S.P., Camp, V.E., Ross, M.E., Wolff, J.A., Martin, B.S., Tolan, T.L., and Wells, R.E., eds., The Columbia River Flood Basalt Province: Geological Society of America Special Paper 497, p. 325–347.

Berger, G.W., and Busacca, A.J., 1995, Thermoluminescence dating of late Pleistocene loess and tephra from eastern Washington and southern Oregon and implications for the eruptive history of Mount St. Helens: Journal of Geophysical Research, v. 100, p. 22361–22374.

Brantley, S.R., and Waitt, R.B., 1988, Interrelations among pyroclastic surge, pyroclastic flow, and lahars in Smith Creek valley during first minutes of 18 May 1980 eruption of Mount St. Helens, USA: Bulletin of Volcanology, v. 50, p. 304–326.

Bronk Ramsey, C., 1998, Probability and dating: Radiocarbon, v. 40, no. 1, p. 461–474.

Bronk Ramsey, C., 2001, Development of the radiocarbon calibration program OxCal: Radiocarbon, v. 43 no. 2A, p. 355–363.

Brugman, M.M., and Meier, M.F., 1981, Response of glaciers to the eruptions of Mount St. Helens, *in* Lipman, P.W., and Mullineaux, D.R., eds., The 1980 eruptions of Mount St. Helens, Washington: U.S. Geological Survey Professional Paper 1250, p. 743–756.

Brugman, M.M., and Post, A., 1981, Effects of volcanism on the glaciers of Mount St. Helens: U.S. Geological Survey Circular 850-D, 11p.

Burk, R.L., Moser, K.R., McCreath, D., Norrish, J.N.L., and Plum, R.L., 1989, Engineering geology of a portion of the Spirit Lake Memorial Highway, *in* Galster, R. W., ed., Engineering geology in Washington: Washington Division of Geology and Earth Resources Bulletin 78, v. II, p. 757–772.

Carey, S., Gardner, J.E., and Sigurdsson, H., 1995, The intensity and magnitude of Holocene plinian eruptions from Mount St. Helens volcano: Journal of Volcanology and Geothermal Research, v. 66, p. 185–202.

Cheney, E.S., 2016, The Neogene eggcrate of the Pacific Northwest, *in* Cheney, E.S., ed., The geology of Washington and beyond—from Laurentia to Cascadia: Seattle, University of Washington Press, p. 206–219.

Cheney, E.S., and Hayman, N.W., 2009, The Chiwaukum structural low—Cenozoic shortening of the central Cascade Range, Washington State, USA: Geological Society of America Bulletin, v. 121, p. 1135–1153.

Claiborne, L.L., Miller, C.F., Flanagan, D.M., Clynne, M.A., and Wooden, J.L., 2010, Zircon reveals protracted magma storage and recycling beneath Mount St. Helens: Geology v. 38, p. 1011–1014, doi:10.1130/G31285.1.

Clynne, M.A., 2003, Mount St. Helens, south flank field trip guide: International Association of Volcanology and

Chemistry of the Earth's Interior (IAVCEI) State-of-the-Arc meeting, Mount Hood, Oreg., August 2003, 30 p.

Clynne, M.A., Ramsey, D.W., and Wolfe, E.W., 2005, Pre-1980 eruptive history of Mount St. Helens, Washington: U.S. Geological Survey Fact Sheet 2005–3045, 4 p.

Clynne, M.A., Calvert, A.T., Wolfe, E.W., Evarts, R.C., Fleck, R.J., and Lanphere, M.A., 2008, The Pleistocene eruptive history of Mount St. Helens, Washington, from 300,000 to 12,800 years before present, *in* Sherrod, D.R., Scott, W.C., and Stauffer, P.H., eds., A volcano rekindled—the renewed eruption of Mount St. Helens, 2004–2006: U.S. Geological Survey Professional Paper 1750, p. 593–627.

Crandell, D.R., 1987, Deposits of pre-1980 pyroclastic flows and lahars from Mount St. Helens volcano, Washington: U.S. Geological Survey Professional Paper 1444, 91p.

Crandell, D.R., and Mullineaux, D.R., 1973, Pine Creek volcanic assemblage at Mount St. Helens, Washington. U.S. Geological Survey Bulletin 1383-A, 23 p.

Crandell, D.R., and Miller, R.D., 1974, Quaternary stratigraphy and extent of glaciation in the Mount Rainier region, Washington: U.S. Geological Survey Professional Paper 847, 59 p.

Crandell, D.R., and Mullineaux, D.R., 1978, Potential hazards from future eruptions of Mount St. Helens volcano, Washington: U.S. Geological Survey Bulletin 1383-C, 36 p.

Criswell, C.W., 1987, Chronology and pyroclastic stratigraphy of the May 18, 1980, eruption of Mount St. Helens, Washington: Journal of Geophysical Research, v. 92, p. 10,237–10,266.

Dethier, D.P., 1988, The soil chronosequence along the Cowlitz River, Washington: U.S. Geological Survey Bulletin 1590-F, 47 p.

Dinehart, R.L., 1998, Sediment transport at gaging stations near Mount St. Helens, Washington, 1980–1990—Data collection and analysis: U.S. Geological Survey Professional Paper 1573, 105 p.

Doukas, M.P., 1990, Road guide to volcanic deposits of Mount St. Helens and vicinity, Washington: U.S. Geological Survey Bulletin 1859, 53 p.

Dzurisin, D., Moran, S.C., Lisowski, M., Schilling, S.P., Anderson, K.R., and Werner, C., 2015, The 2004–2008 dome-building eruption at Mount St. Helens, Washington—epilogue: Bulletin of Volcanology, v. 77, 89, doi:10.1007/s0045-015-0973-4.

Druitt, T.H., 1992, Emplacement of the 18 May 1980 lateral blast deposit ENE of Mount St. Helens, Washington: Bulletin of Volcanology, v. 54, p. 554–572.

Eisele, J.W., O'Halloran, R.L., Reay, D.T., Lindholm, G.R., Lewman, L.V., and Brady, W.J., 1981, Deaths during 18 May 1980 eruption of Mount St. Helens: New England Journal of Medicine, v. 305, p. 931–936.

Endo, E.T., Malone, S.D., Noson, L.L., and Weaver, C.S., 1981, Locations, magnitudes, and statistics of the March 20-May 18 earthquake sequence, *in* Lipman, P.W., and Mullineaux, D.R., eds., The 1980 eruptions of Mount St. Helens, Washington: U.S. Geological Survey Professional Paper 1250, p. 93–107.

Evans, S.G., Hungr, O., and Enegren, E.G., 1994, The Avalanche Lake rock avalanche, Mackenzie Mountains, Northwest Territories, Canada—description, dating, and dynamics: Canadian Geotechnical Journal, v. 31, p. 749–768.

Evarts, R.C., 2004a, Geologic map of the Ariel quadrangle, Clark and Cowlitz Counties, Washington: U.S. Geological Survey, Scientific Investigations Map 2826, scale 1:24,000, 35-p. pamphlet. [Also available at http://pubs.usgs.gov/sim/2004/2826.]

Evarts, R.C., 2004b, Geologic map of the Woodland quadrangle, Clark and Cowlitz Counties, Washington: U.S. Geological Survey, Scientific Investigations Map 2827, scale 1:24,000, 38-p. pamphlet. [Also available at http:/pubs.usgs.gov/sim/2004/2827.]

Evarts, R.C., 2005, Geologic map of the Amboy quadrangle, Clark and Cowlitz Counties, Washington: U.S. Geological Survey, Scientific Investigations Map 2885, scale 1:24,000, 25-p. pamphlet. [Also available at: http://pubs.usgs.gov/sim/2005/2885]

Evarts, R.C., 2006 Geologic map of the Yacolt quadrangle, Clark County, Washington: U.S. Geological Survey, Scientific Investigations Map 2901, scale 1:24,000, 31-p. pamphlet. [Also available at http://pubs.usgs.gov/sim/2006/2901.]

Evarts, R.C., and Ashley, R.P., 1990, Preliminary geologic map of the Goat Mountain quadrangle, Cowlitz County, Washington: U.S. Geological Survey Open-File Report 90-632, 44 p., 1 plate, 1:24,000. [Also available at http://pubs.er.usgs.gov/usgspubs/ofr/ofr90632.]

Evarts, R.C., and Ashley, R.P., 1992, Preliminary geologic map of the Elk Mountain quadrangle, Cowlitz County, Washington: U.S. Geological Survey Open-File Report 92-362, 44 p., 1 plate, 1:24,000. [Also available at http://pubs.er.usgs.gov/usgspubs/ofr/ofr92362.]

Evarts, R.C. and Ashley, R.P., 1993a, Geologic map of the Spirit Lake East quadrangle, Skamania County, Washington: U.S. Geological Survey Geologic Quadrangle Map GQ-1679, 12 p., 1 plate, 1:24,000.

Evarts, R.C., and Ashley, R.P., 1993b, Geologic map of the Vanson Peak quadrangle, Lewis and Skamania Counties, Washington: U.S. Geological Survey Geologic Quadrangle Map GQ-1680, 12 p., 1 plate, 1:24,000.

Evarts, R.C., and Ashley, R.P., 1993c, Geologic map of the Spirit Lake West quadrangle, Skamania and Cowlitz Coun-

ties, Washington: U.S. Geological Survey Geologic Quadrangle Map GQ-1681, 11 p., 1 plate, 1:24,000.

Evarts, R.C., and Ashley, R.P., 1993d, Geologic map of the Cowlitz Falls quadrangle, Lewis and Skamania Counties, Washington: U.S. Geological Survey Geologic Quadrangle Map GQ-1682, 10 p., 1 plate, 1:24,000.

Evarts, R.C., and Swanson, D.A., 1994, Geologic transect across the Tertiary Cascade Range, southern Washington, *in* Swanson, D.A., and Haugerud, R.A., eds., Geologic field trips in the Pacific Northwest: Department of Geological Sciences, University of Washington, v. 2, Chapter 2-H, 31 p.

Evarts, R.C., Ashley, R.P., and Smith, J.G., 1987, Geology of the Mount St. Helens area— record of discontinuous volcanic and plutonic activity in the Cascade arc of southern Washington: Journal of Geophysical Research, v. 92, p. 10,155–10,169.

Evarts, R.C., Gray, L.B., Turrin, B.D., Smith, J.G., and Tosdal, R.M., 1994, Isotopic and fission-track ages of volcanic and plutonic rocks and hydrothermal alteration in the Spirit Lake quadrangle and adjacent areas, southwestern Washington: Isochron/West, no. 61, p. 25–47.

Fairchild, L.H., 1987, The importance of lahar initiation process, *in* Costa, J.E. and Wieczorek, G.F., eds., Debris flows/avalanches—process, recognition, and mitigation: Geological Society of America, Reviews in Engineering Geology, v. 7, p. 51–61.

Fairchild, L.H., and Wigmosta, M., 1983, Dynamic and volumetric characteristics of the 18 May 1980 lahars on the Toutle River, Washington: Proceedings of the symposium on erosion control in volcanic areas, Technical Memorandum 1908, Public Works Research Institute, Tsukua, Japan, p. 131–153.

Fiacco, R.J., Jr., Palais, J.M., Germani, M.S., Zielinski, G. A., and Mayewski, P. A., 1993, Characteristics and possible source of a 1479 A.D. volcanic ash layer in a Greenland ice core: Quaternary Research, v. 39, p. 267–273.

Fleck, R.J., Hagstrum, J.T., Calvert, A.T., Evarts, R.C., and Conrey, R.M., 2014, $^{40}Ar/^{39}Ar$ geochronology, paleomagnetism, and evolution of the Boring volcanic field, Oregon and Washington, USA: Geosphere, v. 10, p. 1283–1314, doi:10.1130/GES00985.1

Folk, R.F., 1980, Petrology of sedimentary rocks: Austin, Texas, Hemphill Publishing Co., 184 p.

Gardner, J.E., Rutherford, M., Carey, S., and Sigurdsson, H., 1995a, Experimental constraints on pre-eruptive water contents and changing magma storage prior to explosive eruptions of Mount St. Helens volcano: Bulletin of Volcanology, v. 57, p. 1–17.

Gardner, J.E., Carey, S., Rutherford, M.J., Sigurdsson, H., 1995b, Petrologic diversity in Mount St. Helens dacites during the last 4,000 years—implications for magma mixing: Contributions to Mineralogy and Petrology, v. 119, p 224–238.

Gardner, J.E., Andrews, B.J., and Dennen, R., 2017, Liftoff of the 18 May 1980 surge of Mount St. Helens (USA) and the deposits left behind: Bulletin of Volcanology, v. 79, article 8, 12 p; doi10.1007/s00446-016-1095-3.

Gawel, J. E., Crisafulli, C. M., and Miller, R., 2018, The new Spirit Lake—Changes to hydrology, nutrient cycling, and biological productivity, chap. 4 *of* Crisafulli, C.M., and Dale, V.H. eds., Ecological responses at Mount St. Helens—revisited 35 years after the 1980 eruption: New York, Springer Science+Business Media, p. 71–95.

Geschwind, C.-H. and Rutherford, M.J., 1992, Cummingtonite and the evolution of the Mount St. Helens (Washington) magma system—an experimental study: Geology, v. 20, p. 1011–1014.

Glicken, H., 1996, Rockslide–debris avalanche of May 18, 1980, Mount St. Helens Volcano, Washington: U.S. Geological Survey Open-File Report 96–677, 90 p, 5 pls., http://pubs.usgs.gov/of/1996/0677.

Greeley, R., and Hyde, J.H., 1972, Lava tubes of the Cave basalt, Mount St. Helens, Washington: Geological Society of America Bulletin, v. 83, p. 2397–2418.

Hammond, P.E., 1987, Lone Butte and Crazy Hills—Subglacial volcanic complexes, Cascade Range, Washington, *in* Hill, M.L., ed., Cordilleran Section field guide: Geological Society of America Centennial Field Guide, v. 1, p. 339–344.

Hammond, P.E., 1998, Tertiary andesite lava-flow complexes (stratovolcanoes) in the southern Cascade Range of Washington—observations on tectonic processes within the Cascade arc: Washington Geology, v. 26, no. 1, p. 20–30.

Hammond, P.E., 2013, Distribution, stratigraphy, and structure of the Grande Ronde Basalt in the upper Naches River basin, Yakima and Kittitas Counties, Washington, *in* Reidel, S.P., Camp, V.E., Ross, M.E., Wolff, J.A., Martin, B.S., Tolan, T.L., and Wells, R.E., eds., The Columbia River Flood Basalt Province: Geological Society of America Special Paper 497, p. 363–400.

Harris, D.M., Rose, W.I., Jr., Roe, R., and Thompson, M.R, 1981, Radar observations of ash eruptions, *in* Lipman, P.W., and Mullineaux, D.R., eds., The 1980 eruptions of Mount St. Helens, Washington: U.S. Geological Survey Professional Paper 1250, p. 323–333.

Hausback, B.P., and Swanson, D.A., 1990, Record of prehistoric debris avalanches on the north flank of Mount St. Helens volcano, Washington: Geoscience Canada, v. 17, p. 142–145.

Hinson, D.R., Steward, C.R., Wills, S.E., Kock, T.J., Kritter, M.A., Liedtke, T.L., and Rondorf, D.W., 2007, Salmonid population trends and recovery in the Toutle River, Washington following the 1980 eruption of Mount St. Helens: Ameri-

can Fisheries Society, Sea Grant Special Symposium, 2007 AFS Annual Meeting, last accessed November 2008 at http://www.fisheries.org/units/afs-sgsymposium/2007/hinson.html.

Hoblitt, R.P., 1978, Emplacement mechanisms of unsorted and unstratified deposits of volcanic rock debris as determined from paleomagnetically-derived emplacement-temperature information: Boulder, University of Colorado, Ph.D. dissertation, 206 p.

Hoblitt, R.P., 1989, Recent volcaniclastic deposits and processes at Mount St. Helens volcano, Washington, Day 3, The Kalama eruptive period, southwest and south flanks, *in* Chapin, C.E., and Zideck, J., eds., Field excursions to volcanic terrains in the western United States II—Cascades and intermountain West: New Mexico Bureau of Mines and Mineral Resources Memoir 47, p. 65–69.

Hoblitt, R.P., 2000, Was the 1980 lateral blast at Mount St. Helens the product of two explosions?: Philosophical Transactions of the Royal Society of London, series A, v. 258, p. 1639–1661.

Hoblitt, R.P., and Kellogg, K.S., 1979, emplacement temperatures of unsorted and unstratified deposits of volcanic rock debris as determined by paleomagnetic techniques: Geological Society of America Bulletin, v. 90, pt. 1, p. 633–642.

Hoblitt, R.P., and Miller, C.D., 1984, Comment on "Mount St. Helens and Mount Pelée—flow or surge?": Geology, v. 12, p. 692–693.

Hoblitt, R.P., Crandell, D.R., and Mullineaux, D.R., 1980, Mount St. Helens eruptive behavior during the past 1,500 yr: Geology, v. 8, p. 555–559.

Hoblitt, R.P., Miller, C.D., and Vallance, J.W., 1981, Origin and stratigraphy of the deposit produced by the May 18 directed blast, *in* Lipman, P.W. and Mullineaux, D.R., eds., The 1980 eruptions of Mount St. Helens, Washington: U.S. Geological Survey Professional Paper 1250, p. 401–419.

Holasek, R.E.., and Self, S., 1995, GOES weather satellite observations and measurements of the May 18, 1980, Mount St. Helens eruption Journal of Geophysical Research, v. 100, p. 8469–8487.

Hooper, P.R., and Conrey, R.M., 1989, A model for the tectonic setting of the Columbia River basalt eruptions, *in* Reidel, S.P. and Hooper, P.R., Volcanism and tectonism in the Columbia River flood-basalt province: Geological Society of America Special Paper 239, p. 293–306.

Howard, K.A., 2002, Geologic map of the Battle Ground 7.5-minute quadrangle, Clark County, Washington: U.S. Geological Survey Miscellaneous Field Studies Map MF-2395, scale 1:24,000, 18-p. pamphlet, http://geopubs.wr.usgs.gov/map-mf2395/.

Hyde, J.H., 1975, Upper Pleistocene pyroclastic-flow deposits and lahars south of Mount St. Helens volcano, Washington: U.S. Geological Survey Bulletin 1383-B, 20 p.

Janda, R.J., Scott, K.M., Nolan, K.M., and Martinson, H.A., 1981, Lahar movement, effects and deposits, *in* Lipman, P.W. and Mullineaux, D.R., eds., The 1980 eruptions of Mount St. Helens, Washington: U.S. Geological Survey Professional Paper 1250, p. 461–478.

Kanamori, H., Given, J.W., and Lay, T., 1984, Analysis of seismic body waves excited by the Mount St. Helens Eruption of May 18, 1980: Journal of Geophysical Research, v. 89, p. 1856–1866.

Kane, P., 1968, Wanderings of an Artist—Among the Indians of North America—from Canada to Vancouver's Island and Oregon through the Hudson's Bay Company's territory and back again, 2d ed.: Rutland, Vt., Charles E. Tuttle Co.

Lipman, P.W., Moore, J.G., and Swanson, D.A., 1981, Bulging of the north flank before the May 18 eruption—geodetic data, *in* Lipman, P.W., and Mullineaux, D.R., eds., The 1980 eruptions of Mount St. Helens, Washington: U.S. Geological Survey Professional Paper 1250, p. 143–155.

Lisiecki, L.E., and Raymo, M.E., 2005, A Pliocene–Pleistocene stack of 57 globally distributed benthic δ18O records: Paleoceanography, v. 20, PA-1003, 17 p.

Major, J.J., 2004, Posteruption suspended sediment transport at Mount St. Helens: Decadal-scale relationships with landscape adjustments and river discharges: Journal of Geophysical Research, v. 109, F01002, doi:10.1020/2002JF000010, 22 p.

Major, J.J., and Scott, K.M., 1988, Volcaniclastic sedimentation in the Lewis River valley, Mount St. Helens, Washington—processes, extent, and hazards: U.S. Geological Survey Bulletin 1383-D, 38 p.

Major, J.J., and Mark, L.E., 2006, Peak flow responses to landscape disturbances caused by the cataclysmic 1980 eruption of Mount St. Helens, Washington: Geological Society of America Bulletin, v. 118, p. 938–958, doi:10.1130/B25914.1.

Major, J.J., Pierson, T.C., Dinehart, R.L., and Costa, J.E., 2000, Sediment yield following severe volcanic disturbance—a two decade perspective from Mount St. Helens: Geology, v. 28, p. 819–822.

Major, J.J., Pierson, T.C., and Scott, K.M., 2005, Debris flows at Mount St. Helens, Washington, USA, *in* Jakob, M., and Hungr, O., eds., Debris flow hazards and related phenomena: Springer-Verlag Berlin Heidelberg, p. 685–731.

Major, J.J., Crisafulli, C.M., Frenzen, P., and Bishop, J., 2009, After the disaster—the hydrogeomorphic, ecological, and biological responses to the 1980 eruption of Mount St. Helens, Washington: Geological Society of America Field Guide 15, p. 111–134.

Major, J.J., Mosbrucker, A.R., Spicer, K.R., 2018, Sediment erosion and delivery from Toutle River basin after the 1980 eruption of Mount St. Helens—a 30-year perspective, *in*

Dale, V.H., and Crisafulli, C.M., eds., Ecological responses revisited 35 years after the 1980 eruptions of Mount St. Helens: New York, Springer-Verlag, p. 19–46, doi:10.1007/978-1-4939-7451-1_2.

McCracken, B., 1989, Storing sediment and freeing fish: American Society of Civil Engineers, Civil Engineering, v. 59, p. 58–60.

Moore, J.G., and Albee, W.C., 1981, Topographic and structural changes, March–July 1980— photogrammetric data, *in* Lipman, P.W., and Mullineaux, D.R., eds., The 1980 eruptions of Mount St. Helens, Washington: U.S. Geological Survey Professional Paper 1250, p. 123–134.

Moore, J.G., and Sisson, T.W., 1981, Deposits and effects of the May 18 pyroclastic surge, *in* Lipman, P.W. and Mullineaux, D.R., eds., The 1980 eruptions of Mount St. Helens, Washington: U.S. Geological Survey Professional Paper 1250, p. 421–438.

Moore, J.G., and Rice, C.J., 1984, Chronology and character of the May 18, 1980 explosive eruptions of Mt. St. Helens, *in* Explosive volcanism—Inception, evolution, and hazards: Washington, D.C., National Academy Press, p. 133–142.

Moore, J.G., Nakamura, K., and Alcarez, A., 1966, The 1965 eruption of Taal volcano: Science, v. 151, p. 955–960.

Mullineaux, D.R., 1986, Summary of pre-1980 tephra-fall deposits erupted from Mount St. Helens, Washington State, USA: Bulletin of Volcanology, v. 48, p. 17–26.

Mullineaux, D.R., 1996, Pre-1980 tephra-fall deposits erupted from Mount St. Helens, Washington: U.S. Geological Survey Professional Paper 1563, 99 p.

Mullineaux, D.R., and Crandell, D.R., 1981, The eruptive history of Mount St. Helens, *in* Lipman, P.W., and Mullineaux, D.R., eds., The 1980 eruptions of Mount St. Helens, Washington: U.S. Geological Survey Professional Paper 1250, p. 3–15.

Mundorff, M.J., 1964, Geology and ground-water conditions of Clark County, Washington, with a description of a major alluvial aquifer along the Columbia River: U.S. Geological Survey Water-Supply Paper 1600, 268 p., scale 1:48,000.

Mundorff, M.J., 1984, Glaciation of the lower Lewis River basin, southwestern Cascade Range, Washington: Northwest Science, v. 58, p. 269–281.

Paguican, E.M.R., van Wyk de Vries, B., and Lagmay, A., 2014, Hummocks—how they form and how they evolve in rockslide–debris avalanches: Landslides, v. 11, p. 67–80.

Pallister, J.S., Hoblitt, R. P., Crandell, D. R., and Mullineaux, D. R., 1992, Mount St. Helens a decade after the 1980 eruptions: magmatic models, chemical cycles, and a revised hazards assessment: Bulletin of Volcanology, v. 54, p. 126–146.

Pallister, J.S., Miller, C.D., Thompson, R.A., Clynne, M.A., and Schilling, S.P., 2003, Mount St. Helens, north flank field trip guide: International Association of Volcanology and Chemistry of the Earth's Interior (IAVCEI) State-of-the-Arc meeting, Mount Hood, Oreg., August 2003, 37 p.

Pierson, T.C., 1985, Initiation and flow behavior of the 1980 Pine Creek and Muddy River lahars, Mount St. Helens, Washington: Geological Society of America Bulletin, v. 96, p. 1056–1069.

Pringle, P.T., 2002, Roadside geology of Mount St. Helens National Volcanic Monument and vicinity: Washington Department of Natural Resources Division of Geology and Earth Resources Information Circular 88, rev. ed., 122 p.

Pringle, P.T., 2008, Roadside geology of Mount Rainier National Park and vicinity: Washington Department of Natural Resources Division of Geology and Earth Resources Information Circular 107, 190 p.

Rowley, P.D., Kuntz, M.A., and MacLeod, N.S., 1981, Pyroclastic-flow deposits, *in* Lipman, P.W., and Mullineaux, D.R., eds., The 1980 eruptions of Mount St. Helens, Washington: U.S. Geological Survey Professional Paper 1250, p. 489–512.

Sarna-Wojcicki, A.M., Shipley, S., Waitt, R.B., Dzurisin, D., and Wood, S.H., 1981, Areal distribution, thickness, mass, volume, and grain size of air-fall ash from six major eruptions of 1980, *in* Lipman, P.W. and Mullineaux, D.R., eds., The 1980 eruptions of Mount St. Helens, Washington: U.S. Geological Survey Professional Paper 1250, p. 577–600.

Schilling, S.P., Carrara, P.E., Thompson, R.A., and Iwatsubo, E.Y., 2004, Posteruption glacier development within the crater of Mount St. Helens, Washington, USA: Quaternary Research, v. 61, p. 325–329.

Scott, K.M., 1988a, Origins, behavior, and sedimentology of lahars and lahar-runout flows in the Toutle-Cowlitz River system, Mount St. Helens, Washington: U.S. Geological Survey Professional Paper 1447-A, 74 p.

Scott, K.M., 1988b, Origins, behavior, and sedimentology of prehistoric catastrophic lahars at Mount St. Helens, Washington, *in* Clifton, H.E., ed., Sedimentologic consequences of convulsive geologic events: Geological Society of America Special Paper 229, p. 23–36.

Scott, K.M., 1989, Magnitude and frequency of lahars and lahar-runout flows in the Toutle-Cowlitz River system, Mount St. Helens, Washington: U.S. Geological Survey Professional Paper 1447-B, 33 p.

Sherrod, B.L., Blakeley, R.J., Lasher, A., Lamb, S.A., Mahan, S.A., Foit, F.F., Jr., and Barnett, E.A., 2016, Active faulting on the Wallula fault zone within the Olympic-Wallowa lineament, Washington State, U.S.A.: Geological Society of America Bulletin, v. 128, p. 1636–1659.

Smith, D.R., and Leeman, W.P., 1987, Petrogenesis of Mount St. Helens magmas: Journal of Geophysical Research, v. 92, p. 10,313–10,334.

Smith, D.R., and Leeman, W.P., 1993, The origin of Mount St. Helens andesites: Journal of Volcanology and Geothermal Research, v. 55, p. 271–303.

Smith, G.A., 1988, Neogene synvolcanic and syntectonic sedimentation in central Washington: Geological Society of America Bulletin, v. 100, p. 1479–1492.

Sparks, R.S.J., Moore, J.G., and Rice, C.J., 1986, The initial giant umbrella cloud of the May 18th, 1980, explosive eruption of Mount St. Helens: Journal of Volcanology and Geothermal Research, v. 28, p. 257–274.

Swanson, D.A., and Holcomb, R.T., 1989, Regularities on growth of the Mount St. Helens dacite dome 1980–1986, *in* Fink, J., ed., Lava flows and domes: IAVCEI proceedings in volcanology, v. 2, p. 3–24.

Vallance, J.E., Schneider, D.J., and Schilling, S.P., 2008, Growth of the 2004–2006 lava-dome complex at Mount St. Helens, Washington, *in* Sherrod, D.R., Scott, W.C., and Stauffer, P.H., eds, A volcano rekindled—the renewed eruption of Mount St. Helens, 2004–2006: U.S. Geological Survey Professional Paper 1750, p. 169–208.

Van Eaton, A.R., Muirhead, J.D., Wilson, C.J.N., and Cimarelli, C., 2012, Growth of volcanic ash aggregates in the presence of liquid water and ice—an experimental approach: Bulletin of Volcanology, v. 74, p. 1963–1984; doi:10.1007/s00445-012-0634-9.

Voight, B., 1981, Time scale for the first moments of the May 18 eruption, *in* Lipman, P.W. and Mullineaux, D.R., eds., The 1980 eruptions of Mount St. Helens, Washington: U.S. Geological Survey Professional Paper 1250, p. 69–86.

Voight, B., Glicken, H., Janda, R.J., and Douglass, P.M., 1981, Catastrophic rockslide avalanche of May 18, *in* Lipman, P.W. and Mullineaux, D.R., eds., The 1980 eruptions of Mount St. Helens, Washington: U.S. Geological Survey Professional Paper 1250, p. 347–377.

Waitt, R.B., 1981, Devastating pyroclastic density flow and attendant air fall of May 18—stratigraphy and sedimentology of deposits, *in* Lipman, P.W., and Mullineaux, D.R., eds., The 1980 eruptions of Mount St. Helens, Washington: U.S. Geological Survey Professional Paper 1250, p. 439–458.

Waitt, R.B., 1984, Comment on "Mount St. Helens and Mount Pelée—flow or surge?": Geology, v. 12, p. 693.

Waitt, R.B., 1989, Swift snowmelt and floods (lahars) caused by great pyroclastic surge at Mount St. Helens volcano, Washington, 18 May 1980: Bulletin of Volcanology, v. 52, p. 138–157.

Waitt, R.B., 2015, In the path of destruction—eyewitness chronicles of Mount St. Helens: Pullman, Washington State University Press, 413 p.

Waitt, R.B., and Dzurisin, D., 1981, Proximal air-fall deposits from May 18 eruption— stratigraphy and field sedimentology, *in* Lipman, P.W., and Mullineaux, D.R., eds., The 1980 eruptions of Mount St. Helens, Washington: U.S. Geological Survey Professional Paper 1250, p. 601–616.

Waitt, R.B., and Pierson, T.C., 1994, The 1980 (mostly) and earlier explosive eruptions of Mount St. Helens volcano, chapter 2-I *of* Swanson, D.A., and Haugerud, R.A., eds., Geologic field trips in the Pacific Northwest [for Geological Society of America]: Seattle, University of Washington Department of Geological Sciences, v. 2, 37 p.

Waitt, R.B., and Begét, J.E., 2009, Volcanic processes and geology of Augustine Volcano, Alaska: U.S. Geological Survey Professional Paper 1762, 78 p., 2 plates, scale 1:25,000.

Waitt, R.B., and Hoblitt, R.P., 2017, The 18 May 1980 pyroclastic surge at Mount St. Helens as two separate events [abs.]: Proceedings of the International Association of Volcanology and Chemistry of the Earth's Interior (IAVCEI) 2017 General Assembly, Abstracts, Abstract VH41A-4.

Waitt, R.B., Hansen, V.L., Sarna-Wojcicki, A.M., and Wood, S.M., 1981, Proximal airfall deposits of eruptions between May 24 and August 7, 1980—stratigraphy and field sedimentology, *in* Lipman, P.W., and Mullineaux, D.R., eds., The 1980 eruptions of Mount St. Helens, Washington: U.S. Geological Survey Professional Paper 1250, p. 617–628.

Waitt, R.B., Pierson, T.C., MacLeod, N.S., Janda, R.J., Voight, B., and Holcomb, R.T., 1983, Eruption-triggered avalanche, flood, and lahar at Mount St. Helens—effects of winter snowpack: Science, v. 221, p. 1394–1397.

Waitt, R.B., Hoblitt, R.P., Criswell, C.W., Scott, K.M., Glicken, H., and Brantley, S.R., 1989, Recent volcaniclastic deposits and processes at Mount St. Helens, Washington, *in* Chapin, C.E., and Zideck, J., eds., Field excursions to volcanic terranes in the western United States, II—Cascades and intermountain West: New Mexico Bureau of Mines and Mineral Resources Memoir 47, p. 51–89.

Waitt, R.B., Mosbrucker, A.R., and Crisafulli, C.M., 2014, Spirit Lake at Mount St. Helens— surge, landslide, giant wave, long-term effects [abs.]: Geological Society of America, Abstracts with Programs, v. 46, no. 6, p. 41, Abst 7-9.

Waitt, R.B., Dzurisin, D., and Schilling, S., 2016, Living, working, dying at Mount St. Helens 1980 to 2008, *in* Cheney, E.S., ed., The geology of Washington and beyond—from Laurentia to Cascadia: Seattle, University of Washington Press, p. 311–328.

Walder, J.S., Schilling, S.P., Vallance, J.W., and LaHusen, R.G., 2008, Effects of lava-dome growth on the Crater

Glacier of Mount St. Helens, Washington, *in* Sherrod, D.R., Scott, W.C., and Stauffer, P.H., eds., A volcano rekindled—the renewed eruption of Mount St. Helens, 2004–2006: U.S. Geological Survey Professional Paper 1750, p. 257–276.

Walker, G.P.L., and McBroome, L.A., 1983, Mount St. Helens and Mount Pelée—flow or surge?: Geology, v. 11, p. 571–574.

Wanke, M., Clynne, M.A., von Quadt, A., Vennemann, T.W., and Bachmann, O., 2019, Geochemical and petrological diversity of mafic magmas from Mount St. Helens: Contributions to Mineralogy and Petrology, v. 174, no. 10, https://doi.org/10.1007/s00410-018-1544-4.

Wells, R.E., Weaver, C.S., and Blakely, R.J., 1998, Fore-arc migration in Cascadia and its neotectonic significance: Geology, v. 26, p. 759–762.

White, J.D.L., and Houghton, B.F., 2006, Primary pyroclastic rocks: Geology, v. 34, p. 677–680; doi:10.1130/G22346.1.

Yamaguchi, D.K., 1983, New tree-ring dates for recent eruptions of Mount St. Helens: Quaternary Research, v. 20, p. 246–250.

Yamaguchi, D.K., 1985, Tree-ring evidence for a two-year interval between recent prehistoric explosive eruptions of Mount St. Helens: Geology, v. 13, p. 554–557.

Yamaguchi, D.K., 1986, Interpretation of cross correlation between tree-ring series: Tree-Ring Bulletin, v. 46, p. 47–54.

Yamaguchi, D. K., 1993, Old-growth forest development after Mount St. Helens' 1480 eruption: National Geographic Research and Exploration, v. 9, p. 294–325.

Yamaguchi, D.K., and Hoblitt, R.P., 1995, Tree-ring dating of pre-1980 volcanic flowage deposits at Mount St. Helens, Washington: Geological Society of America Bulletin, v. 107, p. 1077–1093.

Yamaguchi, D.K., Hoblitt, R.P., and Lawrence, D.B., 1990, A new tree-ring date for the "floating island" lava flow, Mount St. Helens, Washington: Bulletin of Volcanology, v. 52, p. 545–550.

Zheng, S., Wu, B., Thorne, C.R., and Simon, A., 2014, Morphological evolution of the North Fork Toutle River following the eruption of Mount St. Helens, Washington: Geomorphology, v. 208, p. 102–116.

Menlo Park Publishing Service Center, California
Manuscript approved August 12, 2019
Edited by Claire Landowski
Design and layout by Katie Sullivan

ISSN 2328-0328 (online)
https://doi.org/10.3133/sir20175022E